Groundwater Salinization Process in Coastal Aquifer of Saijo Plain, Ehime Prefecture, Japan

A Dissertation Submitted to
the Graduate School of Life and Environmental Sciences,
the University of Tsukuba
in Partial Fulfilment of the Requirements
for the Degree of Doctor of Philosophy in Science
(Doctoral Program in Geoenvironmental Sciences)

Pankaj KUMAR

ABSTRACT

The expansion of brackish and saline water bodies towards inland in coastal aquifers associated with rising sea levels/climate change/periodic sea level fluctuation is being an area of thirst for scientific knowledge since a long time and recognized as a potential health hazard to coastal communities. Considering the current poor understanding about the sea water- fresh water (SW-FW) interaction pattern at dynamic hydro-geological boundary of coastal aquifers, this work strives to study tidal effect on ground water quality/chemistry for different aquifers in case of Saijo plain, Western Japan, using chemical tracers combined with environmental isotopes as well as to estimate aquifer parameters by tidal response method.

To achieve this objective, ground water samples were collected during three different sampling campaigns, from different monitoring sites at hourly basis in a representative array of locations for over twenty four hour period. Physical and chemical parameters of groundwater samples obtained through in situ and laboratory analysis were compared with tidal level data measured by Hydrographic and Oceanographic Department, Saijo city for time series analysis. Data interpretation was done using different plots and calculation to delineate the physical process responsible for water quality change with tidal phase. Numerical simulation was also done to confirm the validity of result from hydrochemical investigation.

Findings of this work are concluded in following points: First, tidal fluctuation on diurnal basis, significantly affects ionic signature of groundwater along with Piezometric level for unconfined aquifer whereas effect is less prominent for confined

aquifer. The mechanism responsible here is horizontal mass movement i.e. mass flux generated due to change in boundary condition towards sea. However, mobilization for heavy metal (oxidation-reduction process) in groundwater samples from both aquifers occurs mainly because of second process i.e. local mass movement across Piezometric level. Though changes/fluctuations in magnitude of many chemical parameters caused by these processes are not very high but the process is significantly necessary to be pointed out. Second, seasonal rainfall amount also one of the important factor affecting the intensity of tidal effect on water quality. Third, presence of aquitard /aquiclude (eg. Clay) hinder partially or completely the propagation of tidal wave to affect water quality parameters in coastal aquifers. In other words, location/position of screen depth for the borehole is the important factor controlling the characteristics of tidal effect on the ground water type at point scale. Fourth, from the above work it was found that for samples taken from bore well with deeper screen depth (about 25 meter) has a problem of salinization in case of Saijo plain; so it will be recommended to have an alternate tube/bore well with shallow screen depth (about 15 meter) in order to prevent the encounter of SW–FW interface as a short term solution.

The results obtained from above mentioned research works will not only contribute to scientific/research community and sustainable groundwater management but also for the local people, who depends on the salinized coastal aquifers for their living. With the help of this information, government bodies can promote local people to change in their water consumption pattern in order to minimize intake of more deteriorated ground water. Finally it must contribute to the sustainable development of

coastal aquifer system and solving one of the most vital challenges, world is facing today i.e. ground water salinization.

TABLE OF CONTENTS

LIST OF TABLES

LIST OF FIGURES

List of Abbreviations

Short Form
Full Form

GW……Ground Water

FW……..Fresh Water

SW……..Sea Water

MSL……Mean Sea Level

BGL……Below Ground Level

EC……...Electrical Conductivity

ORP……Oxidation Reduction Potential

BEX……Base Exchange Indices

VSMOW……Vienna Standard Mean Ocean Water

LMWL……Local Meteoric Water Line

SI…….Saturation Index

WHO……..World Health Organization

t_{lag} ……...Time Lag

TE……Tidal Efficiency

SGD…….Submarine Groundwater Discharge

Chapter 1

Introduction

1.1 General introduction

Coastal zones, especially low-lying deltaic areas (within sixty km of the shoreline), accommodate about fifty percent of the world population, so it is very important to know hydrological processes at coastal aquifers. Since the ancient time, humankind is fascinated to these areas because of the availability of an abundance of food (e.g. fisheries) and the presence of economic activities (e.g. trade, ports, harbors and infrastructure). Due to increasing concentration of human settlements, agricultural development and economic activities, the shortage of fresh groundwater for domestic, agricultural, and industrial purposes becomes more striking in these coastal zones. From the distribution of water resources over the planet earth (shown in Fig. 1.1), it was found that only about 2.5 % of all the water available is fresh in nature. Moreover out of this freshwater storage, only 30 % is potentially available (10.53×10^6 km^3) (shown in Table 1.1), primarily as groundwater. Despite of this, because of high quality and huge availability at spatial scale in compare to surface water; demand pressure on ground water resources increasing day by day. At present, one third of fresh water consumption for domestic purposes is maintained by groundwater and this fraction is growing further due to rapid rise of world population and economic growth and the loss of surface water resources due to its pollution/contamination. Shortcomings of using groundwater compare to that of surface water are high extraction costs, risk of the land subsidence

and most important the danger of salt water intrusion. Here sea water intrusion is defined as the migration of saltwater into freshwater aquifers under the influence of ground water development (Freeze and Cherry, 1979).

A list of the factors affecting coastal aquifers, their effect and countermeasures are summarized in Fig. 1.2. It is shown here that it's a cumulative role of the natural geological/geomorphological processes along with anthropogenic activities which affect the water resources at the coastal aquifers. Natural processes like processes at coastal zone (e.g. coastal erosion, shoreline retreat, tidal effect), sea level rise, backwater effect, seepage through the geological formations (presence of inland faults/fracture), and change in hydraulic regime (e.g. evapotranspiration, precipitation, recharge amount) leads to change in sea water – fresh water equilibrium and favors the ground water salinization.

Anthropogenic activities such as such as excessive extraction of groundwater, mining of natural resources (sand, oil and gas) and land reclamation triggers land subsidence and change in hydraulic regime which ultimately results into sea water intrusion/ salt water upconing. As a result of these factors mentioned above, coastal aquifers have main issues of salt water intrusion, decrease of ground water resources and ecosystem degradation.

To prevent these hazards, main countermeasures includes infiltration of the surface water in the salinized zone of the aquifer, increasing natural recharge and through creating natural barrier to prevent sea water intrusion. The response of the groundwater system is to reach a new state of equilibrium, with amongst others a different

distribution of fresh and saline groundwater. This may last decades or even centuries, as groundwater flow is, in general, a very slow process. Although this may sound rather reassuring, it also means that once an unwanted effect is observed, it will also take a long time before countermeasures become effective.

In summary, lack of regular monitoring network for groundwater in coastal regions, can't give the status of the deterioration of the water resources and thus it will be hard to execute the plan for its diligent sustainable management (Steyl, 2010).

1.2 Groundwater salinization at coastal aquifers all over the world: a short glance

The hydrogeological/hydrogeochemical study at coastal aquifers to decipher the hydrological processes is consistently being hot research topic during the past few decades, motivated by both scientific interest and societal relevance; considering the fact that many coastal aquifers in the world, especially shallow ones, experiencing an intensive salt water intrusion caused by both natural as well as man-induced processes (Oude Essink, 2001). Study of ground water – surface water interaction to represent dynamics of sea water intrusion has been done through various following methods:

1. **Cations exchange as a main process**- Piper and Durov diagrams (in original and modified versions) along with hydrochemical facies evolution diagram have been consistently applied to study the cation exchange and reverse cations reaction during dynamics of sea water intrusion or freshening occurring in alluvial coastal aquifer (Ray et al., 2008; Petalas et al., 2009; Forcada, 2010).
2. **Rock-water interaction as a main process** - Integrated approach of geochemical

and isotopic analysis proved as an efficient tool to understand interaction between groundwater and its surrounding environment which contribute to its better management (Adams et al., 2001; Schiavo et al., 2009; Forcada et al., 2010). Combined study of chemical tracers (all major and minor ions) and environmental isotopes (δD, $\delta^{18}O$ and $^{87}Sr/^{86}Sr$) is an efficient investigative tool to understand the aquifer matrix chemistry and water–rock interaction along the flow path in the aquifer to trace groundwater evolution and mechanism of salt water – fresh water mixing (Kim et al., 2003; Vengosh et al., 2005; Chen et al., 2007; Jorgensen et al., 2008; Langman et al., 2010).

3. **Study of SW-GW interface** – From Ghyben-Herzberg equation, it is known that depends on the ratio of specific weights for freshwater and seawater, freshwater drawdown will affects or induce the inland elevation of the salt water-fresh water interface. Keeping this in mind Depth vs Cl- ratio was calculated to know the exact position of sea water- fresh water interface in order to judge the safe limit of extraction to prevent further deterioration of ground water quality. (Sophocleous, 2002).
4. **Water imbalance as a main reason** – Here scientific community traced out ground water budget through calculating the balance between total amount of recharge and extraction of ground water and what the safe limit of extraction is in order to meet sustainable future demand (Voudouris, 2006).
5. **Numerical simulation** - Numerical simulation approach mainly used finite element based flow and transport simulation model to predict of future saltwater distribution in coastal aquifer (Datta, 2009; Kopsiaftis, 2009). In parallel there are lots of works

have been done to investigate tidal effects mainly focused on submarine ground water discharge (SGD), aquifer leakage and Oxidation- reduction process eventually to investigate the mechanism for sea water – fresh water interaction and sea water intrusion (Yim et al., 1992; Mao et al., 2006, Xia et al., 2007). Using SEEP/W a 2-Dimension model, even with low input dataset, it is easy to interpret the tide-aquifer interaction pattern (Hughes et al., 1998; Aryafar et al., 2009)

1.3 Strontium isotopes - a fine indicator to study sea water intrusion

Among the various isotopes available to study sea water intrusion or ground water-surface water interaction, strontium isotopes has been widely used since few decades. The reason behind this is the abundance of ^{87}Sr, daughter of ^{87}Rb, is directly linked to the geochemistry of potassium, for which Rb^{+} will readily substitute, thus groundwater that have geochemically evolved in differing geological terrains will have contrasting strontium isotope ratios. In this way, different groundwater bodies can be distinguished, mixing relationships examined, and allochthonous versus autochthonous sources of salinity can be identified (Bullen et al., 1998). For waters developed in multi-mineralic rocks or soils, $^{87}Sr/^{86}Sr$ in any water parcel usually represents a mixture of Sr from several sources, and thus the exact contributions from individual minerals are difficult to determine with the Sr isotopic data alone. However, when considered in conjunction with water chemistry, the Sr isotopes provide a powerful tool for distinguishing among solute sources (Faure and Mensing, 2005). Since its approximate value in modern oceanic seawater is 0.7092, it is a very sensitive parameter to check seawater influence on groundwater even at primary stage (Frost et al., 2004).

1.4 Importance of study of tidal effect on coastal groundwater

Coastal aquifers are unique because of tidal effects which causes complicated ground water flow and contaminant transport phenomena (Kim et al., 2005). Strong response of groundwater characteristics to the intertidal phase are of great interest to a range of researchers examining physical, chemical and biological processes in coastal systems. Numerous previous researches have already proved the importance of studying tide-induced groundwater flow in coastal aquifer to decipher problems arising in different sectors (e.g. hydrogeology, ecology and environment) of coastal areas (Grant, 1948; Harbison, 1986; Weisman et al., 1995; Li et al., 1997; Gibbes et al., 2007). Time series analysis of tidal effect on coastal ground water gave an in-depth sight for correlation between sea tides and ground water quality (specially pH, EC and Piezometric level) as well as it avoids the need of pump testing to determine aquifer characteristics (Carr et al., 1969; Harbison, 1986; Erskine, 1992; Li et al., 1997; Kim et al., 2005; Kim et al., 2006; Robinson et al., 2007; Jha et al., 2008; Shalev et al., 2009). Abdullah et al., (1997) investigate change in water quality (pH, temperature, electrical conductivity by diurnal tides in Sipadan Island, Malaysia and found that diurnal variation in pH with respect to tidal level is negligible or very less and it seems preceding the tidal fluctuation pattern. The reason because natural water normally contains dissolved carbon dioxide and bicarbonate ions, which make a buffer system with carbon dioxide and hence small changes in pH value of GW occurs with tides. The coastal GW table fluctuates in response to high frequency sea level oscillation due to wave run-up. These high frequency water table fluctuations significantly affect the infiltration/exfiltration as well as controls oxidation-reduction processes. (Li et al.,

1997). It was stated that for unconfined aquifers, large storage coefficient (high porosity of the aquifer) which is several orders of magnitude larger than that of confined aquifer, pressure (tidal) waves tend to be damped and hence time lag is higher and tidal efficiency is lower. However for confined aquifer, because of low porosity and storage coefficient, damping of tidal wave is relatively lower resulting into shorter time lag and larger tidal efficiency (Fakir et al., 2003). GW level responds directly with the change in tidal level because of transportation mechanism by the tide is advection. However, EC level responds with tidal phase by the combined effect of advection and diffusion. Also, for above two conditions, tidal level must cross the minimum barrier level so that big difference in hydraulic pressure created between SW and FW and trigger the flow of SW towards the land (Kim et al., 2005). Turner (1993) stated that existence of capillary fringe above water table in coastal aquifer helps for inland propagation of tidal waves. Despite a lot of attention on tide-aquifer interaction issues in recent time, the effect of tides on water quality at ionic level and its relation with the geological signature of the aquifer is still sparse throughout the world.

Importance of numerical simulation based on tidal effect

As mentioned above social and economic development in coastal areas are the main factors causes various hydrogeological, engineering, ecological and environmental problems such as seawater intrusion, stability of coastal engineering structures, beach dewatering for construction purposes, and coastal ecological environment deterioration. A great deal of previous literature review show that research work of the coastal groundwater flow induced by sea tides plays an important and active role in solving

these problems. For example, Gregg (1966) investigated relation of tidal efficiency with the distance from coast (or influencing tidal body) and with the well depth. Carr (1969) investigated the tide-related salt-water intrusion for different aquifers. Lanyon et al. (1982) provided a comprehensive description of water table changes over time for particular points along beach profiles and related those changes to tidal fluctuation and variation in beach-face configuration. Erskine (1992) described the tidal aquifer interaction methodology can be efficiently applied to determine aquifer characteristics and avoids the necessity of pumping test. Chan et al. (1992) used a one-dimensional numerical model to simulate the migration process of a contaminant plume within tidally influenced aquifers. Marquis et al. (1994) assessed groundwater flow and chemical transport in a tidally influenced aquifer using geostatistical filtering and hydrocarbon fingerprinting. Farrell (1994) analyzed groundwater flow through leaky marine retaining structures using analytical and numerical methods.

The coastal groundwater table fluctuates in response to high frequency sea level oscillation due to wave run-up. These high frequency water table fluctuations significantly affect the infiltration/exfiltration as well as controls oxidation-reduction processes (Li et al., 1997). It was found that tide can significantly influence the temporal and spatial patterns of groundwater discharge as well as the salt concentration in the near-shore groundwater for unconfined coastal aquifers (Robinson et al., 1998; Robinson et al., 1999). Estimations of the submarine groundwater discharge (SGD) and net inland recharge in coastal areas are of great importance for the correct assessment of the role of groundwater in the global water cycle (Moore, 1996; Church, 1996; Younger, 1996). The distribution of subaerial and submarine discharge is most dependent on the

beach characteristics of the slope, hydraulic conductivity magnitude and distribution, and tidal range (Turner, 1993). In most cases of the sloping beach, the intertidal zone is subjected to salt water flooding and infiltration from the rising tide, which is then a substantial component of the ground water discharge (Urish et al., 2004).

Li et al. (1999) proposed a conceptual model, which shows that SGD consists of the net groundwater discharge, the outflow due to wave-setup induced groundwater circulation, and that due to tidally driven oscillating flow. They also applied their model in field of the South Atlantic Bight and concluded that the outflow due to tidally driven oscillating flow amounts to 37% of the total SGD, implying the importance of the tidal effects in estimating SGD.

Different scenarios taken during analytical studies of tide-induced groundwater flow

1. **One-Dimension problem domain**

The simplest case of tide-induced groundwater flow is the Jacob's (1950) solution that considered the vertical beach, straight coastline and one-dimensional flow in a coastal confined aquifer. The solution indicates that the amplitude of the tide-induced groundwater head fluctuation decreases exponentially with the distance from the coast, whereas the time lag increases linearly with the distance. The attenuation speed decreases with the diffusivity of the aquifer (i.e., the ratio of the transmissivity to the storativity) and increases with the angular velocity of the sinusoidal sea tide.

2. **L-Shaped coastal aquifers**

In the case that the tidal water is in an estuary or a bay, the tidal level fluctuation in the sea will attenuate along the estuary or the bay (e.g., Fisher, 1986; Sun, 1997; Li et al., 2001b; Cheng and Chen, 2001; Li et al., 2002) and the tidal loading boundary condition along the estuary coastline becomes two-dimensional. Li et al. (2002) and Li et al. (2002b) obtained a periodic analytical solution independent of initial condition and generalized the single L-shaped aquifer into an L-shaped coastal leaky aquifer system. Their improvements include the computationally efficient solution form, simple approximate solution as well as consideration of the storativity of the semi-permeable layer.

3. Confined aquifers extending under tidal water

In reality, the roof of a coastal aquifer, i.e., the overlying confining layer, may extend for a certain distance under the tidal water. It is of great importance to estimate the roof length since it represents a key boundary condition in the coastal groundwater flow model for seawater intrusion studies or coastal groundwater resources evaluation. Here many studies have been done to derive a solution to describe the groundwater fluctuation in the aquifer considering the extreme assumption for infinite roof length (van der Kamp, 1972; Maas and De Lange, 1987; Liu, 1996). The unconfined aquifer terminates at the coastline, while the semi permeable layer extends under the sea and its offshore part forms the roof of the confined aquifer. The water level fluctuations in the inland part of the confined aquifer decrease significantly with the roof-length for small roof-lengths and become insensitive to change of roof length for those roof-lengths greater than a certain threshold. The effects of leakage from the offshore and inland portions of the confining unit are different. The leakage from the offshore portion tends

to increase the fluctuations while that from the inland portion to decrease. The fluctuations increase as the tidal efficiency increases but it is important only when the roof-length is great and leakage is small.

4. Three-layered coastal aquifer system

Here during construction of aquifer domain, inclusion of semipermeable layer(s) was also considered (van der Kamp, 1973; Li et al, 1991; Jiao et al, 1999). Jiao et al (1999) derived an analytical solution to study the groundwater head fluctuations in the confined aquifer of a coastal aquifer-aquitard-aquifer system. They ignored the elastic storage of the leaky layer (aquitard) and the water table fluctuation in the shallow unconfined aquifer is negligible. This assumption may not be valid when the leakage of the leaky aquifer system is great (Volker and Zhang, 2001). However, Jiao and Tang (2001) examined the leaky aquifer systems reported in literature and found that the leakage is usually very small for a real leaky aquifer system and there is no problem to use the assumption. Li et al. (2001a) used a perturbation method to investigate the tidal wave interference between the unconfined and confined aquifers, but they ignored the effects of the elastic storage of the leaky layer. Also ignoring the effects of the elastic storage of the leaky layer, Jeng et al. (2002) presented an analytical solution to describe the tidal wave propagation in the unconfined and confined aquifers separated by a thin, no storativity leaky layer. It is found that the leaky layer's storativity behaves as a buffer to the tidal wave interference between the two aquifers. The buffer capacity increases with the leaky layer's thickness, specific storage, and decreases with the leaky layer's vertical permeability. Great buffer capacity can result in negligible tidal wave interference between the upper and lower aquifers so that the solution can be simplified

significantly. The analytical solution indicates that both storativity and leakage of the semi-permeable layer play an important role in the groundwater head fluctuation in the confined aquifer.

Enhancing effect of the sea tide on the mean water table of a coastal unconfined aquifer

Due to the water table-dependent transmissivity of an unconfined aquifer, the sea tides has an enhancing effect on the mean water table even for a vertical beach and in the absence of net inland recharge. This nonlinear effect has been studied by many researchers under the assumptions that the coastal unconfined aquifer is isotropic, homogeneous and the tide comprises only one sinusoidal component (Philip, 1973; Knight, 1981; Nielsen, 1990; Li and Jiao, 2003a).

An important finding was that the water table-enhancing effect is independent of the vertical permeability and can be reinforced if the horizontal permeability decreases with depth. Seawater is pumped into the unconfined aquifer by the sea tide and divided into two parts. One part returns to the sea driven by the mean water table gradient. The rest part leaks into the confined aquifer through the semipermeable layer, and returns to the sea through the confined aquifer driven by the mean head gradient. The total discharge through the confined aquifer is significant for coastal leaky aquifer system with typical parameter values. This seawater–groundwater circulation has impacts on better understanding of submarine groundwater discharge and exchange of various chemicals such as nutrients and contaminants in coastal areas. If the observed mean water levels in coastal areas are used for estimating the net inland recharge, the

enhancing processes of sea tide on the mean groundwater levels should be taken into account. Otherwise, the net inland recharge will be overestimated.

There are still a great deal of new situations to be investigated, for example, the effects of the elastic storage of a semipermeable roof of a confined aquifer extending under tidal water, the effect of the sloping beach in a coastal aquifer or aquifer system, the enhancing effect of the sea tide on the water table in a generic unconfined aquifer with sloping beach. All of them are meaningful task full of challenge.

1.5 Previous studies in Saijo plain, Japan

Despite a lot of attention on tide-aquifer interaction issues in recent time, the effect of tides on water quality at ionic level and its relation with the geological signature of the aquifer is still sparse throughout the world. In terms of coastal aquifer, water locked country like Japan is one of the most important regions to study the SW-GW interaction for its sustainable future ground water use. In case of Saijo plain, Western Japan, Kurihara (1972) described that geological structure in Saijo plain is very complex because of subsidence took place in alluvial fan of Kamo River. In northern coastal area of the Saijo plain, sea water intrusion into groundwater is caused by a decline water level (Tanikawa, 1998; Saijo city, 2008). Nakamura (2005) stated that in Saijo plain, along the sea water and fresh water interface groundwater is of stagnant flow and sea water of very long residence time indicates very low proportion of direct mixing. On the other hand, Saijo plain is known for its plenty of good quality ground water in western Japan but despite its importance little is known about the natural

phenomena that govern the chemical composition of groundwater. Hence this study attempts to deepen its ideas on the items where limited information exists.

1.6 Objectives of the present study

To make a clear understanding about factors controlling the chemical signature of groundwater in coastal area of Saijo plain, objectives of this study are listed below:

1. To clarify the significance of tidal influence on sea water/ fresh water mixing using array of environmental isotopes ($^{87}Sr/^{86}Sr$, $\delta^{18}O$ and $\delta^{2}H$) and chemical tracers (eg. Na^{+}, Cl^{-} , HCO_3^{-} and heavy metals).
   a) Evaluate hydrochemistry at spatial-temporal scale in northern coastal area in Saijo Plain.
   b) Comparative study of tidal effect on groundwater quality for different aquifer types.
   c) To estimating phreatic aquifer parameters by the tidal response technique.
2. Numerical simulation for the validation of tide- aquifer interaction through investigation of tidal effect on dynamics of the submarine groundwater discharge (SGD).

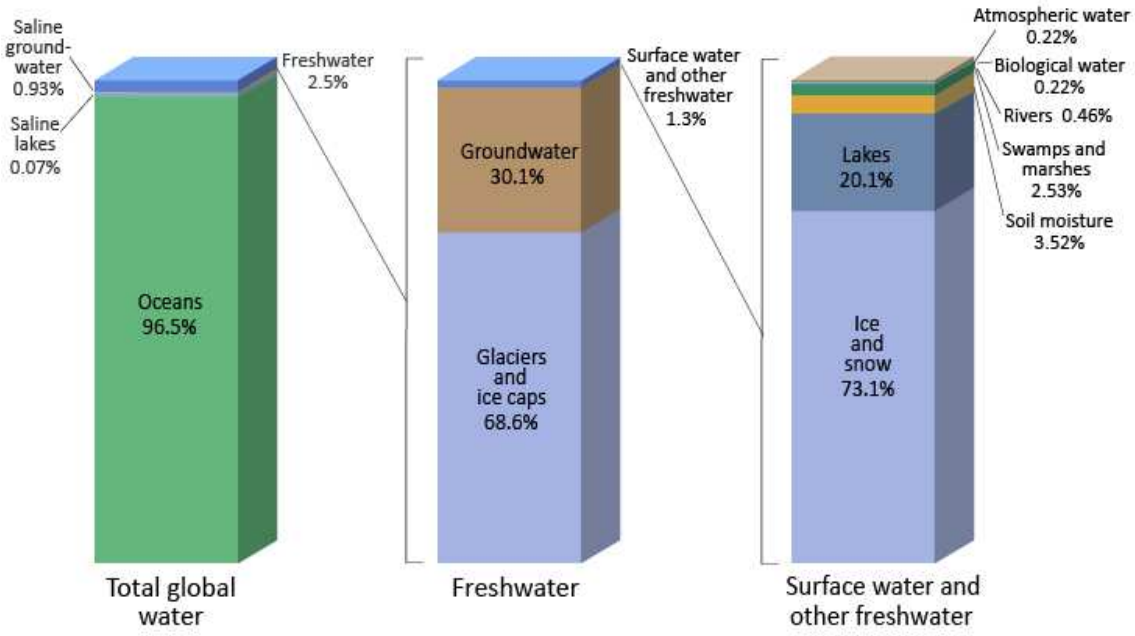

Fig. 1.1 Distribution patterns of water resources over the planet earth (Shiklomanov, 1993)

Table 1.1 Amount estimates of global water distribution in different sectors (USGS, 2011)

Water Source	Water Volume (in Km^3)	Percent of Fresh Water	Percent of Total Water
Oceans, Seas & Bays	1,338,000,000	--	96.5
Ice caps, Glaciers & Permanent Snow	24,064,000	68.6	1.74
Ground water	23,400,000	--	1.7
Fresh	10,530,000	30.1	0.76
Saline	12,870,000	--	0.93
Soil Moisture	16,500	0.05	0.001
Ground Ice & Permafrost	300,000	0.86	0.022
Lakes	176,400	--	0.013
Fresh	91,000	0.26	0.007
Saline	85,400	--	0.007
Atmosphere	12,900	0.04	0.001
Swamp Water	11,470	0.03	0.0008
Rivers	2,120	0.006	0.0002
Biological Water	1,120	0.003	0.0001

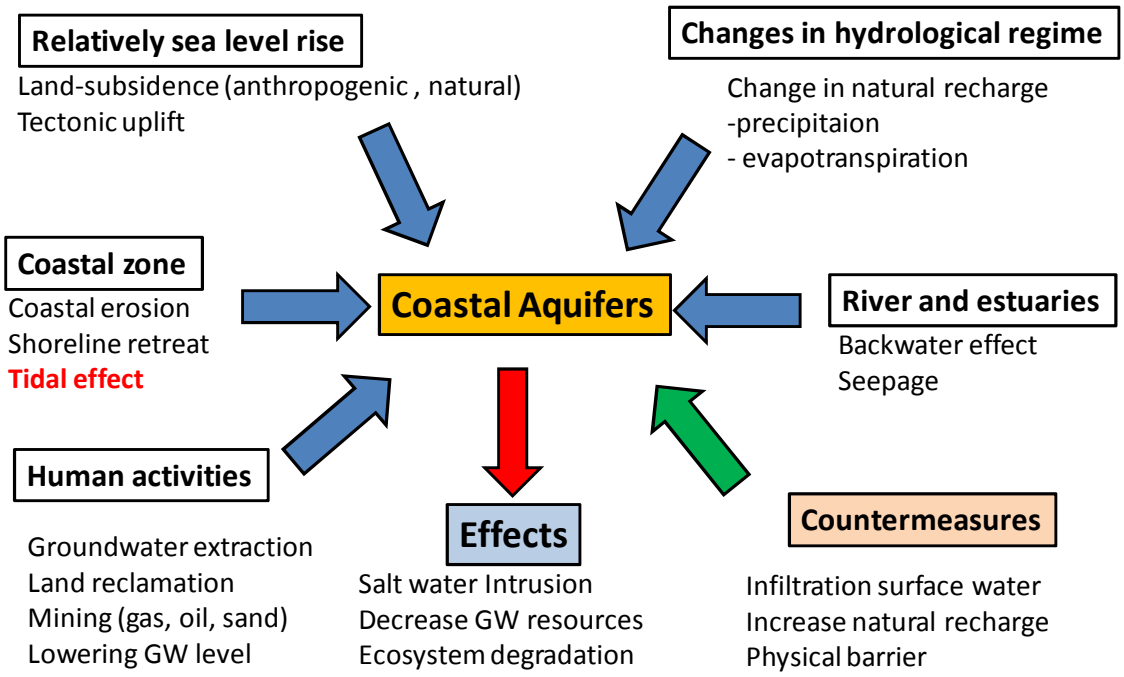

Fig. 1.2 Factors affecting fresh water/groundwater resources at coastal aquifers, list of major effects and countermeasures to restore the quality/quantity

Chapter 2

Study Area

2.1 Topography and geology

Saijo city, known as the water capital of the Ehime prefecture located in Shikoku Island, Western Japan (Fig. 2.1). Topographic gradient is huge within a small stretch of area. Whole area is divided into the eastern Saijo plain and the western Shuso plain respectively, each one of which is composed of sediments of Pliocene to Quaternary age (Fig. 2.2). Average thickness of both the plain is approximately one km. Saijo plain which is focus of this research work is located in between latitude 33.85 to 33.99 ºN and longitude 133.00 to 133.26 ºE. Geographically, it is bounded on the south by the Ishizuchi mountainous ranges (1982 masl), the highest peak in western Japan, on the north by the Seto Inland Sea, on the west by Shuso plain and on the east by Toyo region. Saijo plain belong to Setouchi climate, a temperate climate with a relatively small amount of mean annual precipitation (1433 mm). The mean annual temperature is approximately 15°C.

Geological map of the area is shown in Fig. 2.2. It can be found that mountainous area is primarily composed of Sambagawa metamorphic rocks (i.e. basic schist and conglomerate) (Banno and Sakai, 1989). North and Western part of the area is dominated by Ryoke granitic rocks and the Izumi Group (gravelly sediment) (Kubota and Takeshita, 2008), both of which are of Cretaceous age (Nakano et al., 2008). Mineralogically mountainous part is dominated by Green schist, Black schist, Conglomerate, sand Stone, Shale, Tuffaceous rocks etc.; where as plain area is mainly

dominated by Clay, sand, Gravel, Gravely Sediment, Granitoid rocks etc. There are many active faults distributed in the area along east to west direction viz. Ishizuchi fault, Okamura fault etc. The boundary of Ishizuchi mountainous area and plain are along an active fault of median tectonic line fault system (Mizuno et al., 1993).The Komatsu fault is one which is considered to be occurring in the plain, physically mean that most probably it occur in older rock of hard nature but also affecting the overlying sediment. Alluvial fans are developed around the rivers coming from mountains. Spring water discharges around the end of alluvial fans. The groundwater occurs in Pliocene sandy sediments and forms extensive unconfined to leaky confined aquifers, i.e. the area has both confined and unconfined aquifers. There is artesian water zone in the central part of the Saijo plain.

Lithological cross section of the plain is shown in Fig. 2.3. It was found that unconfined aquifers mainly lies within a depth of less than 10 meter below ground level (bgl) and confined aquifers mainly lies after a depth of 15 meter bgl. However this classification can't be considered perfect for each point in the study area because of non uniform nature of aquitard/aquiclude layer (separating unconfined and confined aquifers) especially in eastern part of the study area and presence of the faults all along the plain.

2.2 Land Use/Land Cover (LU-LC) pattern

LU-LC map of the Saijo city is shown is Fig. 2.4. It is found that coastal region is mainly occupied by manufacturing plants and other built ups while plain area is mainly occupied by agriculture fields/ residential areas. As a whole Saijo city is mainly

categorized into nine major land use categories viz. Paddy field, other agricultural area, forest, waste land, residential/industrial area, arterial traffic area, river/lake, golf course and other areas.

2.3 Hydrogeological setting

Whole area of Saijo city is intersected by numerous streams like Daimyojin, Nakayama, Kamo and Uzui etc., however Saijo plain is mainly inhabited with Kamo and Uzui rivers. Kumasaka (2010) stated that unconfined groundwater of Saijo alluvial fan gets recharged mainly from the Kamo and Uzui rivers where as confined groundwater is estimated to be mainly recharged at an altitude of approximately 1000 m in Ishizuchi mountainous regions.

Classification for groundwater resources

Groundwater resources in the Saijo plain can be divided into three zones spreading from southern mountains to northern coast consisting spring, artesian and coastal groundwater zones respectively. It is supposed that artesian and coastal zone is separated by the Komatsu fault.

The artesian water zone also called ‘Uchinuki’ in Japanese lies in the central part of the Saijo plain. Uchinuki which literally means self-pumping water permeates through the surrounding land and is widely distributed throughout the old Saijo City. It is found that there are approximately 2000 artesian flow wells in the Saijo plain. Amount of water flows through Uchinuki is approximately 90,000 Cubic meters a day, which is commonly used as water for living, agricultural and industrial use, taking advantage of its stability in temperature throughout the four seasons. The water obtained

through Uchinuki is selected as one of the 100 famous spring waters throughout Japan. Spring water discharges around the end of alluvial fans (Saijo City, 2008).

The groundwater in the Saijo plain is mainly recharged by the stream like Kamo and Uzui rivers. Except the flood period, the stream flow at the lower course of the river is not seen. It can be suggested that amount of current flow for Kamo river (728 Cubic kilometers per sec) is much greater than that of Uzui river (340 Cubic kilometers per sec) which results into relatively higher oxidizing condition near the western site of the plain in compare to that of the eastern site.

2.4 Importance to select Saijo plain, Japan as a study area

Presence of good quality ground water, complex geological structure and fairly new point scale ground water salinization triggers many researcher groups to conduct several studies at Saijo plain, Western Japan. Kurihara (1972) described that geological structure in Saijo plain is very complex because of subsidence took place in alluvial fan of Kamo River. Nakamura (2005) stated that in Saijo plain, along the sea water and fresh water interface, groundwater is of stagnant flow and sea water of very long residence time indicates very low proportion of direct mixing. Nakano et al. (2008) reported that groundwater in this area shows a different quality between the eastern Saijo plain and western Shuso one, indicating that each groundwater constitutes an independent aquifer system. In northern coastal area of the Saijo plain, sea water intrusion into groundwater is caused by a decline water level (Tanikawa, 1998; Saijo city, 2008). High conc. of $^{87}Sr/^{86}Sr$ and $\delta^{34}S$ was also observed in northern coastal groundwater of Saijo plain (Nakano et al., 2008). With the integrated use of CFC-11,

chemical constituents and stable isotopic compositions, Kumasaka (2010) found that in the Saijo plain, unconfined water is mainly recharged by Kamo river and local flow with short residence times, whereas confined water is recharged at the altitude of approximately 1000 m in Ishizuchi mountainous regions, and deep flow with long residence times contributes to the unconfined groundwater. Also, there is an interaction between unconfined and confined aquifer in the eastern part of the artesian zone. Hachani (2011) applied Self-potential (SP) measurements to investigate groundwater flow in the Saijo Plain, and found that, the general trend of SP value changes from negative to positive when the transect was drawn from the mountain to the coast which is mainly because of natural groundwater flow course. Also, high correlation found between distributions of SP and Piezometric level in case of confined aquifer.

From above literature review, still very little is known about the natural phenomena that govern the chemical composition of groundwater. This study attempts to deepen its ideas on the items where limited information exists. The prime objective of this study is to elucidate interaction between sea water and ground water in order to know the factors controlling the ground water quality. Considering the poor understanding about the sea water- fresh water (SW-FW) interaction pattern at dynamic hydro-geological boundary of coastal aquifers, this work strives to study tidal effect on ground water quality for different aquifers as well as to estimate aquifer parameters by tidal response method. No study about tidal effect on water quality at ionic level and presence of mixed aquifer types within a small area makes Saijo plain an ideal place to choose it as a study area.

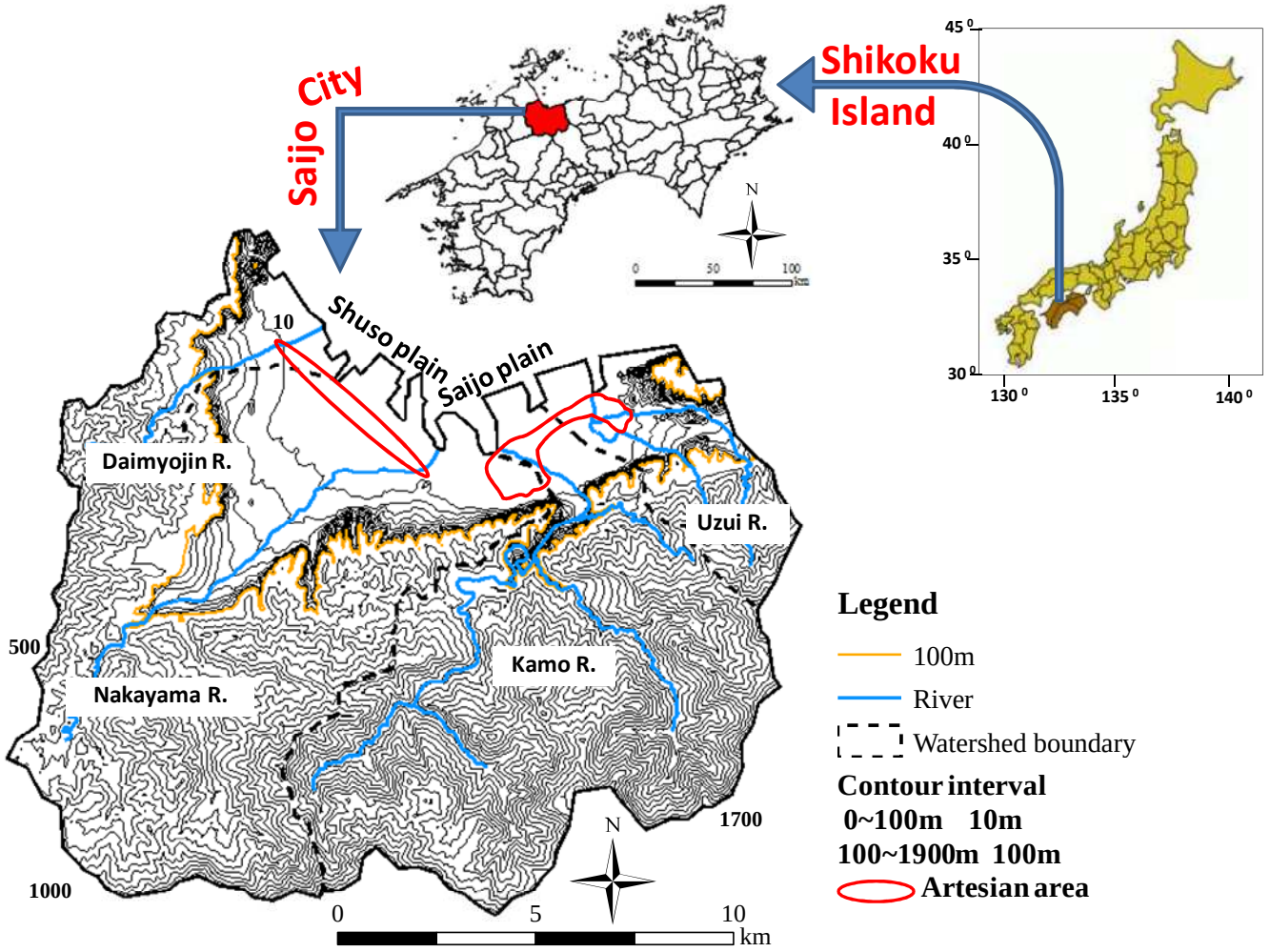

Fig. 2.1 Topographical map of the Saijo plain, Japan

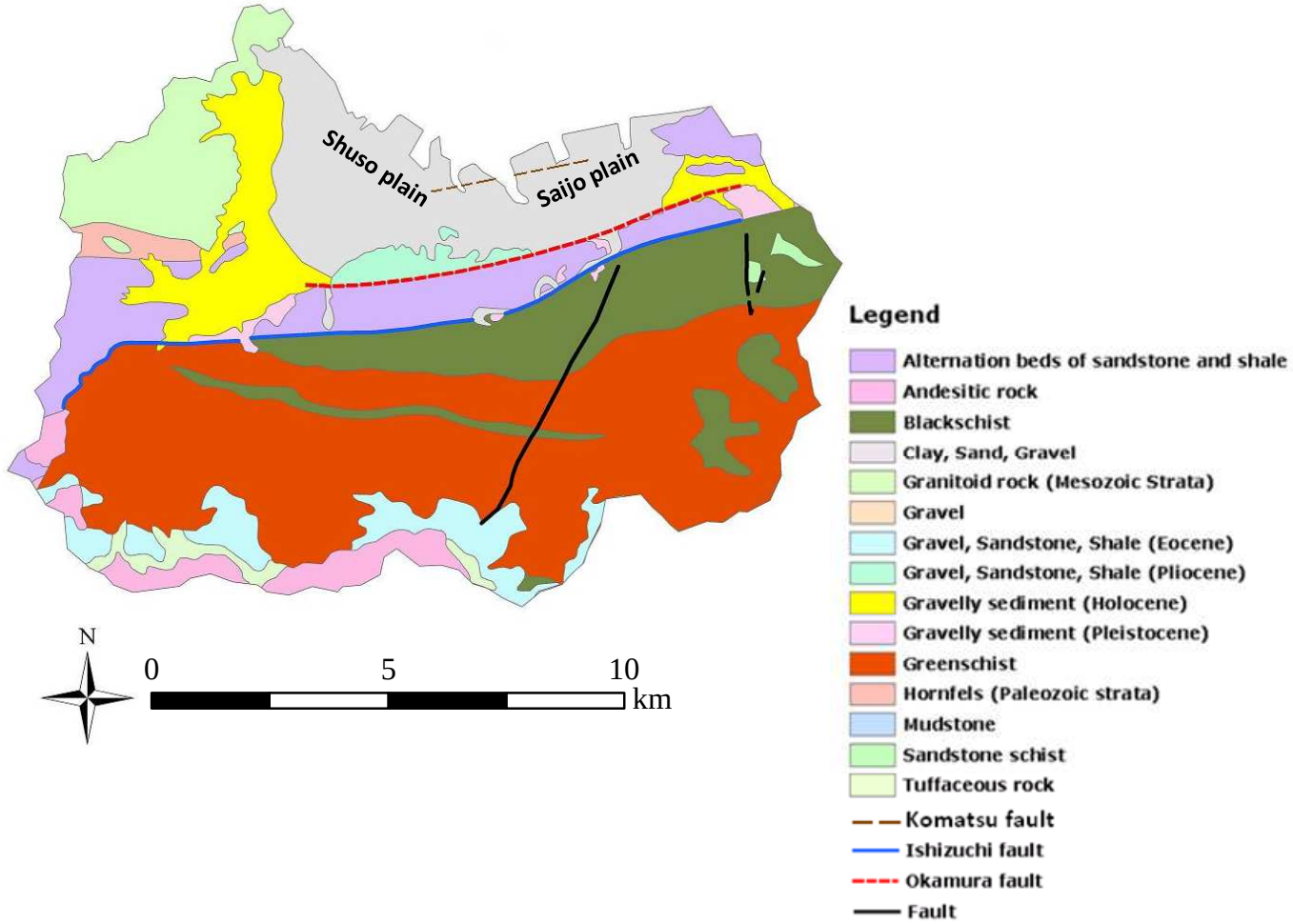

Fig. 2.2 Geological map of the Saijo plain, Japan

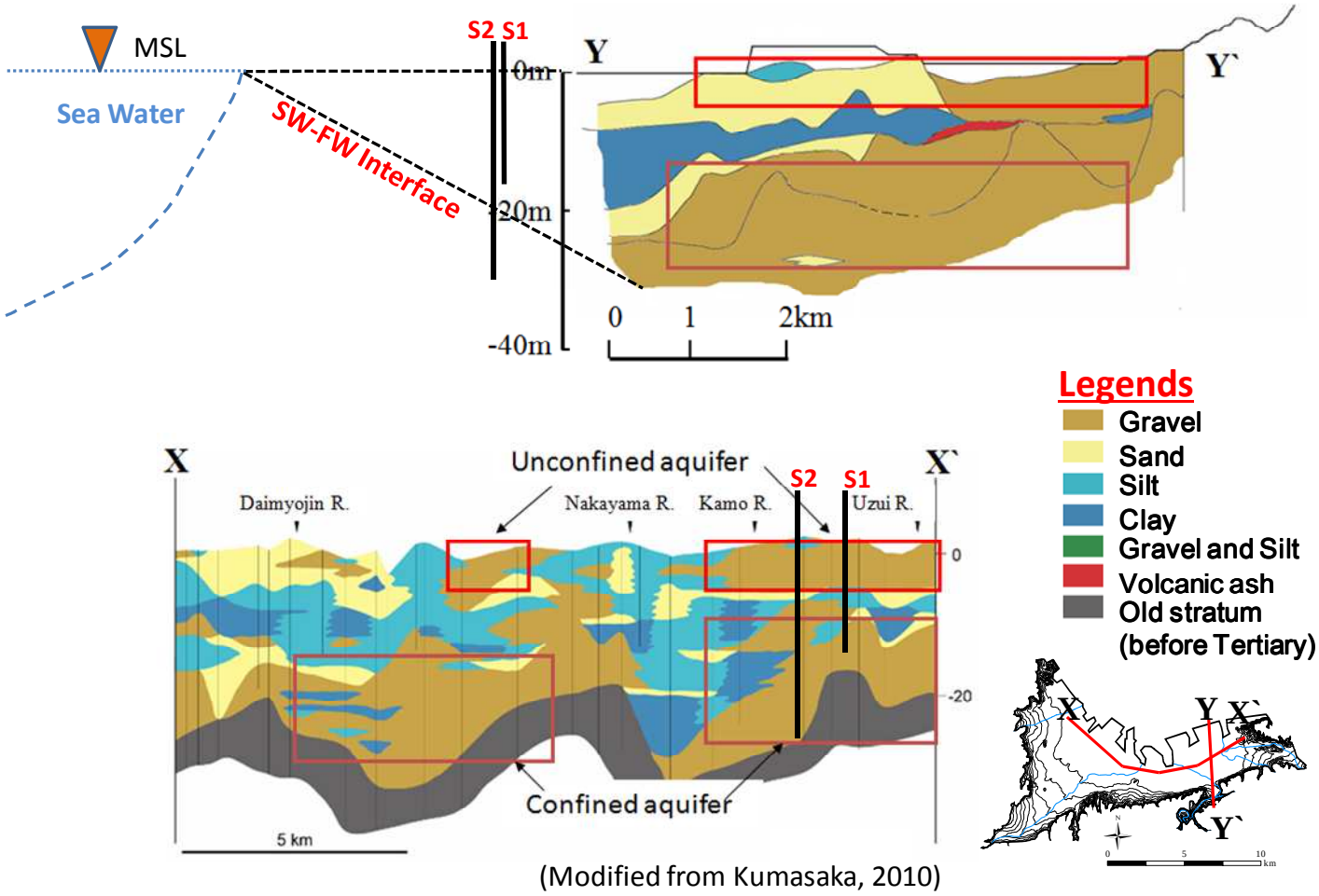

Fig. 2.3 Lithological cross section of the plain showing the location of monitoring wells considered for tidal effect observation

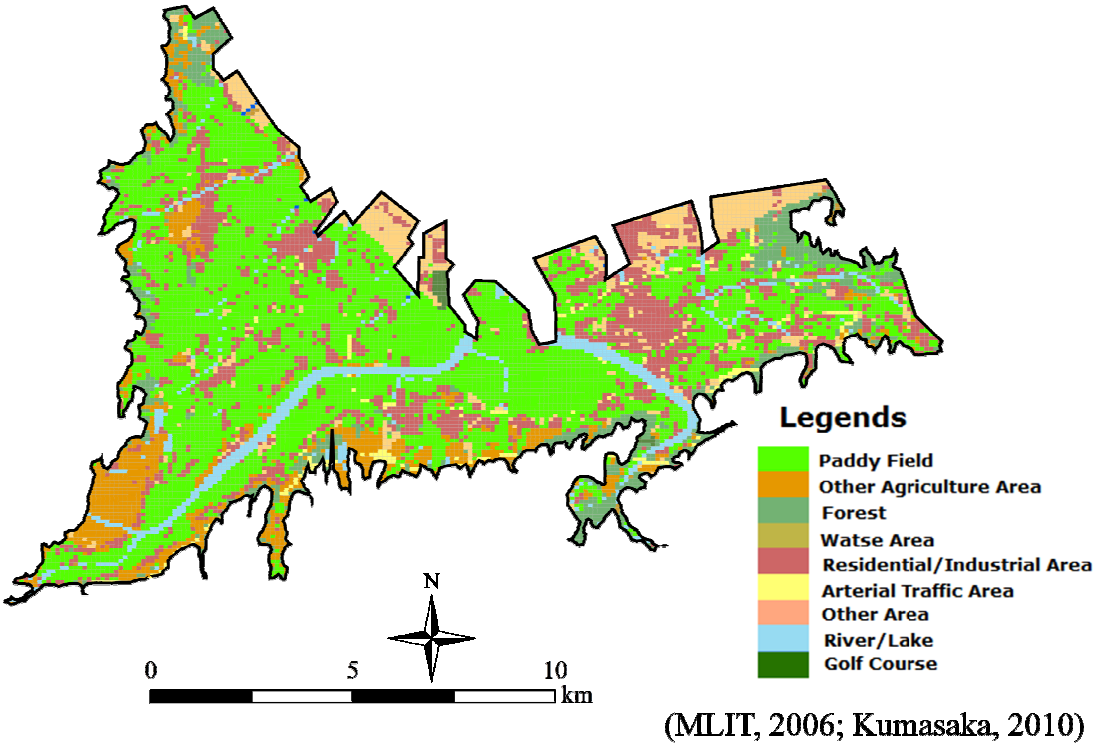

Fig. 2.4 Land Use/Land Cover map of the Saijo plain, Japan

Chapter 3

Methodology

Flow chart for the research methodology is shown in Fig.3.1. It mainly includes two parts geochemical characterization and numerical simulation. Geochemical characterization parts include field observation, solute concentration analysis and interpretation of the results.

3.1 Field observation

As a preliminary observation, seven sampling wells were selected from northern coastal area of Saijo plain in such a way that they represent varying topography of the northern coastal area of Saijo plain (Fig. 3.2). Approximate screen depth for S1 and S2 are 15 and 24 meter below ground level respectively. Lithological cross section at points near to both S1 and S2 shown in Fig. 3.3, which indicates the difference in aquifer types as screen for S1 and S2 belongs to unconfined and confined aquifers respectively. Based on above two characteristics, these two sampling locations were selected to observe effect of diurnal tidal fluctuation. Ground water samples were collected during three field campaigns during July and October, 2010 and June, 2011 with different objectives shown in Fig. 3.4. First campaign was conducted to get an idea

about the behavior of tidal effect on different aquifers. Second campaign was decided in period with relatively very low precipitation in order to see the effect of change in precipitation amount on the tidal response pattern. Final and third campaign was conducted to see the effect of location/geology/well depth on the response pattern and validation of the previous results undertaking an additional observation for monitoring well “S6” (with a screen depth of approximately 18 meter below ground level) located in vicinity of sample “S2” (Fig. 3.2). In the parallel seven ground water samples (taken for preliminary survey for the first time in July, 2010) were collected again during the field campaign of October, 2010 to observe the spatio-temporal variation in water chemistry at small coastal area of the Saijo plain, Japan.

During all three campaigns hourly tidal level data was procured from Hydrographic and Oceanographic Department, Japan. Ground water samples were collected from these different sites at hourly basis in a representative array of locations for over twenty four hour period. Piezometric level was measured (followed up with tidal fluctuation) through automatic recorder and water level dipper (Million Corp.) in case of S1 and S2 respectively (Fig. 3.4). For bore wells, collection and in-situ analysis was done after pumping out the water for 2–5 minutes. Electrical conductivity (EC) was measured using its probe (Yokogawa Model Number SC82) where as measurement of

water temperature and oxidation-reduction potential (ORP) was done using their respective probes (HORIBA Ltd. D-52) with a precision of 1%. The water samples were collected in pre-rinsed clean polyethylene bottles after getting filtered through 0.2-µm cellulose acetate disposable filter paper (Millipore). The collected groundwater samples were classified for cations and anions analysis.

3.2 Laboratory analysis

Following the collection, water samples brought back to Research Institute for Humanity and nature (RIHN), Kyoto and laboratory in Graduate School of Life and Environmental Science, University of Tsukuba, Tsukuba City for the chemical analysis. The concentration of HCO_3^- was determined by acid titration (using Metrohm Multi-Dosimat). Other major anions like Cl^-, NO_3^-, SO_4^{2-}, Br^- and PO_4^{3-} were analyzed by ion chromatograph (DIONEX ICS-90) with a detection limit of 10µg/L and an error percentage of less than 2% using duplicates. Major cations and trace elements were determined with inductively coupled plasma-mass spectrometry (ICP-MS) (AGILENT-7500) with a detection limit of 0.1 parts per trillion (ppt) and precision of 1%. Before the analysis with ICP-MS, water samples were prepared with 1% HNO_3. The Sr isotopes were determined by using a Thermo Fisher mass spectrometer

(NEPTUNE) installed at the Research Institute for Humanity and Nature. Before the analysis with NEPTUNE, samples were prepared with column experiment, centrifugation and drying at hotplate for overnight (Fig. 3.5 & 3.6). The $^{87}Sr/^{86}Sr$ ratio of standard samples of NBS987 during this study was 0.710256 (2σmean: ±0.000005), and all measurements were normalized to a recommended 87Sr/86Sr ratio of 0.710250. Oxygen and hydrogen isotopes were analyzed by mass spectrometer (MODEL MAT 252, Thermo Finnigan Inc.) in university of Tsukuba. The results for both isotopes are expressed through deviation from the VSMOW (Vienna Standard Mean Ocean Water) standard using the δ-scale according to the equation and unit is per mil using equation (3.1).

$$\delta‰ = \left[\frac{R_{Sample} - R_{VSMOW}}{R_{VSMOW}}\right] \times 1000 \quad \text{.....(3.1)}$$

Where R is the isotopic ratio (i.e. $^{2}H/^{1}H$ and $^{18}O/^{16}O$) for the sample and standard. For the sample preparation before isotopic measurement, we adopted hydrogen gas equilibrium method using platinum catalyst with 6 hours for δD and carbon dioxide gas equilibrium method with 9 hours for $\delta^{18}O$. Analytical precisions of stable isotopes were better than 0.1‰ for $\delta^{18}O$, 1.0‰ for δD and ±0.000007 for $^{87}Sr/^{86}Sr$. Milli-Q water (Model Milli-Q Biocel) was used for all analysis. For major ions, analytical precision

was checked by normalized inorganic charge balance (NICB) (Kumar et al., 2010). This is defined as [(Tz+ - Tz-)/(Tz+ + Tz-)] and represents the fractional difference between total cations and anions.

Hourly tidal level data was procured from Hydrographic and Oceanographic Department, Saijo City, Japan for time series analysis. Piezometer readings taken over 24-hour period were compared with tidal level over the same period obtained from tidal information for Japan. Where the time of actual Piezometer reading was not coincident with the hourly tidal reading, then the appropriate tidal level was determined by interpolation method.

Relationship between Piezometric level and tidal height was determined by the tidal response technique which was further used for estimating phreatic aquifer parameters using Darcy's law. In order to understand the origin of trace metal mobilization, speciation calculations were performed using the program PHREEQC (Parkhurst and Appelo, 1999) and thermodynamic data compiled from databases of minteq.dat and llnl.dat. To support the result from hydrochemical characterization, a 2-Dimensional numerical model, SEEP/W (a product of Geo-Slope, 2007) was used to infer the time varying extent of the saturated and unsaturated regions of inter tidal

profile. For second part, numerical simulation has been done using SEEP/W (a product of Geo-Slope, 2007) to support the findings from hydrochemical analysis.

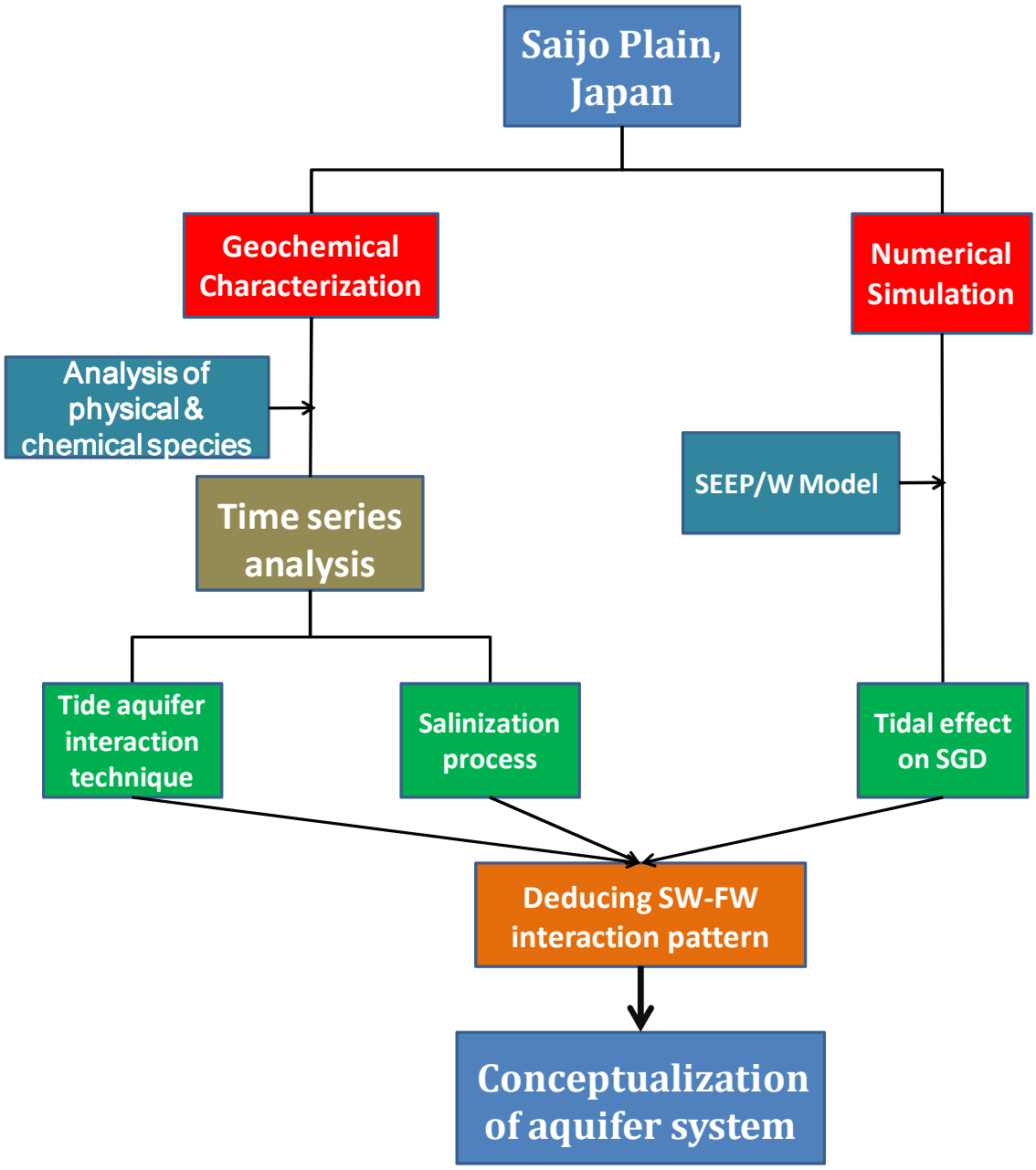

Fig.3.1 Flow chart showing the steps taken into consideration in this research

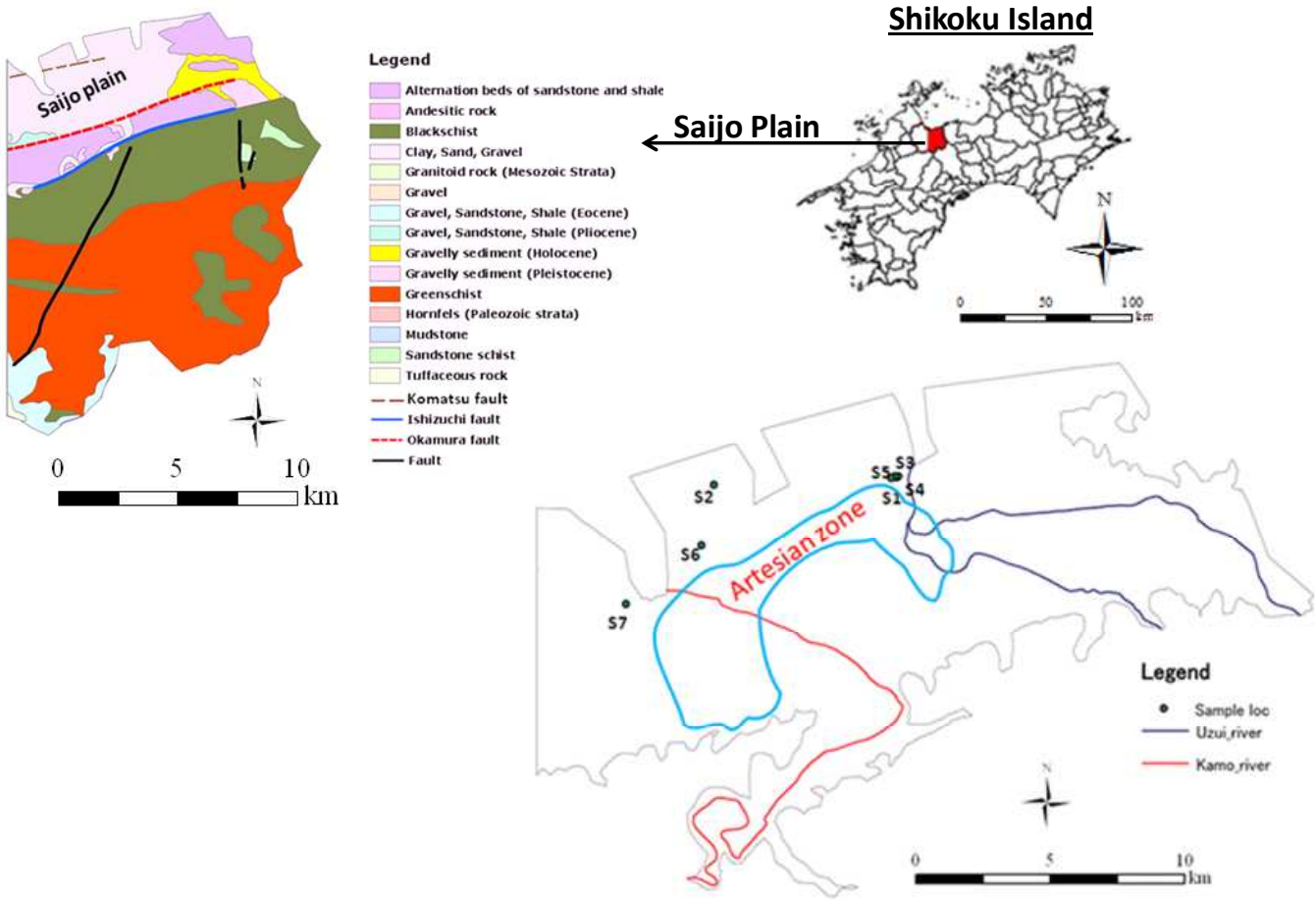

Fig. 3.2 Saijo plain map with ground water sampling locations

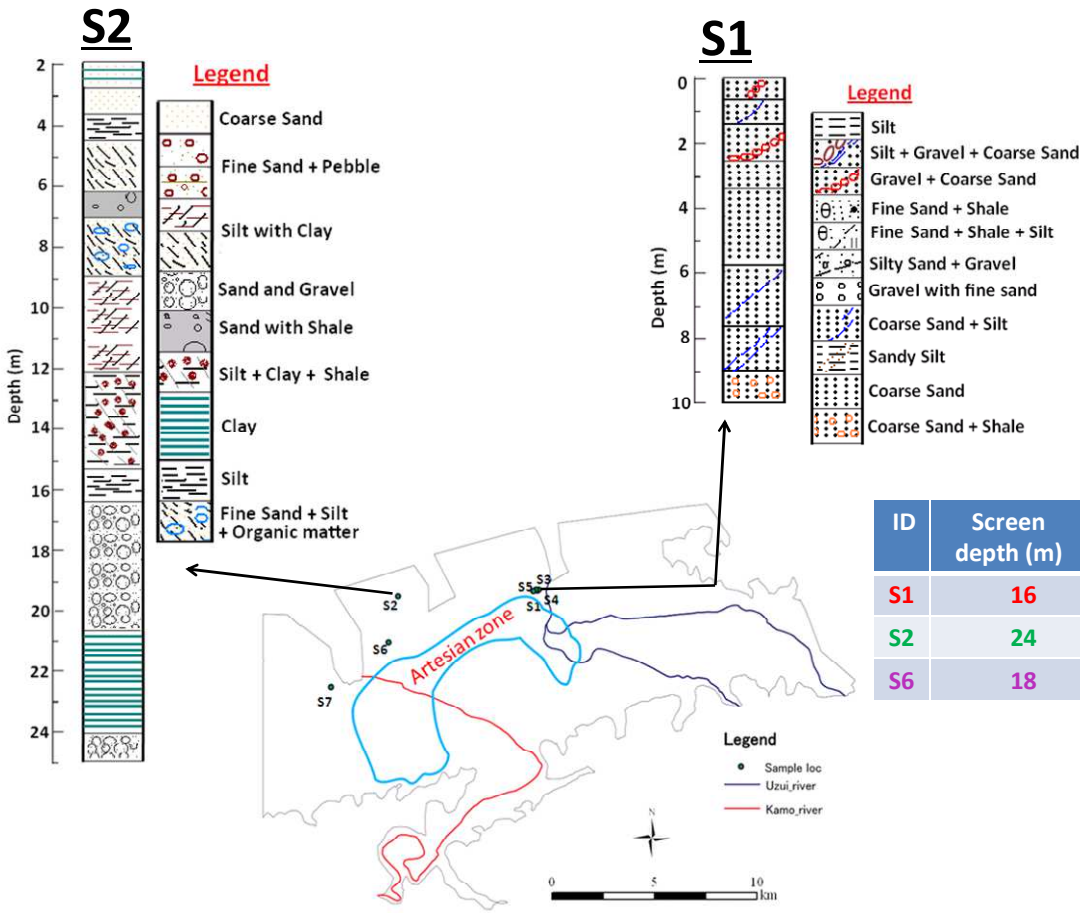

Fig. 3.3 Lithological cross section of the points near to the monitoring wells considered for tidal effect observation

Fig. 3.4 Location of Piezometric reading points (measurement done through automatic recorder and water level dipper respectively)

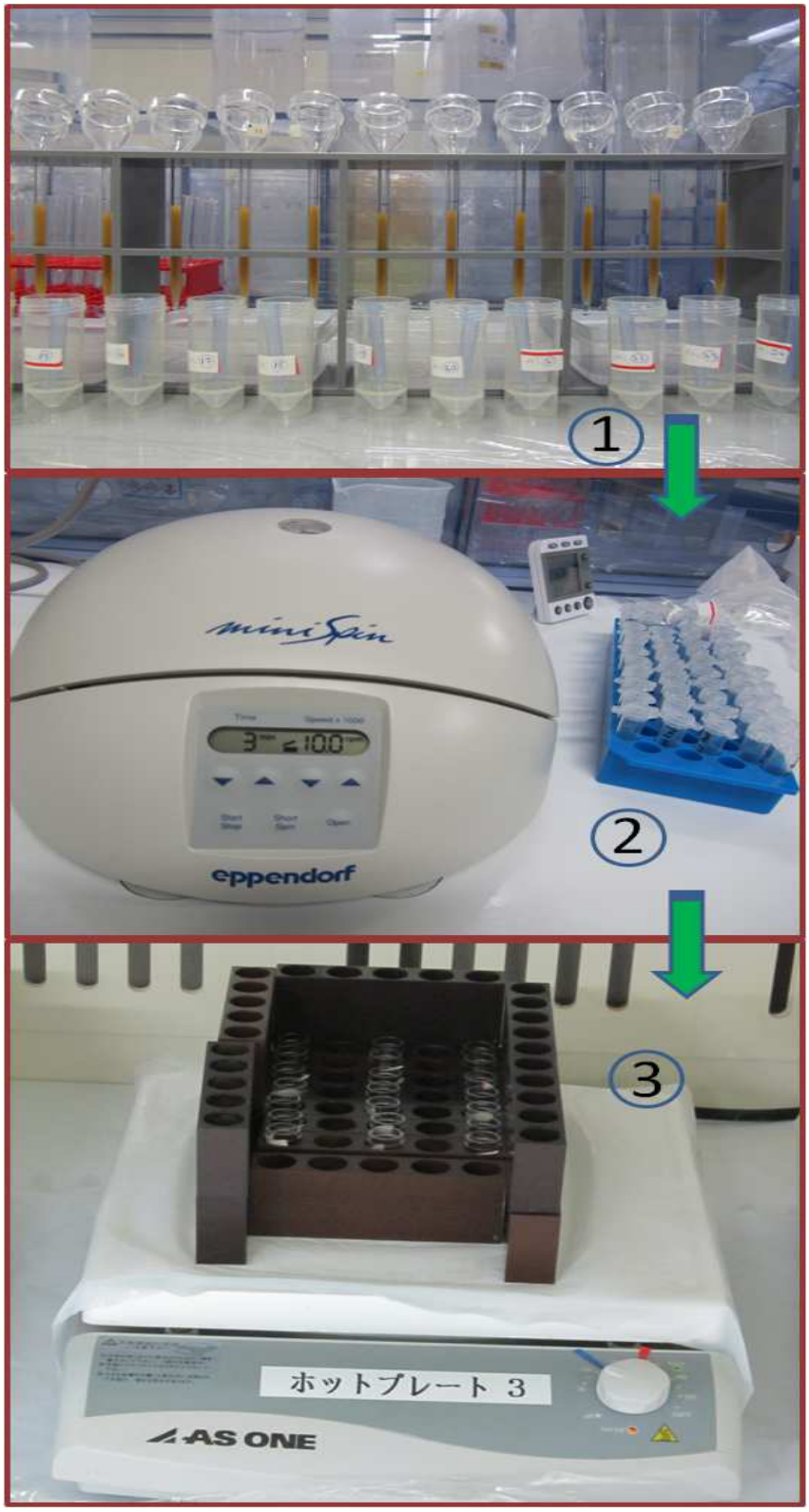

Fig. 3.5 Experiment setup used for strontium isotope analysis (1. Column experiment 2. Centrifugation, 3. Drying at hot plate for overnight)

Fig. 3.6 Thermo Fisher mass spectrometer (NEPTUNE) used for strontium isotopes analysis

Chapter 4

Results and Discussion

Whole section is divided into three parts:

1. Geochemical characterization of ground water at spatio temporal scale.
2. Effect of tidal fluctuation on ground water quality in case of different aquifers.
3. Conceptual diagram showing the tidal effect on groundwater quality for different aquifers in coastal zone.

Part - I

4.1 Geochemical characterization of ground water at spatio- temporal scale

4.1.1 General ground water chemistry

Fourteen water samples were collected from coastal area of Saijo plain during July and October, 2010. In general, chemical analysis result for observed charge balance for ground water samples was better than ±5% and they showed a charge imbalance mainly in favor of positive charge. Statistical summary (i.e. minimum, maximum, average and the standard deviation) of the analytical results for each water-quality characteristic analyzed is given in Table 4.1. Average value ionic trend for water samples was found as $Na^{+}>Ca^{2+}>Mg^{2+}>K^{+}$ and $Cl^{-}>HCO_3^{-}>SO_4^{2-}$ during both the sampling campaign. All the physico-chemical parameters for both surveys were within the highest desirable or maximum permissible limit set by WHO (World Health Organization), (2004), except Cl− at some sampling points with screen depth more than 25 meter. This shows that average high value of Cl- might be because of encounter of screen depth to the sea water – fresh water interface. In addition to that input from sewage effluents in the village areas also cannot be neglected. Higher average values of pH, EC and some of the ions in the second survey are the combined effect of the higher concentration of dissolved solids, local variation in soil type and amount of less precipitation (Fig. 4.1). Piper diagrams were used to analyze the water quality data in order to gain better insight into the hydro-geochemical processes operating in the

coastal aquifer of Saijo plain which resulted in the spatio-temporal variation in hydrochemistry (Fig. 4.2). From this diagram, water type found very heterogeneous in nature, which is an indicator of complex and patchy geological setting. Water samples during 1st survey mainly fallen in three categories i.e. Na-HCO_3, Mg-Cl and Na-Cl where as for 2nd survey, it has fallen in four categories i.e. Na-HCO_3, Mg-Cl, Na-Cl and Ca-Cl type. Two samples (i.e. S3 & S6) have shown temporal variation in water type. For 1st survey, S3 has shown Na-HCO_3 facies which might be the result of weathering of carbonaceous sandstone (consistent with its geological signature), while for 2nd survey it has shown Na-Cl facies which may be the results of precipitation of HCO_3 along with other cations or mixing of groundwater from different aquifers with variable Cl^- concentration. For sample S6, water quality has shown a seasonal shift from Na-Cl to Ca-Cl type, which may be as a result of mixing of groundwater from different aquifers. To distinguish the mechanism controlling water quality for different campaign, sodium - chloride equiline plot was drawn (Fig. 4.3), which suggests that geochemical process that controls water chemistry for both surveys in case of most samples is same except sample S3. For sample S3, water quality was being controlled by silicate weathering during 1st survey where as it was ion exchange process which mainly controls water quality in 2nd survey. The Ca versus $^{87}Sr/^{86}Sr$ plot yielded a nice correspondence in case of sample S3 and S6 (Fig. 4.4), which also supported the fact that for salinized water sample points, base exchange reactions add radiogenic Sr from the clay mineral.

To further confirm the ion exchange process, *BEX* (Base Exchange indices) was calculated for different surveys using following equation (4.1) (Stuyfzand, 2008):

$$BEX = Na + K + Mg - 1.0716\,Cl\ (all\ in\ meq/L) \ldots\ldots (4.1)$$

If value of *BEX* for any water sample is negative, it indicates state of salinization. However when value of *BEX* is positive but with increasing Cl concentration, if there is a decreasing trend of *BEX*, this can be considered as a preliminary sign of salinization with cation exchange process is one of the main mechanism responsible for it. For sample S3, concentration of Cl- were 0.18 and 1.42 meq/L in 1st and 2nd survey respectively where as corresponding *BEX* were 0.82 and 0.21 respectively, which firmly supports the nascent state of aquifer salinization (Stuyfzand, 2008).

A significant spatio-temporal variation was observed for heavy metals (like Fe and Mn) concentration (Fig. 4.5). To understand the spatial variation, study area was divided into reducing or oxidizing zone based on the distribution of ORP value for groundwater samples and amount of current flow in the nearby stream to the sampling site (Fig. 4.6). Kamo River is much greater than that of Uzui River which results into relatively higher oxidizing condition near the western site of the plain in compare to that of the eastern site. Temporal variation can be understood by relatively less amount of precipitation during 2nd survey in compare to that of 1st survey ultimately results in to adsorption of metals on soil matrix. To support the two different zones based on ORP, geological cross sections to represent bed rock outcrop from north to south ward passing through both reducing and oxidising zone (shown in Fig. 4.7). Along X-X` stretch there are two types of aquifers in the Saijo plain, a shallow unconfined aquifer (0-15 m) and a deep confined aquifer (>15 m) separated by a thick and continuous aquiclude. Along Y-Y` stretch, the clay layer is thin and patchy.

4.1.2 Isotopic chemistry

4.1.2.1 Hydrogen and oxygen isotopes

Relationship between $\delta^{18}O$ and δD values for Saijo groundwater samples is shown in Fig. 4.8. Value for $\delta^{18}O$ varies from (-9.13 to -8.81‰) and (-9.13 to -8.97 ‰) for 1st and 2nd survey respectively, whereas corresponding value for δD ranges from (-61.10 to -56.51‰) and (-62.12 to -58.42‰) respectively. This huge variation in isotopic composition of groundwater samples might be due to altitude effect as shown by Nakano et al. (2008). Most of the result points were plotted near the LMWL except fewer samples in 1st survey, which indicates that origin of ground water is meteoric in principle; however point away from the LMWL might be because of evaporation and exchange with rock minerals. Since the hydro-geological condition of Saijo plain allows quick infiltration into groundwater and no chance of much evaporation after raining, so isotopic composition points away from LMWL mainly favors exchange with rock minerals. Temporal variation for isotopic composition shows that water samples having lower values of both $\delta^{18}O$ and δD during 2nd survey in spite of lower rainfall in compare to 1st survey might be because of propagation of lower value of $\delta^{18}O$ and δD through moisture transport from the nearby areas.

4.1.2.2 Strontium isotopes

In order to understand ground water-sea water interface dynamics, spatio-temporal plot between 1/Sr versus $^{87}Sr/^{86}Sr$ ratio is shown in Fig. 4.9. Though value of $^{87}Sr/^{86}Sr$ varies from a narrow range of 0.7087-0.7090 for both sampling period but the large range of Sr content (i.e. (23.24-476.21µg/L) and (19.43-507.08µg/L) in 1st and 2nd

survey respectively) supported with high precision of $^{87}Sr/^{86}Sr$ analysis result were sufficient to depict the water-rock interaction pattern for different aquifer. For both survey, sample number 2 shown value of $^{87}Sr/^{86}Sr$ ratio approaching to that of modern sea water (i.e. 0.709) which clearly indicates the state of salt water intrusion. From Fig. 4.9, it was found that no temporal change in SW-FW interaction/mixing pattern for most of the samples except for sample number 3 and 6, which is quite consistent with the previous ionic ratio analysis. For these two samples, there is a trend showing salinization (SW-FW mixing) during 2^{nd} survey. Fewer amounts of precipitation decrease in Piezometric level, distance from the coast, rate of groundwater extraction and rock-water interaction at point scale might be the factors resulting in to this phenomenon.

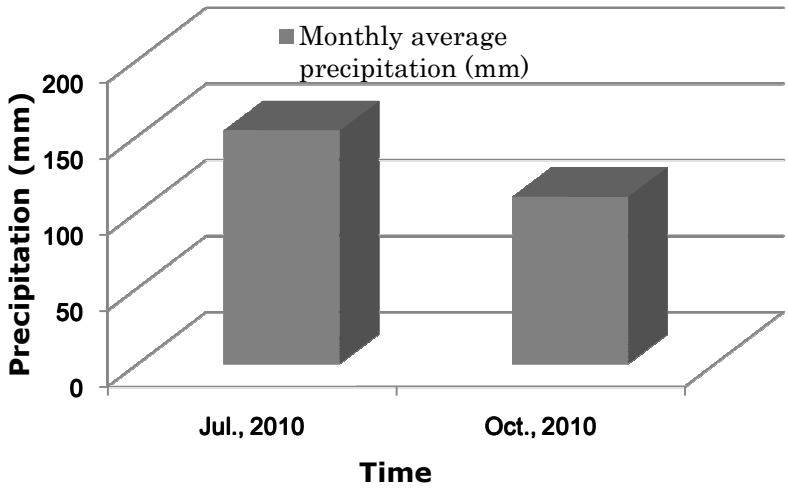

Fig. 4.1 Average antecedcent monthly precipitation during both sampling period for hydrochemical analysis

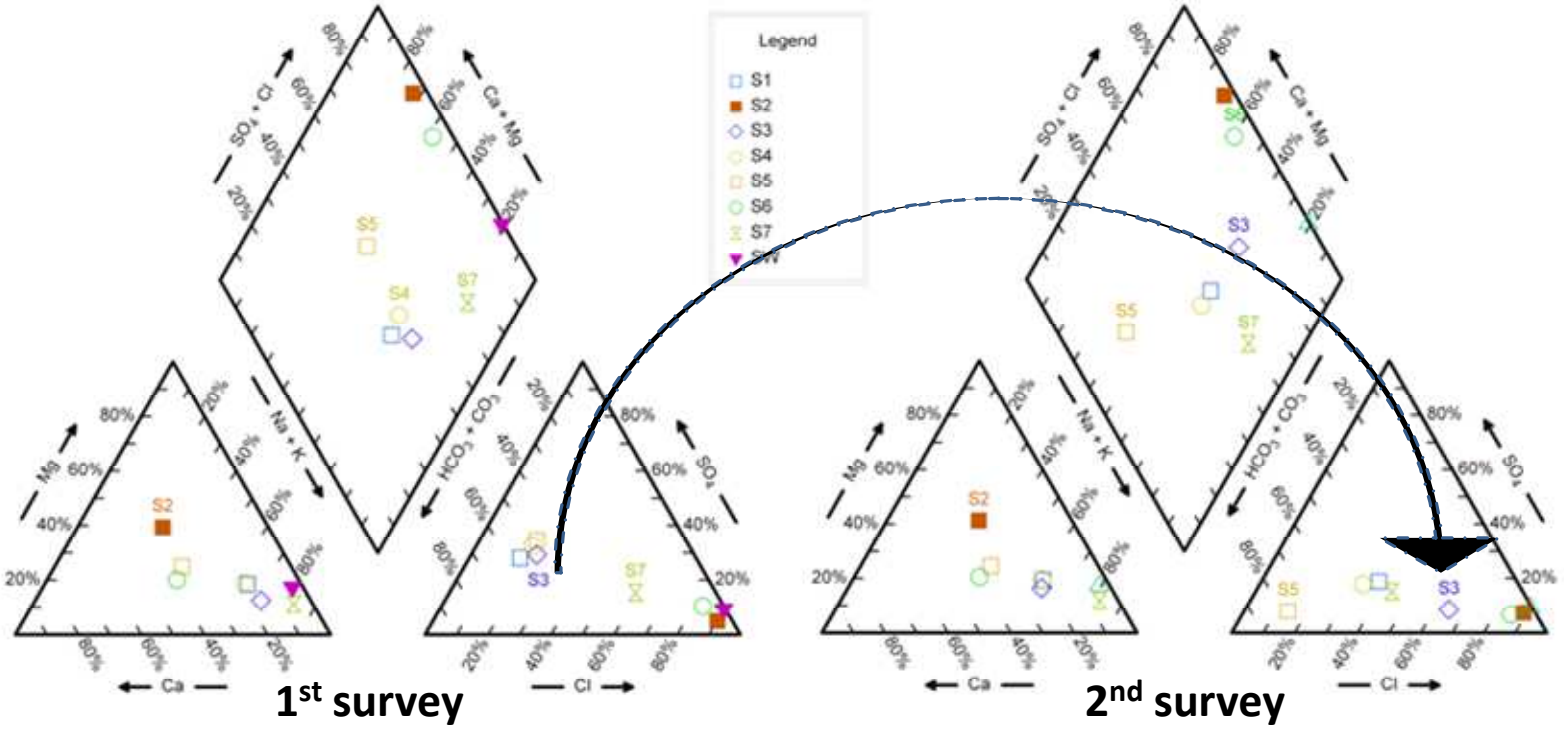

Fig. 4.2 Piper diagram showing temporal change in water type

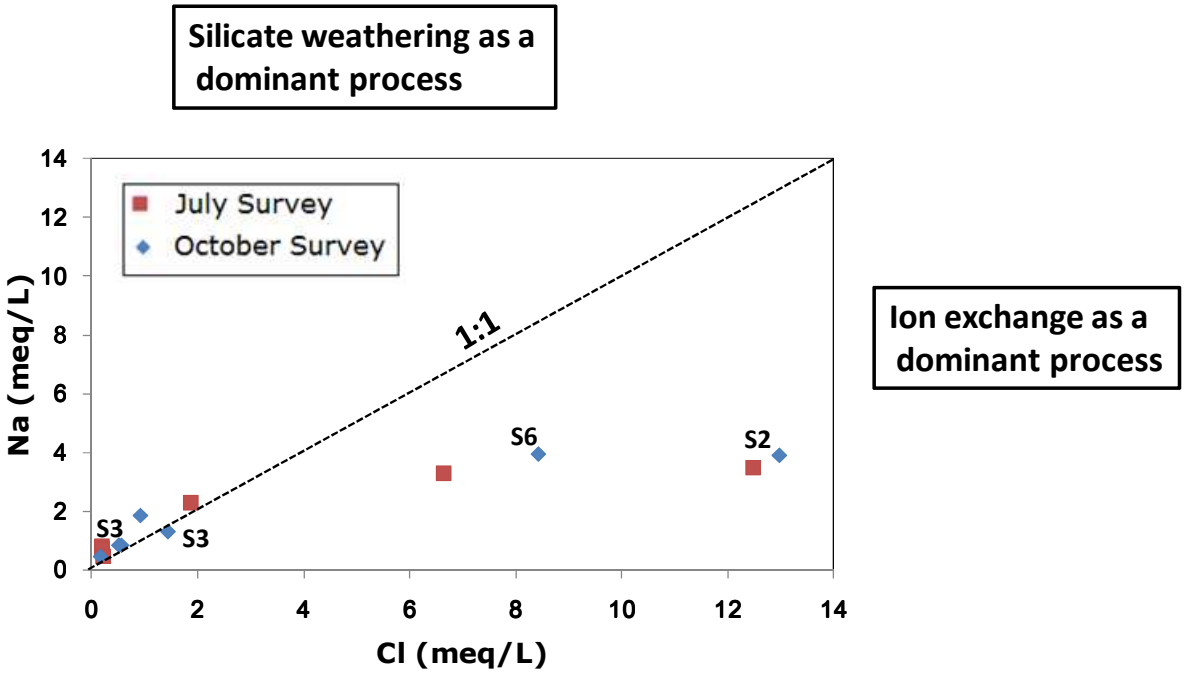

Fig. 4.3 Scatter plot showing sodium-chloride equiline for both survey

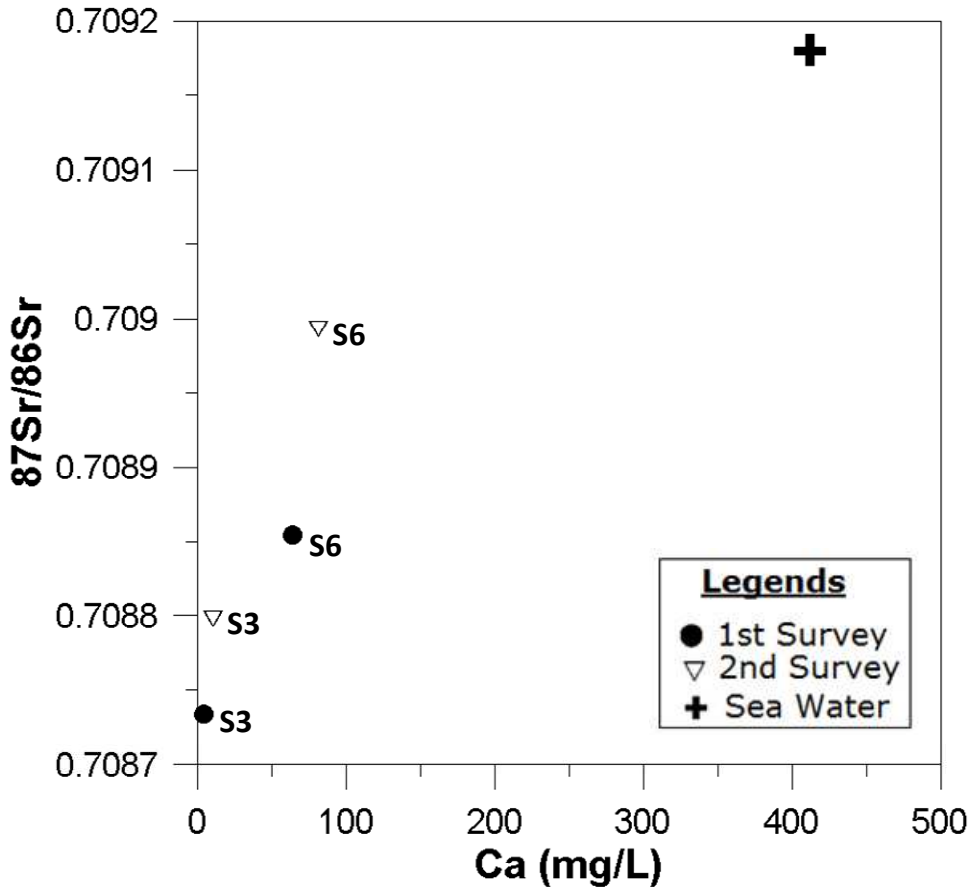

Fig. 4.4 Scatter plot showing temporal variation between Ca and $^{87}Sr/^{86}Sr$

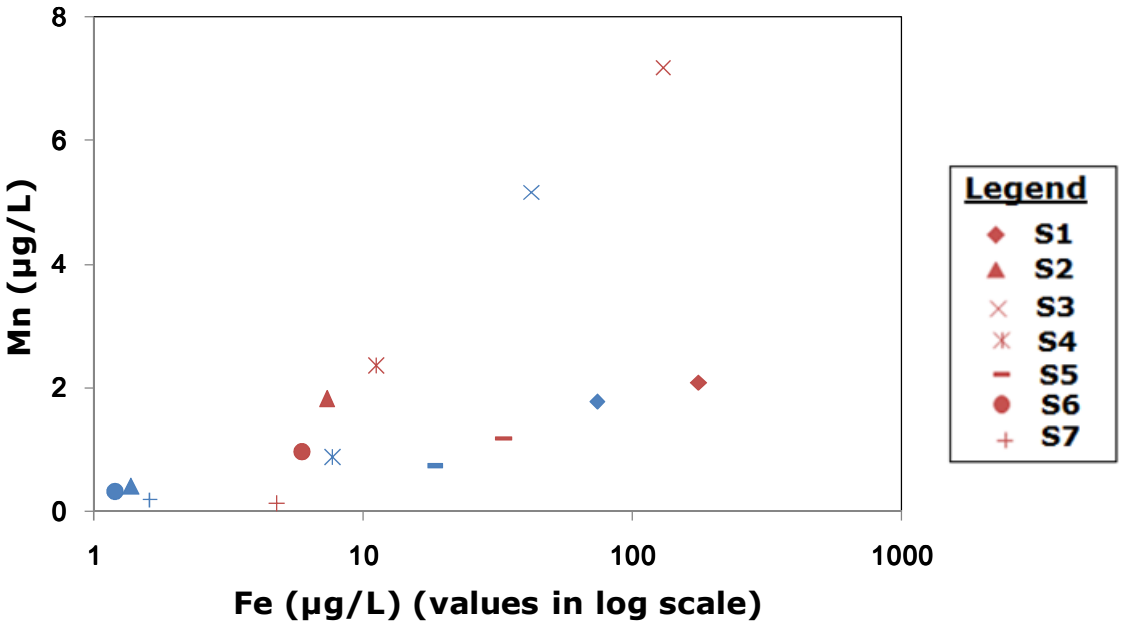

Fig. 4.5 Spatiotemporal variation of trace metals in water samples (Red and blue colors represents July and October survey results respectively)

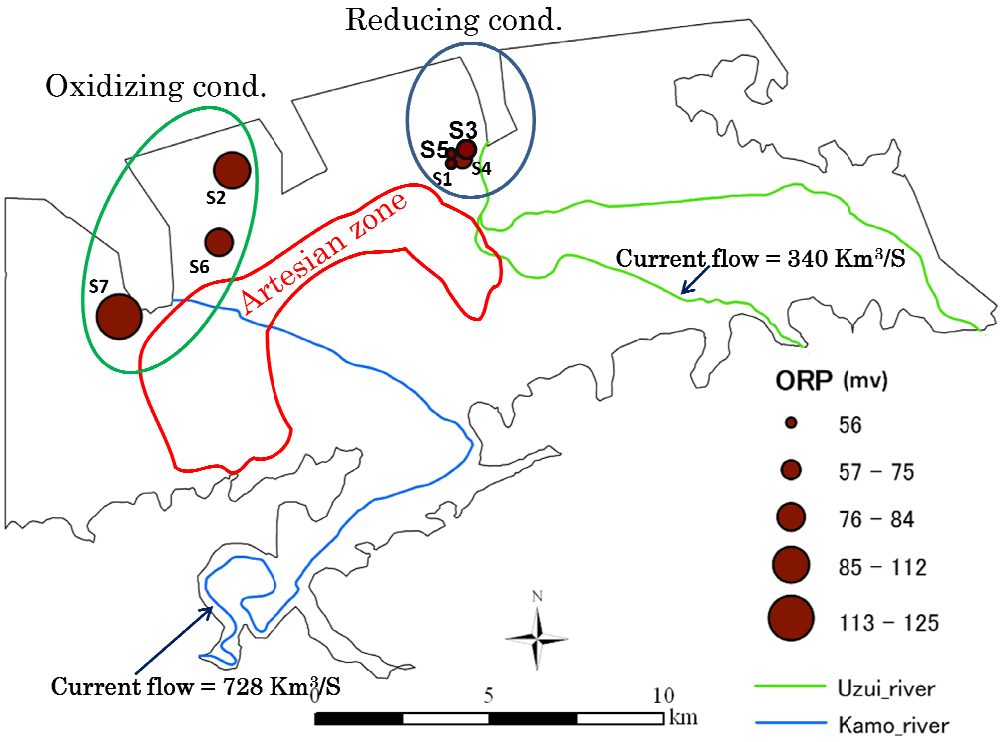

Fig. 4.6 Hypothetical diagram showing different redox zone of the study area

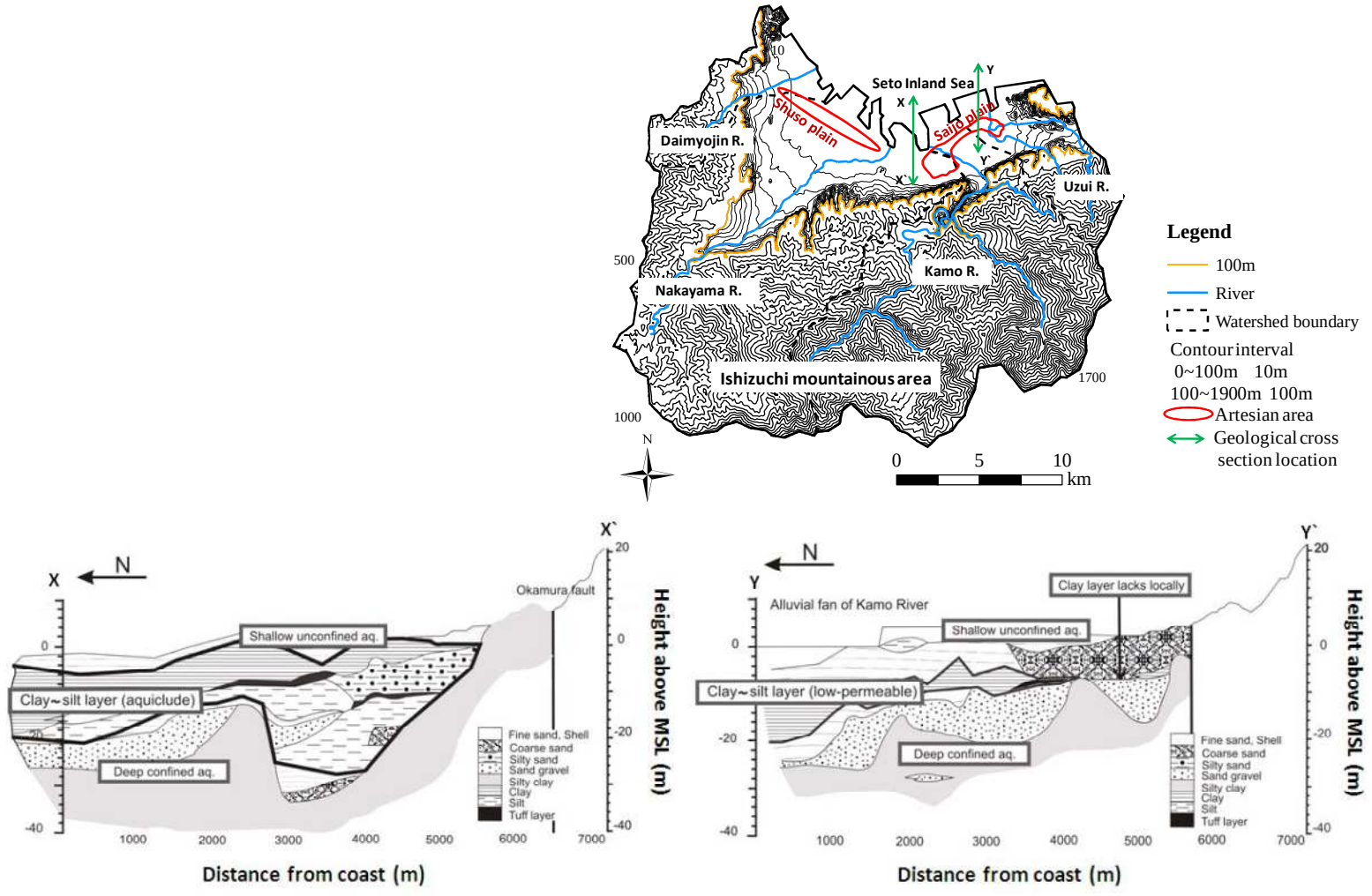

Fig. 4.7 Geological cross section for the stretches X-X` & Y-Y`

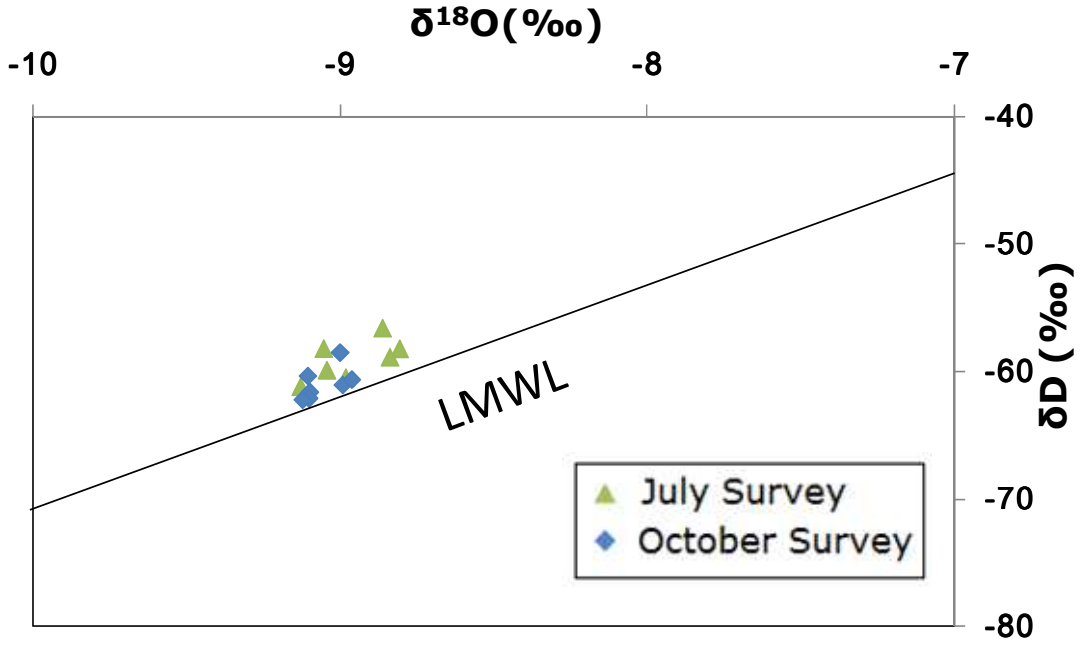

Fig. 4.8 Relationship between δ18O and δD values of water samples for both survey. (Here LMWL – local meteoric water line)

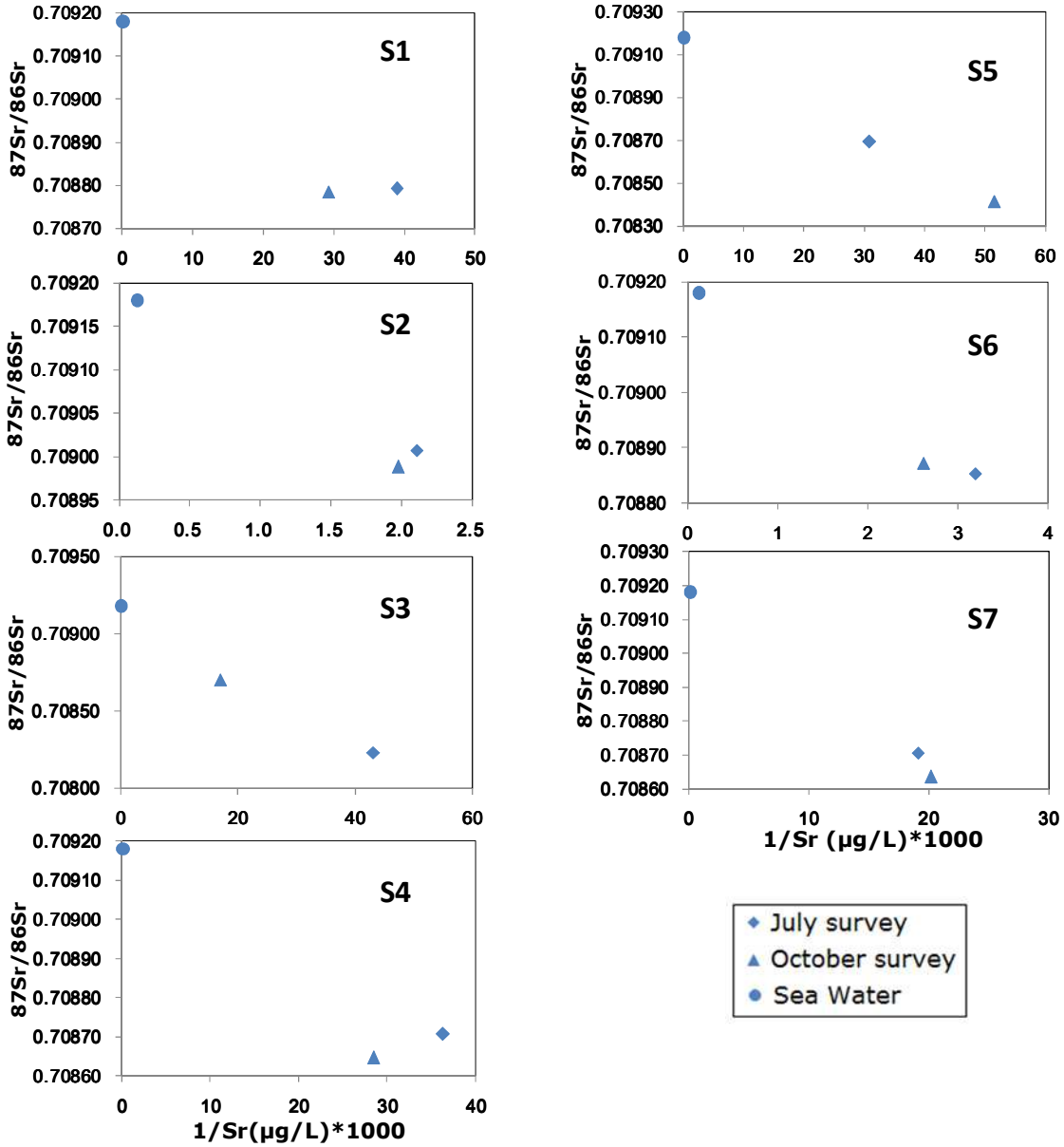

Fig. 4.9 Scatter plot between 1/Sr versus $^{87}Sr/^{86}Sr$ for all 7 samples during both sampling period to show ground water- sea water mixing pattern

Table 4.1 Statistical summary of hydrochemical parameters for groundwater samples

	July (1st survey)		October (2nd survey)	
Parameters	Range	Average± St.Dev.	Range	Average± St.Dev.
Temp.(°C)	14.20 – 19.10	18.03 ± 1.66	14.20 - 22.40	19.69 ± 3.19
Ph	6.53 – 7.50	6.88 ± 0.35	6.73 – 8.01	7.19 ± 0.47
EC (µs/cm)	134.10-1562.00	490.83± 538.11	144.50 – 1522.00	522.96 ± 549.65
Na^+ (mg/L)	11.01 – 80.42	39.09 ± 28.90	10.91 – 91.08	43.52 ± 32.35
K^+ (mg/L)	1.06 – 7.36	2.75 ± 2.19	1.45 – 8.14	3.12 ± 2.33
Ca^{+2} (mg/L)	3.52 – 91.03	25.57 ± 34.81	2.84 – 83.67	28.26 ± 35.55
Mg^{+2} (mg/L)	1.81 – 64.74	14.26 ± 22.24	3.33 – 70.86	16.38 ± 24.35
Cl^- (mg/L)	6.37 – 442.35	109.99 ± 162.12	5.54 – 459.93	126.34 ± 172.45
SO_4^{2-} (mg/L)	12.31 – 39.98	22.41 ± 9.88	4.27 – 50.84	19.61 ± 15.50
HCO_3- (mg/L)	28.68 – 56.38	45.00 ± 9.54	25.62 – 62.53	39.48 ± 12.81
SiO_2 (mg/L)	4.91 – 6.70	5.56 ± 0.66	5.19 – 7.12	6.09 ± 0.81
Sr (µg/L)	23.24 – 476.21	135.90 ± 176.08	19.43 – 507.08	155.20 ± 193.41
Mn (µg/L)	0.14 – 7.18	2.25 ± 2.21	0.18 – 5.16	1.36 ± 1.69
Fe (µg/L)	4.78 – 176.10	52.65 ± 67.77	1.20 – 73.32	20.82 ± 26.37
As(tot) (µg/L)	0.03 – 0.86	0.24 ± 0.29	0.02 – 1.14	0.28 ± 0.39
$\delta^{18}O$ (‰)	-9.13 - -8.81	-8.96 ± 0.12	-9.13 - -8.97	-9.06 ± 0.06
δD (‰)	-61.10 - -56.51	-58.98 ± 1.51	-62.12 - -58.42	-60.84 ± 1.23
$^{87}Sr/^{86}Sr$	0.7087 – 0.7090	0.7088 ± .0001	0.7087 – 0.7090	0.7089 ± 0.0001

Part – II

4.2 Effect of tidal fluctuation on ground water quality in case of different aquifers

4.2.1 Relationship between Piezometric and tidal level fluctuation and tide aquifer interaction technique to estimate aquifer parameters

Contour map for electrical conductivity (EC) in the first survey at spatial is shown in Fig. 4.10. Here it is found that S1 and S2 having very contrast EC despite being equidistant from the coast. Also water quality and lithological cross section for the monitoring wells is shown in Fig. 4.11. Based on above contrasting findings, monitoring wells (S1 and S2) were taken for tidal effect observation. Also another monitoring well (S6) was taken into consideration to validate the results from above two monitoring wells.

For both in case of S1 and S2, the forms of the tidal fluctuation and the Piezometer readings were found sinusoidal in nature (Fig. 4.12). One curve was superimposed upon other by applying the concept of time lag and tidal efficiency factors (Erskine, 1992). Here time lag (t_{lag}) is defined as an inverse measure of the velocity of tidal wave propagation as it moves through the aquifer and tidal efficiency (TE) is defined as the ratio of the amplitude of groundwater fluctuations to the amplitude of tidal fluctuations at the aquifer–sea boundary (Jha et al., 2008).Tidal efficiency factor was calculated by the ratio of the standard deviation of Piezometric and tidal readings to reduce the effect of individual reading error. In order to calculate time lag with least square fit method, Piezometer readings were shifted in the amplitude

same to tidal data and then amplified by tidal efficiency factor using following equation (4.2).

$$h`(t) = \bar{T} + \left[h(t) - \bar{h}\right]/E \qquad \text{……..(4.2)}$$

Where, *h (t)* = GW level at time t (m), *h` (t)* = shifted GW level at time t (m),

$\bar{h}$ = Mean GW level (m), $\bar{T}$ = mean tidal level (m), and *E* = Tidal efficiency factor (dimensionless)

The shifted Piezometric level was then compared with tidal level to calculate time lag using following equation (4.3).

$$Min \sum\left[h`(t) - T\left(t - t_{Lag}\right)\right]^2 \qquad \text{…….(4.3)}$$

Where, *T (t)* = Tide level at time t(m), and t_{lag} = Time lag (day)

Using eqn. 1 and 2, tidal efficiency and time lag were calculated for both the site (Table 4.2), and found that time lag for "S2" is larger than in case of sample "S1" despite of being equidistant from coast, which confirms the difference in aquifer type (Gregg, 1966). It seems that for "S1", water quality shows tidal effect through direct movement of tidal water into and out of aquifer like an unconfined aquifer while for "S2", water quality responds by compression and expansion of the aquifer and its confining layers due to the weight of the incoming and outgoing tidal waters like a confined aquifers.

Based on this time lag value, other properties of the aquifers (viz. transmissivity and hydraulic conductivity) have been calculated (using equation (4.4) and (4.5)) in order to delineate nature of the aquifers.

$$Time\ Lag\ (day) = X\sqrt{t_o S/4\pi T} \qquad \text{……..(4.4)}$$

$$T = Kb \qquad \text{…….(4.5)}$$

Where X = distance from sea (ft), S= Storage of the aquifer (dimensionless)

t_o = Period of tidal oscillation (ft), T =Transmissivity of the aquifer (ft^2/day),

K= Hydraulic conductivity of the aquifer, b= Thickness of the aquifer

Average storage value for unconfined and confined aquifers in this case are 0.17 and 0.0001 respectively (Sugita and Tanaka, 2009). After calculation, hydraulic conductivity for S1 and S2 were found 0.01 and 2.8 x 10^{-6} m/s respectively. These values look reasonable and consistent with the geological cross section at the screen depth of both the well (Freeze and Cherry, 1979) (Fig. 2.3).

4.2.2 Tidal implication on diurnal variation in chemical signature of groundwater for different aquifers

In order to see the tidal implication, time series plot for specific chemical characteristics of monitoring groundwater samples (S1, S2 and S6) from for all three surveys are shown in Fig. 4.13, 4.16 & 4.17. It was found that in case of S1 (i.e. unconfined aquifer), tidal level has strong implication on electrical conductivity, specially there was an antagonistic relation found between electrical conductivity with tidal height during lower low tide situation. However very little correlation was observed between electric conductivity and tidal height in case of S2 (i.e. confined aquifer) during all three survey except at lower low tide situation when electrical conductivity sharply decreases.

To support this finding, time series plot for different chemical characteristic (eg. Na^+, Cl^- , Sr, $^{87}Sr/^{86}Sr$ and HCO_3^-) (conservative for both fresh water and sea water system) were plotted. For sample “S1”, it was found that most of the parameters also shown a sharp altercation in ground water type/characteristics at the low tide situation.

For parameters like Sr, $^{87}Sr/^{86}Sr$ the value gets decreases where as value for Na/Cl ratio gets decreases indicating the enhancement of salt water characteristics while decrease in HCO_3^- strongly indicates lowering down of fresh water components in the ground water samples. It was also noted that during lower low tide situation, Piezometric level for sample "S1", goes down below the mean sea level (Fig. 4.12), which results in to disturbance in sea water- fresh water equilibrium and ultimately causes water quality change in case of sample "S1". On the other hand, for sample "S2", although electric conductivity fluctuation is not significant with tides but at ionic level most of the parameters simply showing relatively lower concentration might indicating a case of dilution or freshening during low tide situation. This change might take place either because of simple dilution from nearby pounded water (Fig. 4.10) during low tide situation when Piezometric level lowers down or unconfined water mixing through leaky confining layer.

To explain the relationship between ground water type from monitoring wells (S1 & S2) and tidal fluctuation pattern, piper diagram were drawn for S1 and S2 during this sampling period as shown in (Fig. 4.14). Here it was found that in case of sample "S1", water quality shows a sharp transition from Na-HCO_3 type to Na-Cl type during low tide situation (as shown by S1 (5)) which firmly supports the fluctuation patterns of the parameters discussed above. In case of sample "S2", water quality does not show significant deviation with tidal pattern except at low tide.

Tidal fluctuation on other physiochemical parameters of the ground water samples (e.g. pH, water temperature) is shown for the first survey in Fig. 4.15. It was found that time series plot for pH and temperature didn't have any relation with the tidal fluctuation pattern. Negligible relation between pH with respect to tidal level can be

justified with the reason because natural water normally contains dissolved carbon dioxide and hydrogen carbonate ions, which make a buffer system with carbon dioxide and hence small changes in pH value of GW occurs with tides (Abdullah et al., 1997). On the other hand little correlation between ground water temperature and tidal level can be explained with the reason that temperature of the water samples fluctuates mainly due to the presence and absence of the sunlight rather than interaction between surface and ground water. Role of biological and photosynthetic activities in this small mud flat area also can't be neglected.

4.2.3 Cross validation of the chemical results and relation with screen depth

Results of tidal effect on chemical characteristics for both the monitoring well samples (S1 and S2) were cross validated with considering time series results from another monitoring well (mentioned as "S6" here after). It was found that, despite of being located near to sample "S2" and with high electrical conductivity, tidal response on fluctuation pattern of chemical species for "S6" is similar to sample "S1" (Fig. 4.17). The screen depth for S6 is 18 meter bgl and from lithological cross section (Fig. 4.11), it can be concluded that presence of aquitard /aquiclude (eg. Clay) near 20 meter hinder partially or completely the propagation of tidal wave to affect water quality parameters in coastal aquifers (for sample "S2"), however for "S6" and "S1" screen depth is less than 20 meter which didn't encounter confining layer and thus tidal waves easily propagates through these aquifers. In other words, depth of the borehole (screen depth) is the important factor controlling the characteristics of tidal effect on the ground water type at point scale.

Among all three survey results, fluctuation pattern for all physico-chemical parameters during second survey was found very typical. To understand this, average

antecedent monthly precipitation amount before all sampling campaign is shown in Fig. 4.18. It was found that with the seasonal variation in general precipitation fluctuation pattern, the amount is least during second survey. This leads to high concentration of dissolved solids and/or high ionic strength of ground water. Hence after aquifer get recharged by brackish water/ sea water during low tide, flushing of it takes time to get in to normal fresh condition thus solutes shows periodicity at higher concentration.

4.2.4 Deduction of mechanisms responsible for tidal propagation

To get a deep insight for the process responsible for water quality changes, scatter plot was drawn between $^{87}Sr/^{86}Sr$ vs 1/Sr and $^{87}Sr/^{86}Sr$ vs Cl (shown in Fig. 4.19 and 4.20 respectively). If two water bodies chemical properties are well separated, mixing trend can be plotted without considering two different end members (Langmuir et al., 1978). For plot between $^{87}Sr/^{86}Sr$ vs 1/Sr (Fig. 4.19), it was found that direct mixing of SW-FW is not much obvious for most of the cases (S1, S2 & S6). However in case of second survey, samples showing an increasing trend towards the sea water end member. To further analyze the phenomenon, plot between $^{87}Sr/^{86}Sr$ vs Cl was drawn (Fig. 4.20), from where two conclusion can be made. First, as the $^{87}Sr/^{86}Sr$ fluctuation is very clear and it's increasing in relatively higher order during the second survey. It is known that incorporation of increasing amount of aquifer strontium into groundwater should progressively shift the 87Sr/86Sr ratio of the groundwater towards that of the aquifer material (Woods et al., 2000) which means here also there is a clear contribution from marine environment. But another question arises here about the time required for this short temporal fluctuation of the strontium ratio of the water samples. The two possibilities for the exchange of strontium among the two different aquifer types are simple SW-GW mixing and weathering through flow path. However considering the weathering phenomenon as a function of geological time scale it is next to impossible to

take this in to account for the change in strontium isotopic value during diurnal cycle; so another possibility i.e. simple mixing of SW-GW with different strontium isotopic ratio make sense here. Second, movement of ground water samples towards/away from sea water doesn't follow linear fashion along the mixing line which suggests that not only influx of salt/brackish water is important rather than contribution of other processes like cations exchange; selective ion movement/diffusion for water quality changes can't be neglected. To support this speculation, theoretical sea water – fresh water mixing was calculated predicting the changes in the chloride concentration of monitoring well groundwater and how much it acquires from other aquifer materials during low tide situation.

4.2.5 Calculation of percentage SW-FW mixing rate

Considering chloride concentration as conservative property for sea water, mixing ratio was calculated using equation (4.6) (Appelo and Postma, 2005):

$$f = \frac{(Cl_{Sample} - Cl_{Fresh})}{(Cl_{Sea} - Cl_{Fresh})} \times 100\ [\%] \qquad \text{…….(4.6)}$$

Where, f = Salt water mixing rate (%), Cl_{Sample} = Chloride conc. of sample, Cl_{Fresh} = Average chloride conc. of Kamo river water sample (i.e. 2.6 mg/L (Kumasaka, 2010)), Cl_{Sea} = Chloride conc. of sea water (i.e. 19350 mg/L (Nakano et al., 2008)).

Here, chloride concentration for sea water and Kamo river water (main recharging source for ground water) were considered as two end members. Calculation result is shown for all four main phase of diurnal tidal cycle in Fig. 4.21. Here it was found that though there is an increment in mixing ratio (for S1 and S6) during lower

low tide situation but magnitude is not so significant. The trend is opposite for sample "S2", i.e. mixing ratio getting reduced during lower low tide situation.

To further look into the ion exchange process, *BEX* (Base Exchange indices) was calculated for different surveys using equation (1). From scatter plot between Cl vs *BEX* (Fig. 4.22), it was found that for first and third sampling campaigns, there is an clear inverse relation between Cl and *BEX* during low tide situation which firmly supports the above phenomenon, while trend is not so clear for second survey.

4.2.6 Tidal effect on trace metal chemistry: hydrochemical approach

To understand mechanism for the periodic fluctuation of iron with tidal cycle, time series plot of Fe, ORP, SO_4^{2-} and NO_3^- are shown in Fig. 4.23, 4.24 and 4.25 for all three surveys respectively. Lu et al. (1977) stated that redox potential (Eh) is one of the main variables controlling the solubility of trace metals at sediment/ water interface. Minerals like ferrous hydroxide and pyrite are generally stable in a reducing environment and remains concentrated in organic deposits (under the water table or high tide situation). During low tide situation, in parallel with lowering of Piezometer level, hydraulically saturated pores get partially filled with air which in turn enhance interstitial oxidation and ultimately results into mobilization of these heavy metals. Figure 16 shows fluctuation pattern of Fe along with ORP giving enough supports to the above mentioned mechanism for trace metal mobilization. A strong correlation between fluctuation pattern of Fe and SO_4^{2-} along with inverse correlation with fluctuation pattern of NO_3^- found from in Fig. 4.23, 4.24 and 4.25 (for 1^{st}, 2^{nd} and 3^{rd} survey respectively), which fairly indicates the possible mineral source for iron present in this study site. Here it can be concluded that minerals containing both Fe and SO_4^{2-} is most probable source here and decrease of NO_3^- acts as thermodynamically favored electron

acceptor to mediate this oxidation-reduction process of the mineral responsible for trace metal mobilization (Drever, 1997).

However, in order to confirm the solubility control for iron enrichment in groundwater with tidal level, saturation index (SI) was calculated using PhreeqC (speciation modeling) code (Parkhurst and Appelo, 1999). Saturation indexes (SI) are used to evaluate the degree of equilibrium between water and respective mineral. Changes in saturation state are useful to distinguish different stages of hydrochemical evolution and help to identify which geochemical reactions are important in controlling water chemistry (Coetsiers and Walraevens, 2006; Langmuir, 1997). The saturation index of a mineral can be obtained using following equation (4.7) (Garrels and Christ, 1965).

$$SI = log_{10}(K_{IAP}/K_{SP}) \qquad \ldots\ldots(4.7)$$

Where *SI* is the saturation index, K_{IAP} is the ion activity product of particular solid phase and K_{SP} is the solubility product of the phase. Based on the value of the *SI*, the saturation states are recognized as saturation (equilibrium; $SI = 0$), under saturation (dissolution; $SI < 0$) and oversaturation (precipitation; $SI > 0$). In other words, $SI < 0$ which specifies case of unsaturation; could reflect the character of water from a formation with insufficient amount of the mineral for solution or short residence time and $SI > 0$ specifies that the groundwater is oversaturated with respect to the particular mineral and therefore incapable of dissolving more of the mineral. Such an index value reflects groundwater discharging from an aquifer containing ample amount of the mineral with sufficient resident time to reach equilibrium.

Result for saturation index (*SI*) for five selected minerals (Iron Sulfide, Goethite, Siderite, Scorodite and pyrite) during both sampling campaign is shown in Table 4.3. Here shaded portions are indicating results during lower low tide and low tides situations. Results shows that most of the samples are strongly undersaturated with respect to FeS, goethite, siderite and scorodite, while in case of pyrite, *SI* value approaching towards saturation. It was also found that during lower low tide situation, water samples relatively getting more undersaturated with respect to pyrite mineral suggesting pyrite as a source for dissolved iron. Following the above facts, possible reaction mechanism can be explained by the following equation (4.8).

$$2FeS_2 + 7O_2 + 2H_2O \rightarrow 2Fe^{2+} + 4SO_4^{2-} + 4H^+ \quad \ldots\ldots(4.8)$$

For sample "S1", nitrate consumption during iron mobilization process as indicated in Fig. 4.23, then Pyrite denitrification process can also be considered as a potential mechanism for iron enrichment and reaction can be shown by following equation (4.9) (Spiteri et al., 2008):

$$FeS_2 + 2.8\,NO_3^- + 0.8\,H^+ \rightarrow Fe^{2+} + 2\,SO_4^{2-} + 1.4\,N_2 + 0.4H_2O \quad \ldots(4.9)$$

However trend for nitrate consumption in case of sample "S2" is not significant hence nitrate denitrification can't assigned as the catalyst for the trace metal mobilization.

4.2.7 Tidal effect on trace metal chemistry: quantitative approach

Considering the result from hydro-chemical analysis, it was found that there is a significant effect of diurnal tidal fluctuation on trace metal concentration in groundwater from coastal aquifers. Hence, it is necessary to support this result through numerical simulation to confirm this idea.

Till date so many research has been conducted on numerical modeling on tidally forced aquifer mainly describing (Submarine Groundwater Discharge, aquifer leakage, Oxidation- reduction process) (Li et al., 1997; Xia et al., 2007). However, very few studies are there to model tidal effect on trace metal fluctuation. Considering low availability of field data and aquifer parameters in Saijo plain, SEEP/W model is considered during this work. SEEP-W model (a product of Geo-Slope, 2007) need low input dataset and equally helpful to delineate tide- aquifer interaction (Hughes et al., 1998; Aryafar et al., 2009).

So finally the objective here is to define the time varying extent of the saturated and unsaturated regions of inter tidal profile.

Model description

SEEP/W is a two dimensional finite element analysis computer based program designed to simulate/analyze different flow condition such as saturated/unsaturated flow, confined/unconfined aquifer in a two-dimensional situation. In principle, it is based on mass balance statement and Darcy's law applied to both saturated and unsaturated flow (GEO-SLOPE, 2007).

Governing differential equation:

The governing differential equation used by SEEP/W is shown be equation (4.10):

$$\frac{\partial}{\partial x}\left(K_x \frac{\partial H}{\partial x}\right) + \frac{\partial}{\partial z}\left(K_z \frac{\partial H}{dz}\right) Q = \frac{\partial \theta}{\partial t} \quad \text{.....(10)}$$

Here, H = total head, Kx and Kz are hydraulic conductivity in x and z directions respectively. Q = Applied boundary flux, θ = Volumetric water content, t= time

Model design

Problem domain consisting of finite elements for unconfined aquifers is shown in Figure 4.26. This domain consists of 368 elements and three layers each of four meter thick. It's an anisotropic aquifer with different hydraulic conductivity and other parameters for different layers. All three layers from top to bottom consist of sand, silty sand and sandy silt with horizontal hydraulic conductivities **(K_X)** is equal to $1X10^{-2}$ m/sec, $1X10^{-5}$ m/sec and $1X10^{-4}$ m/sec respectively. Upper and lower boundary of the domain considered as the no flow boundary condition. Left side of the domain considered as the constant head boundary equals to the Piezometric level at the height of four meter high from mean sea level. Right side of the domain considered as the variable head boundary keeping tidal amplitude for different phase at diurnal basis.

After quantitative simulation/iteration, submarine groundwater discharge at three different tidal phases (high tide, zero tide and low tide situation) were calculated at two different lower boundary positions of the problem domain. Lower boundary for two different simulations was considered at two and four meters lower than mean sea level and their simulation result are shown in Figure 4.27 and 4.28 respectively.

Main outcome of the modeling

1. Estimated relative volume of submarine groundwater discharge (SGD) flux value and position of its exit points at the beach slope varies temporally with tidal fluctuation.
2. During low tide situation, value of flux is maximum and exit point is much deeper

in the sea. The aquifer matrix gets oxidized quickly and favors the short term mobilization of trace metals during lower low tide situation (Same as previous finding (Hughes et al., 1998)).

3. Despite changing the lower boundary position, magnitude of the submarine groundwater discharge changes a little however the order of submarine groundwater discharge for different tidal phase remain same which firmly confirms that the oxidation- reduction process prevails with tidal fluctuation at diurnal basis.

Validation of the modeling result

As it is known that flux value of submarine groundwater discharge (SGD) represents the velocity of groundwater discharging toward the coast, so with different tidal phase it is indicating how fast the aquifer system gets saturated/unsaturated. Saturated and unsaturated i.e. reduced and oxidized state of the aquifer is generally measured by oxidation reduction potential (ORP), a physical property of ground water. Considering the above fact, pattern of submarine groundwater discharge fluctuation generated through numerical simulation were compared to the field observed results of oxidation reduction potential value along with tidal cycle. Result is shown in Figure 4.29, where a high correlation was found signifies this phenomenon.

Assumptions made before modeling

1. Mean sea water level considered as datum of the problem domain.

2. Constant boundary head towards coastal aquifer is equal to water table height

3. Variable head boundary towards the sea is the tidal amplitude.

4. Tides composed of only one sinusoidal wave component propagates towards land

5. Aquifer is perfectly stratified i.e. all layering extends from the left side to the right side of the problem domain and layering is same throughout the embankment.

6. No-flow boundary condition at the upper and lower boundaries of the aquifer.

4.2.8 Deduction of physical processes operating at diurnal scale:

It is known that with the oceanic tides, pressure distribution above the coastal aquifer water table changes which results in to inland propagation of tidal oscillation/wave energy as well as local water exchange across water table occurs through capillary effect (Turner, 1993; Li et al., 1997). In other words, during high tide situation, aquifer behaves as saturated soil matrix and there is no pressure gradient between sea and inland aquifer however during low tide situation, aquifer behaves as unsaturated soil matrix and there is pressure gradient created between sea and inland aquifer. Li et al. (1997) described about the two mechanisms which are responsible for Piezometric level fluctuation in response to tidal cycle are a) horizontal mass movement and b) local mass movement across Piezometric level. In general first mechanism is responsible for phase difference between sinusoidal tidal and Piezometric oscillation (Nielsen, 1990). So water quality (for major ions) of "S1 and S6" changes mainly because of horizontal mass movement i.e. mass flux generated due to change in boundary condition towards sea. However, mobilization for heavy metal (oxidation-reduction process) in all samples occurs mainly because of second process i.e. local mass movement across Piezometric level.

Finally summary for the processes responsible for change in water quality with tidal fluctuation is shown in Table. 4.4. Here it is found that mainly three kinds of the processes like cation exchange, local sea water- fresh water mixing and sea water freshening or simple dilution; however the priority order is temporally different for

different kind of aquifers. It can be suggested that cumulative effect of seasonal precipitation amount and local factors might be responsible for this discrepancy.

List of assumptions made in this case study before analyzing tidal effects on surface water - ground water interaction

1) Effect of wind and atmospheric pressure on sea-water levels has not been taken in account.
2) Assumed one dimensional flow which implies no vertical flow or flow parallel to the shoreline. This assumption is not unreasonable here considering that a coastal aquifer system is too much thick compared to the tidal range with a straight shoreline.
3) Homogenous aquifer which is connected with sea in perfect hydraulic manner.
4) The aquifer is in perfect hydraulic connection with sea.

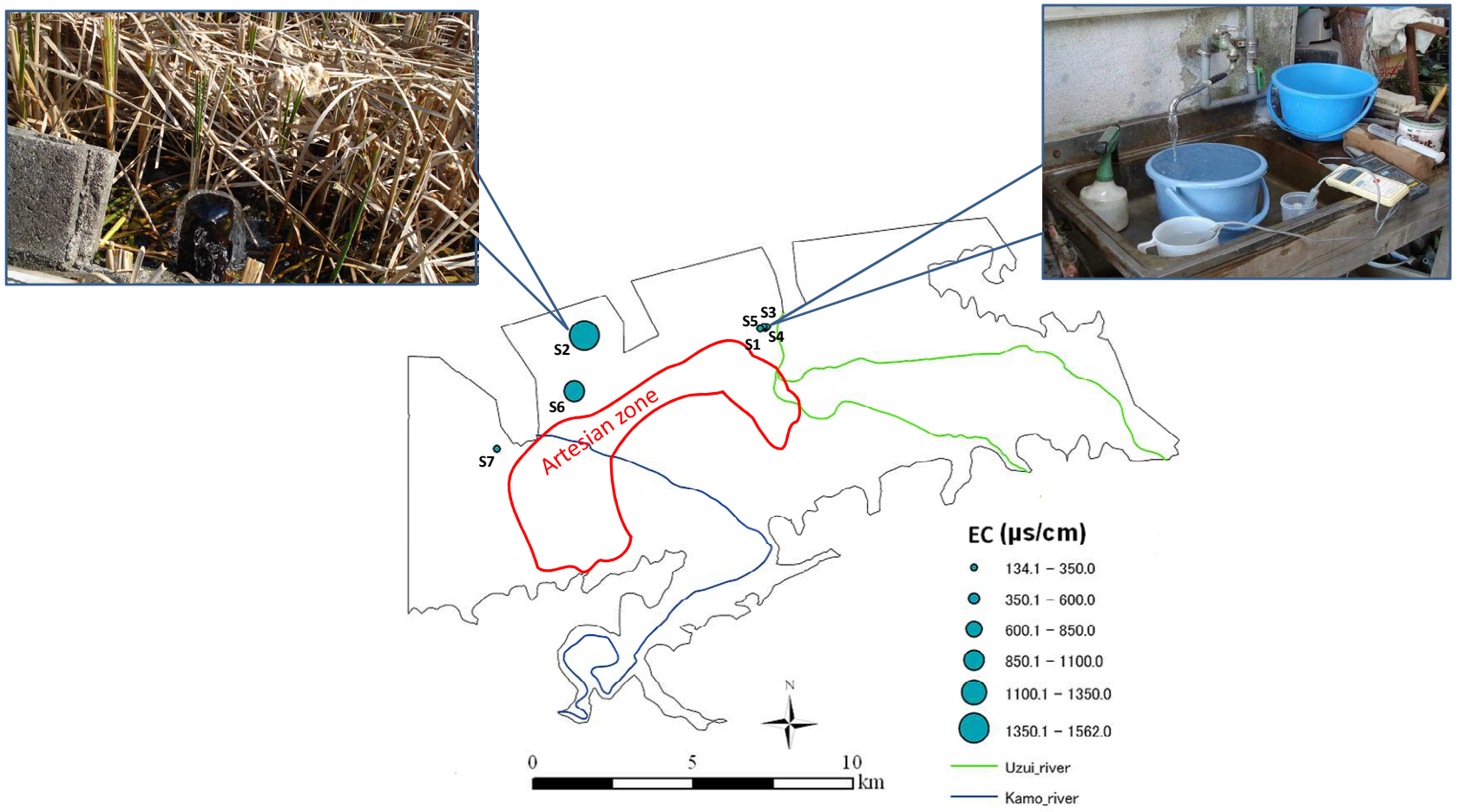

Fig. 4.10 Electrical conductivity (EC) contour map at spatial scale during July, 2010 (here S1 and S2 denotes samples taken for tidal effect observation)

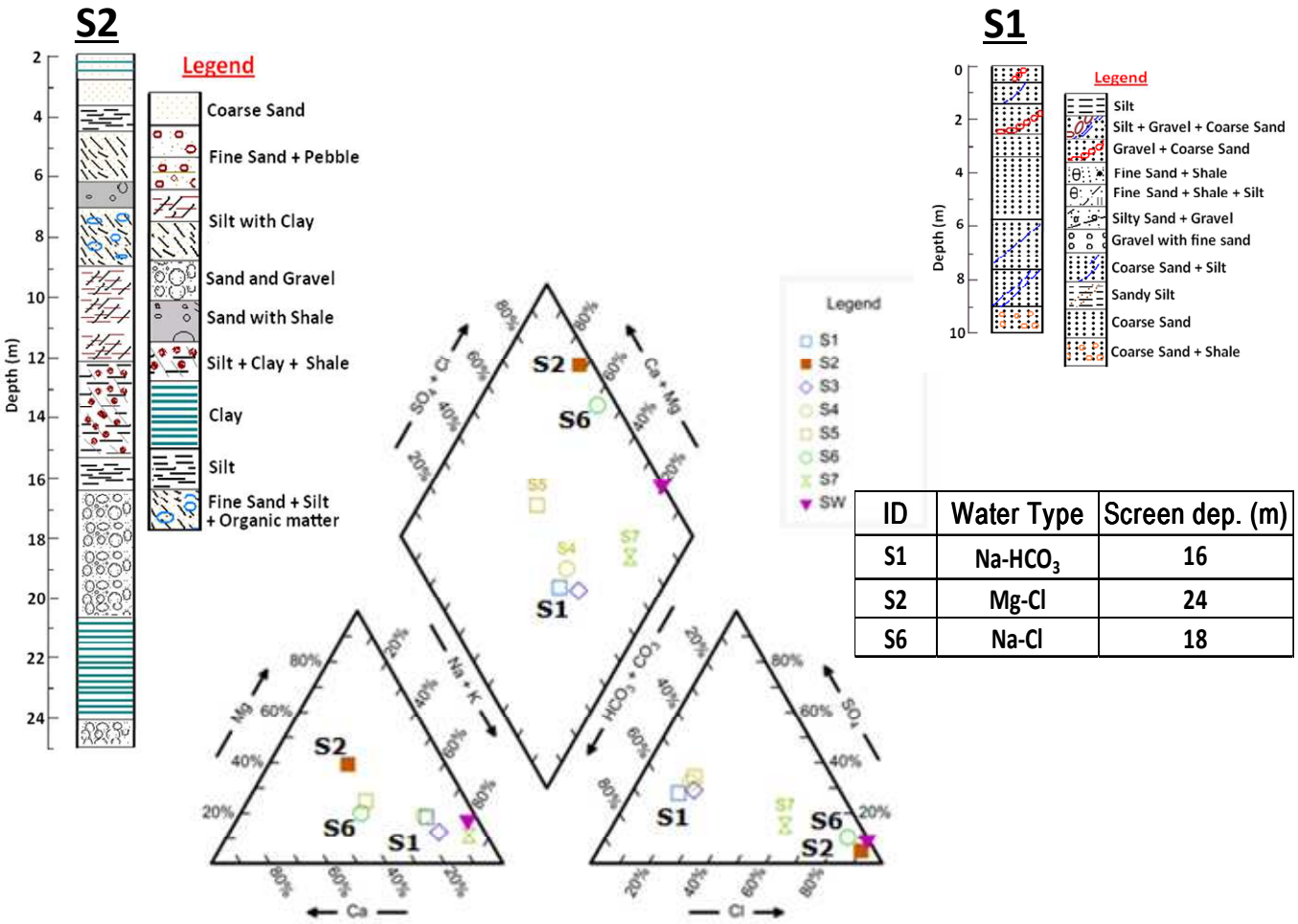

ID	Water Type	Screen dep. (m)
S1	Na-HCO_3	16
S2	Mg-Cl	24
S6	Na-Cl	18

Fig. 4.11 List of criteria to select tidal effect observation points along with lithological cross section for the points near to S1 and S2

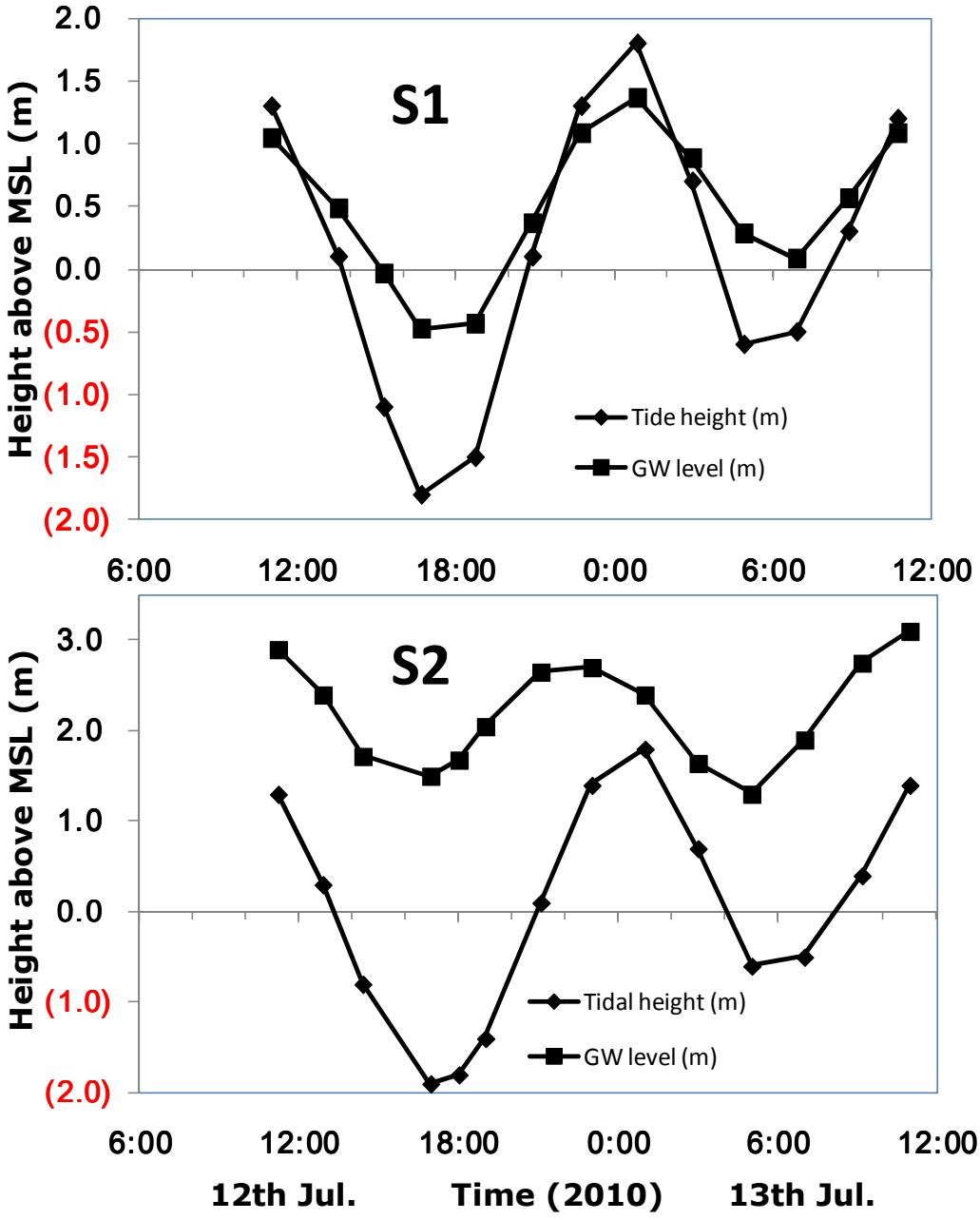

Fig. 4.12 Relationship between Tidal height and Piezometric level for both S1 and S2 for a period of 24 hours during July, 2010 (Digits in parenthesis showing negative value)

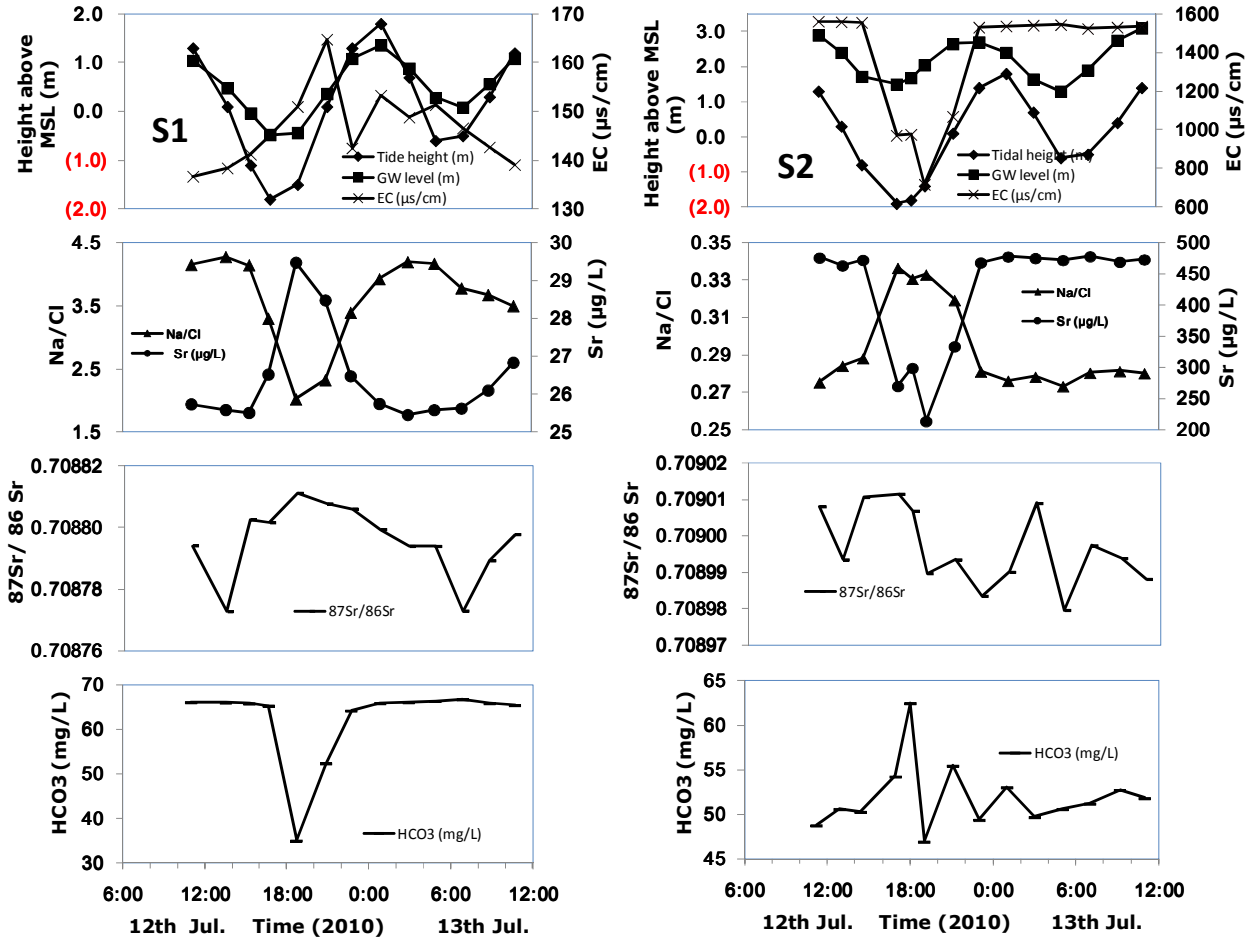

Fig. 4.13 Time series plot to show relationship between Tidal height, GW level and different chemical species for both S1 and S2 for a period of over twenty four hours during July, 2010 campaign. (Digits in parenthesis showing negative value)

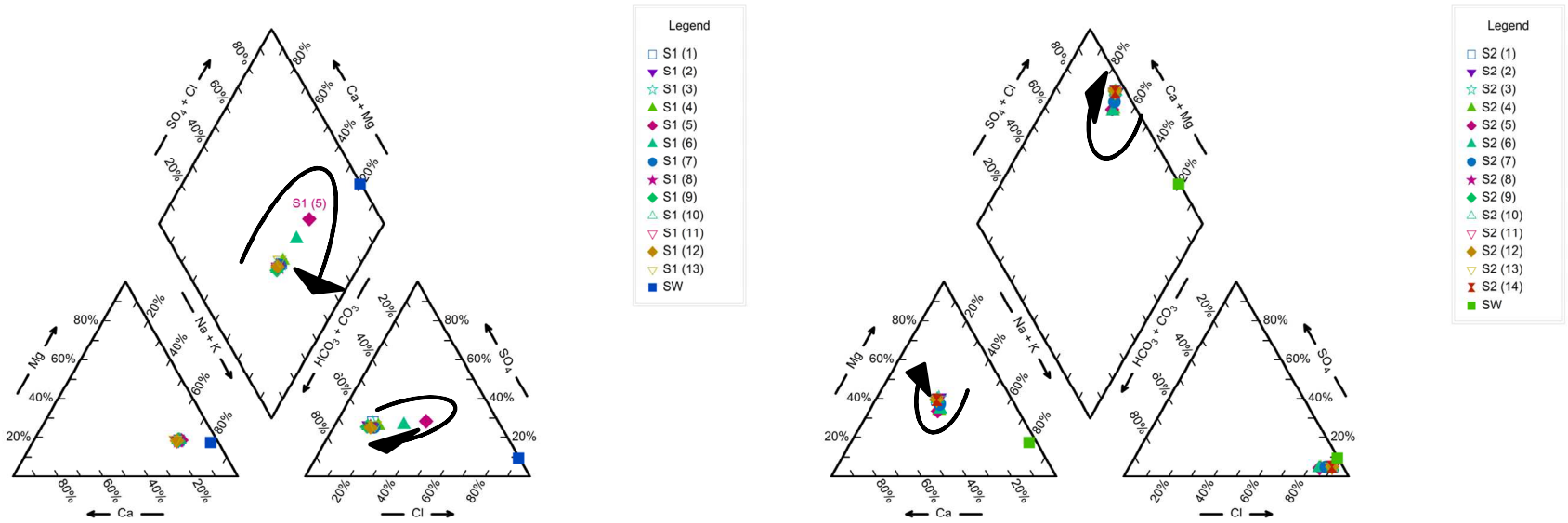

Fig. 4.14 Piper diagram showing water quality changes with the diurnal tidal cycle for the samples S1 and S2 during July, 2010 campaign

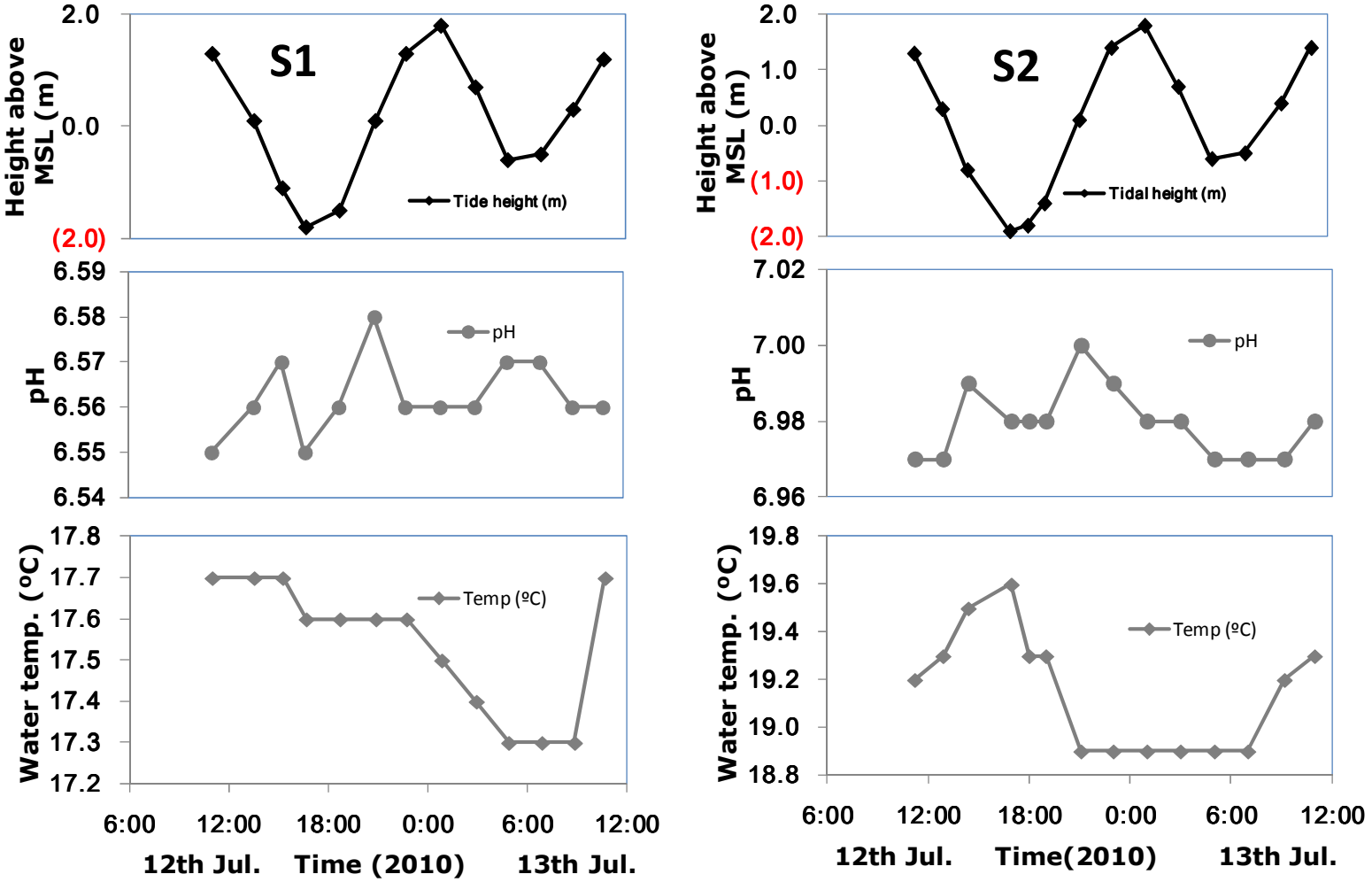

Fig. 4.15 Time series plot for pH and water temperature in case of sample S1 and S2 during July, 2010 campaign

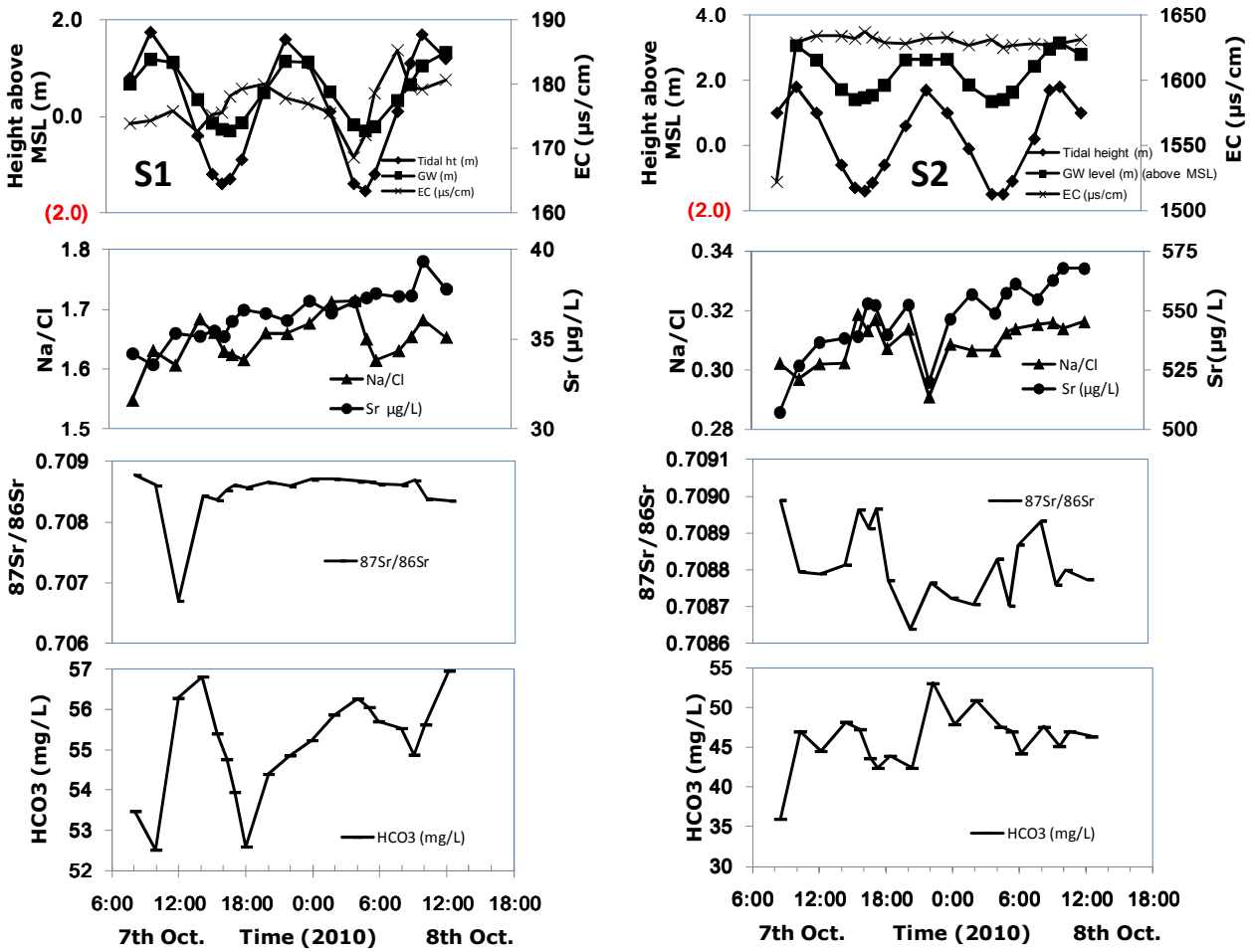

Fig. 4.16 Time series plot to show relationship between Tidal height, GW level and different chemical species for both S1 and S2 for a period of over twenty four hours during October, 2010 campaign. (Digits in parenthesis showing negative value)

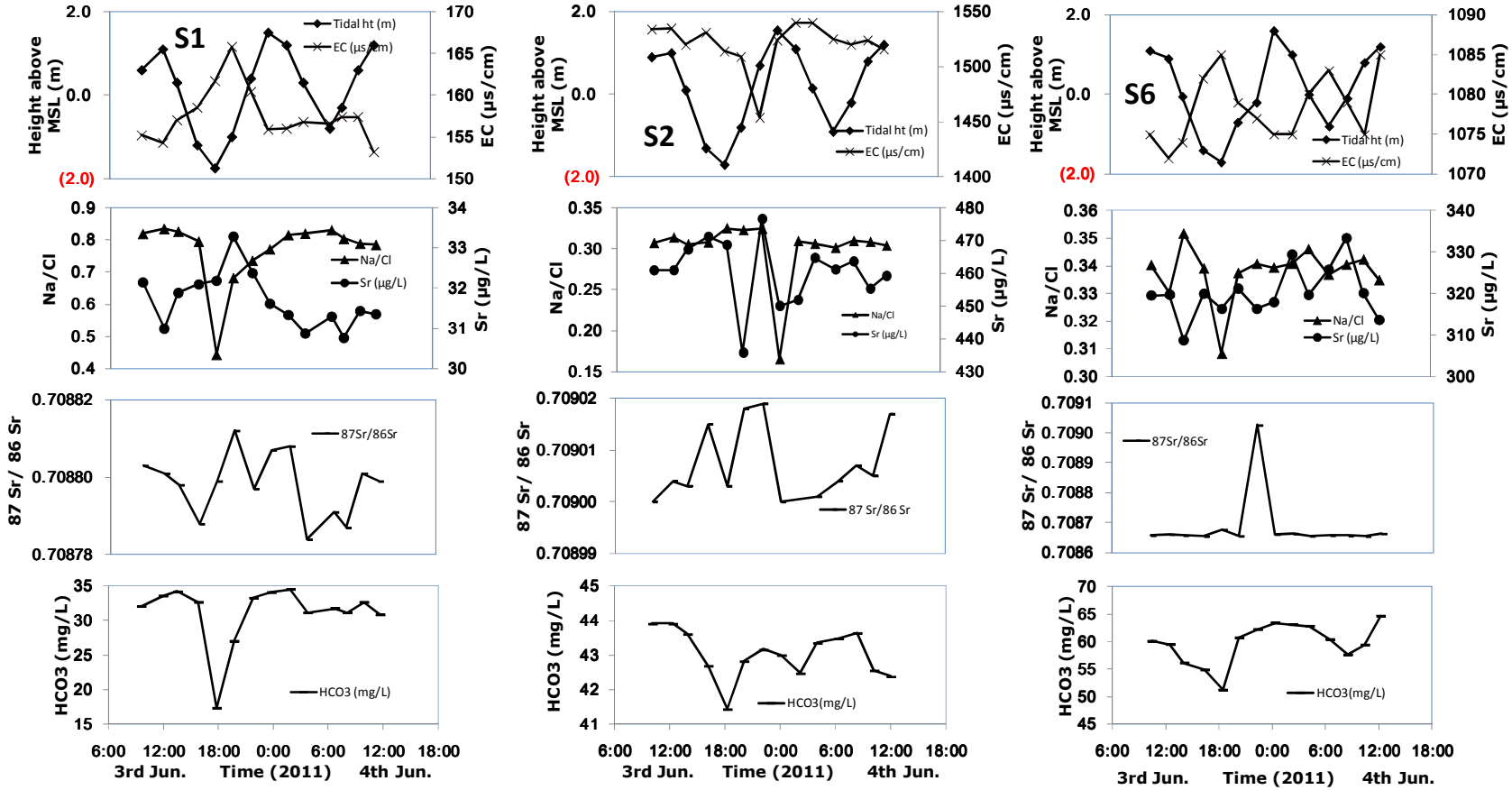

Fig. 4.17 Time series plot to show relationship between Tidal height, GW level and different chemical species for all three samples S1, S2 and S6 for a period of over twenty four hours during June, 2011 campaign. (Digits in parenthesis showing negative value)

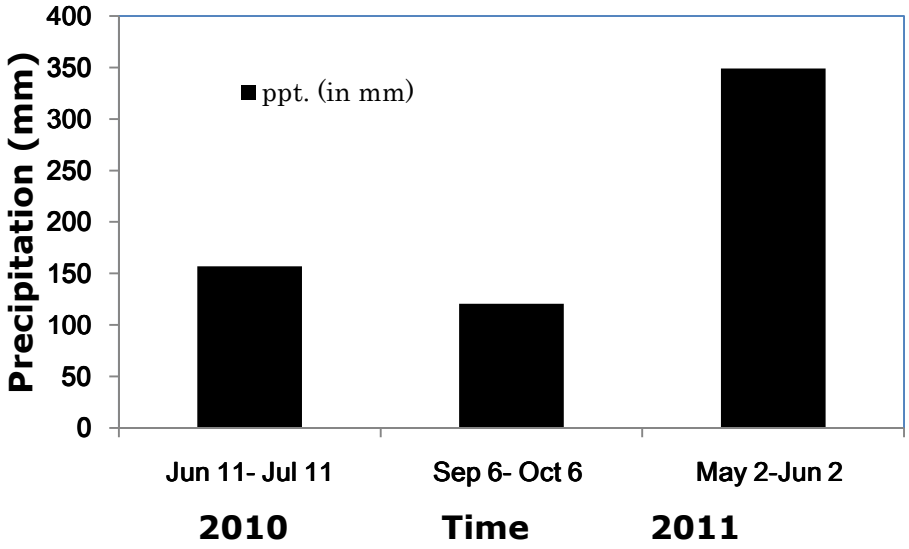

Fig. 4.18 Bar diagram showing amount of antecedent monthly average precipitation for different sampling campaigns for tidal effect observation

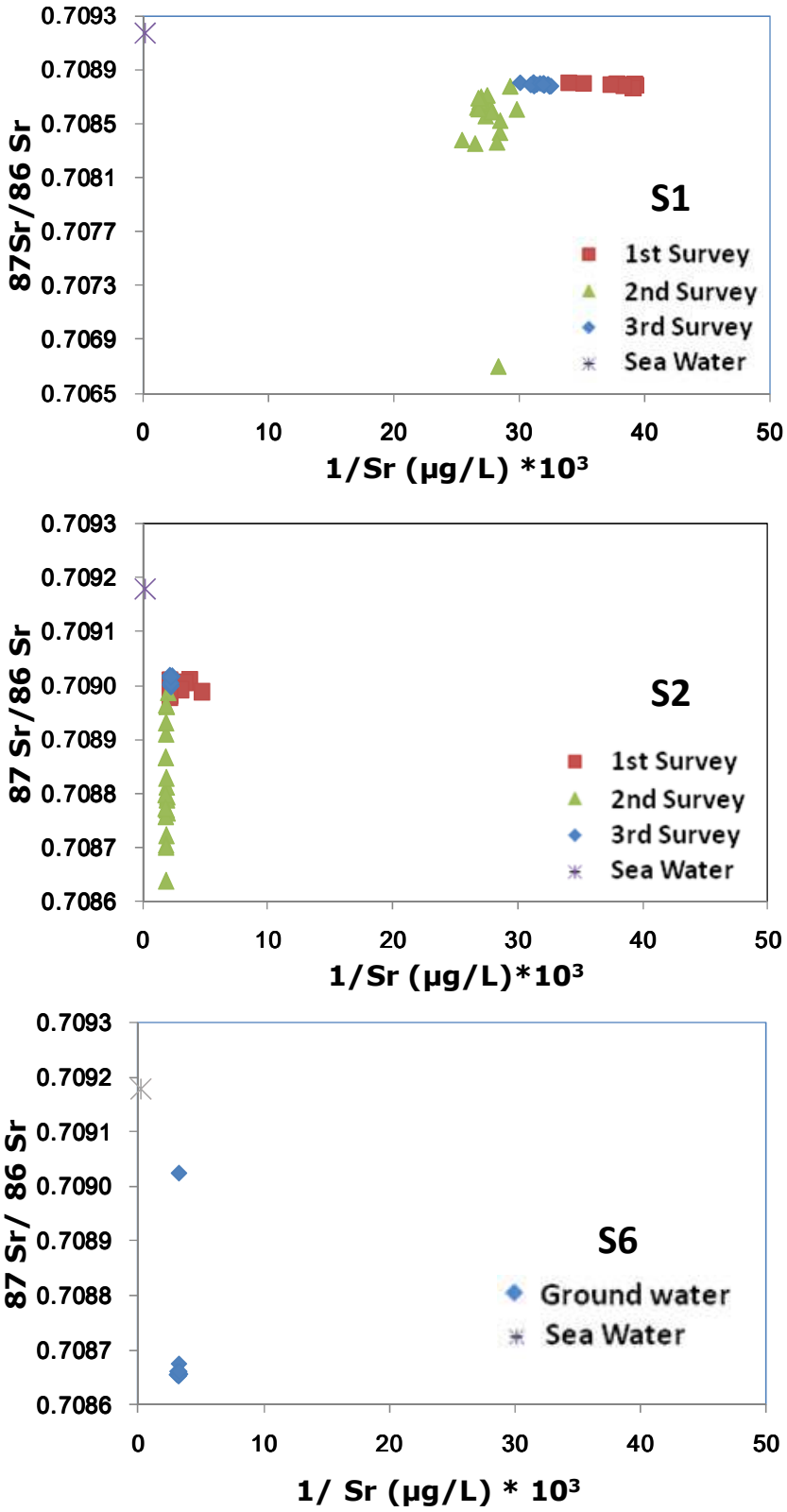

Fig. 4.19 Scatter plot between $^{87}Sr/^{86}Sr$ and 1/Sr for all three samples S1, S2 and S6 showing the SW-FW mixing pattern

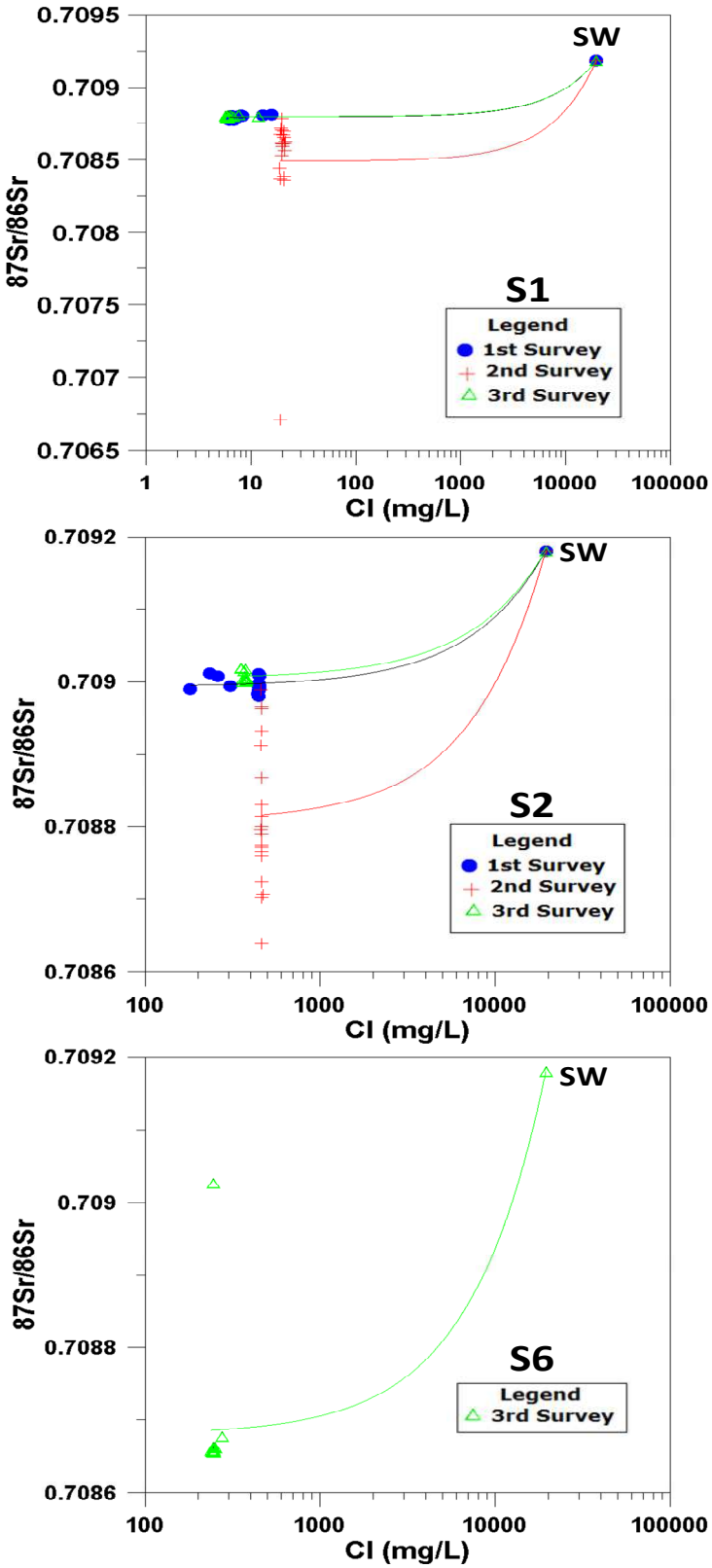

Fig. 4.20 Scatter plot between $^{87}Sr/^{86}Sr$ and Cl (mg/L) for all three samples S1, S2 and S6 showing the SW-FW mixing pattern

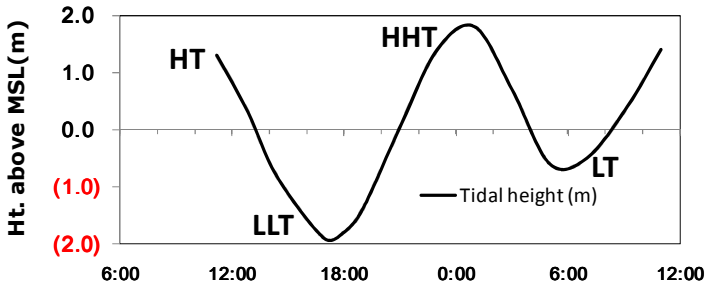

Mix. rate (%)	S1			S2			S6
Phase	1st	2nd	3rd	1st	2nd	3rd	3rd
HT	0.02	0.08	0.02	2.30	2.30	1.90	2.20
LLT	0.07	0.09	0.05	0.90	2.40	1.80	2.50
HHT	0.02	0.09	0.02	2.30	2.40	1.90	2.20
LT	0.03	0.09	0.02	2.30	2.40	1.90	2.20

*HT - High tide, LLT – Lower low tide, HHT – Higher high tide, LT – Low tide

Fig. 4.21 Statistics of Salt Water –Fresh Water mixing ratio in percentage for all the three samples during different tidal phase

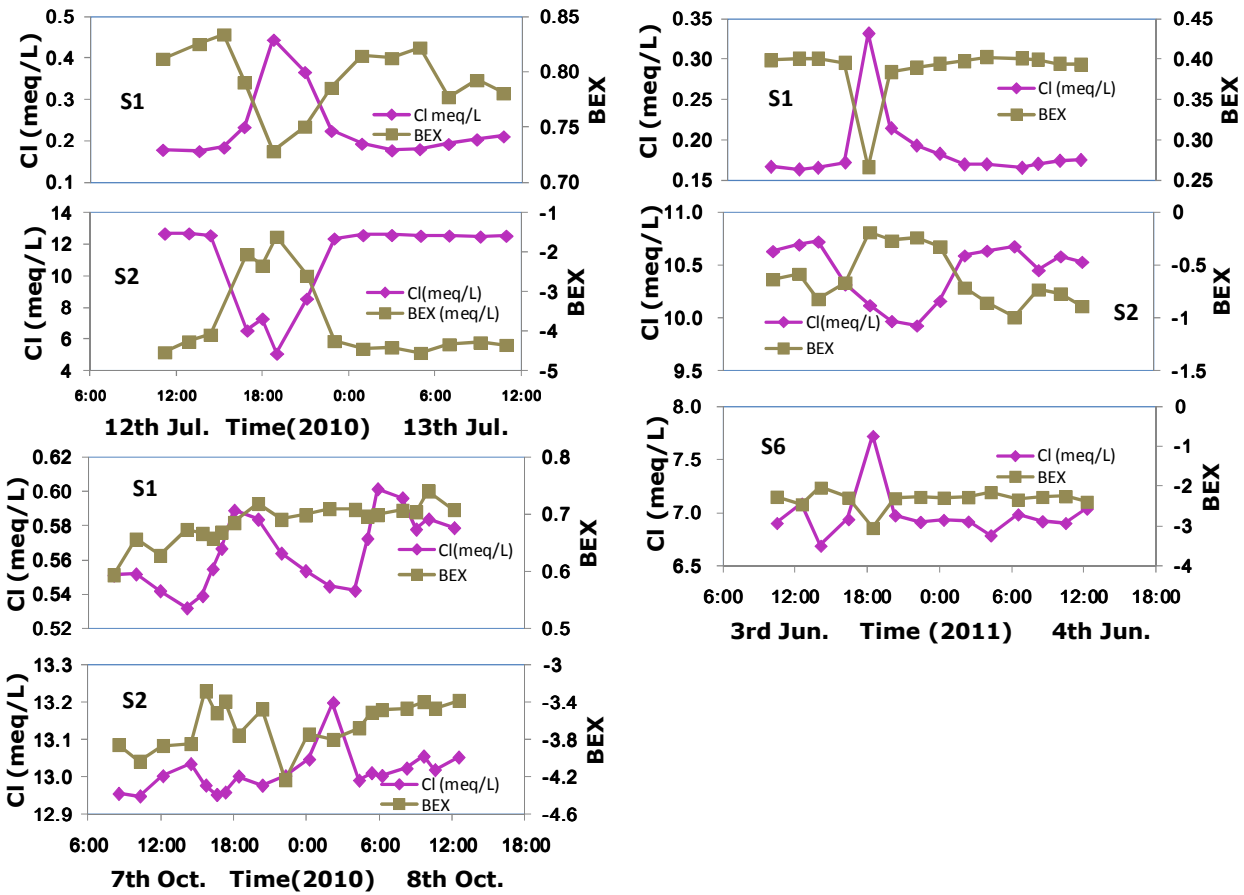

Fig. 4.22 Time series plot to show relationship between BEX and Cl for all three samples S1, S2 and S6 for a period of over twenty four hours during different survey campaign

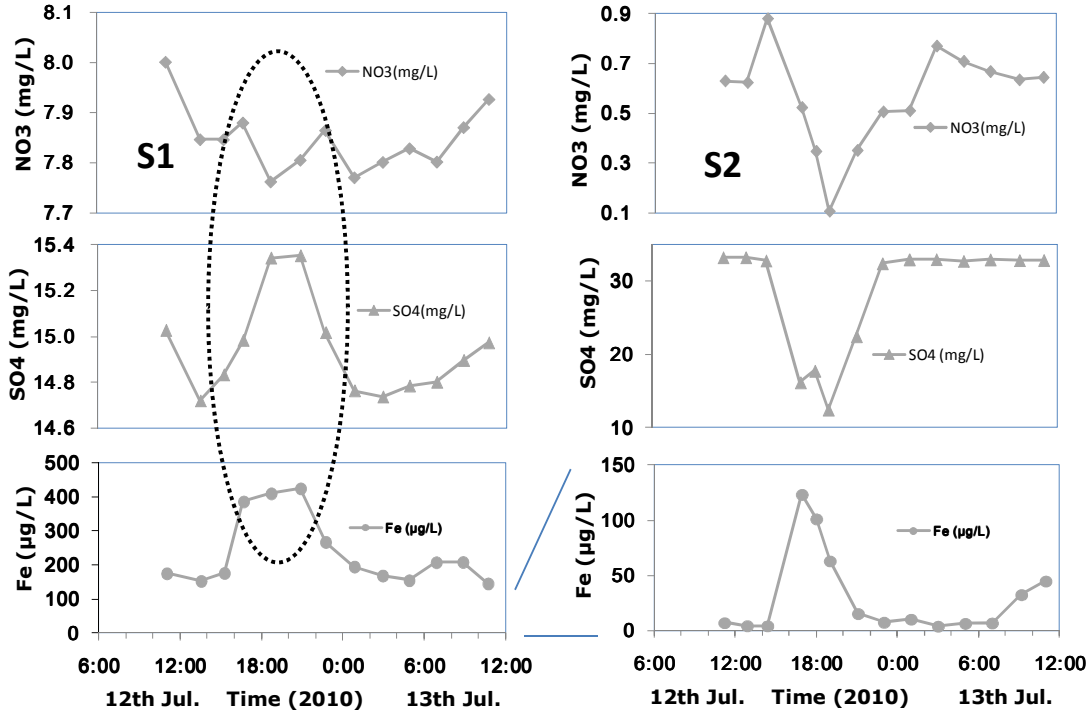

Fig. 4.23 Time series plot to show relationship between trace metal and different ions for samples S1 and S2 during July, 2010 to depict the reaction mechanism responsible for its mobilization.

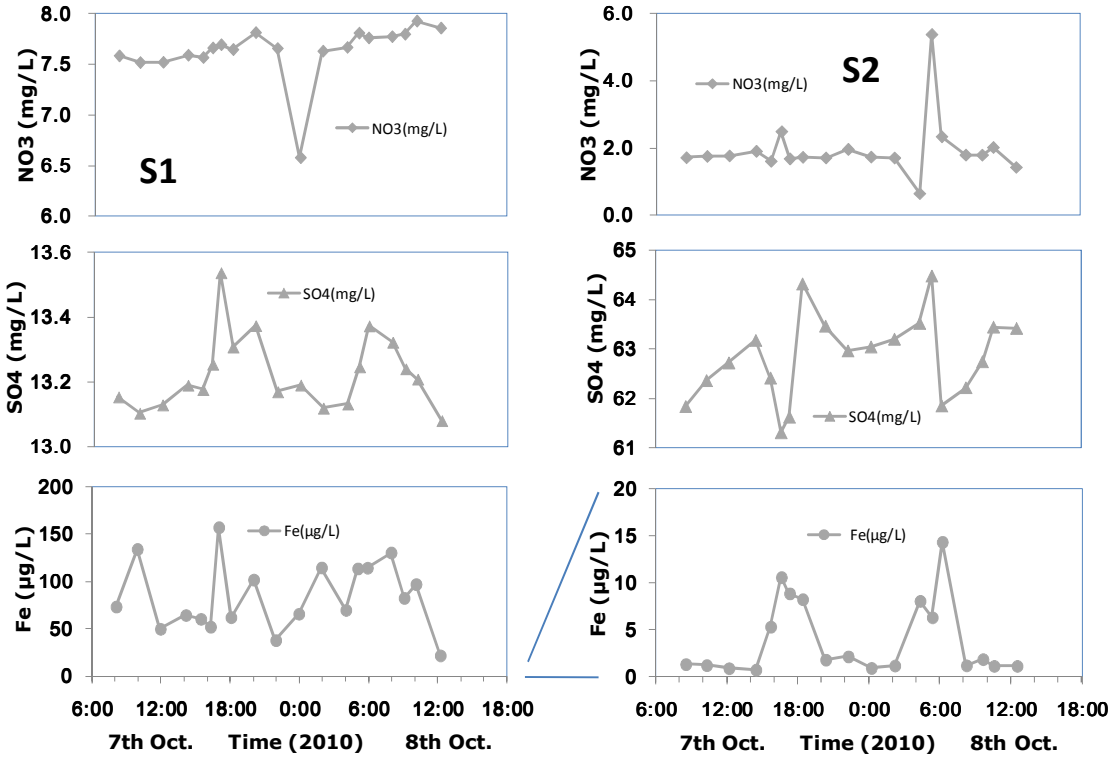

Fig. 4.24 Time series plot to show relationship between trace metal and different ions for samples S1 and S2 during October, 2010 to depict the reaction mechanism responsible for its mobilization

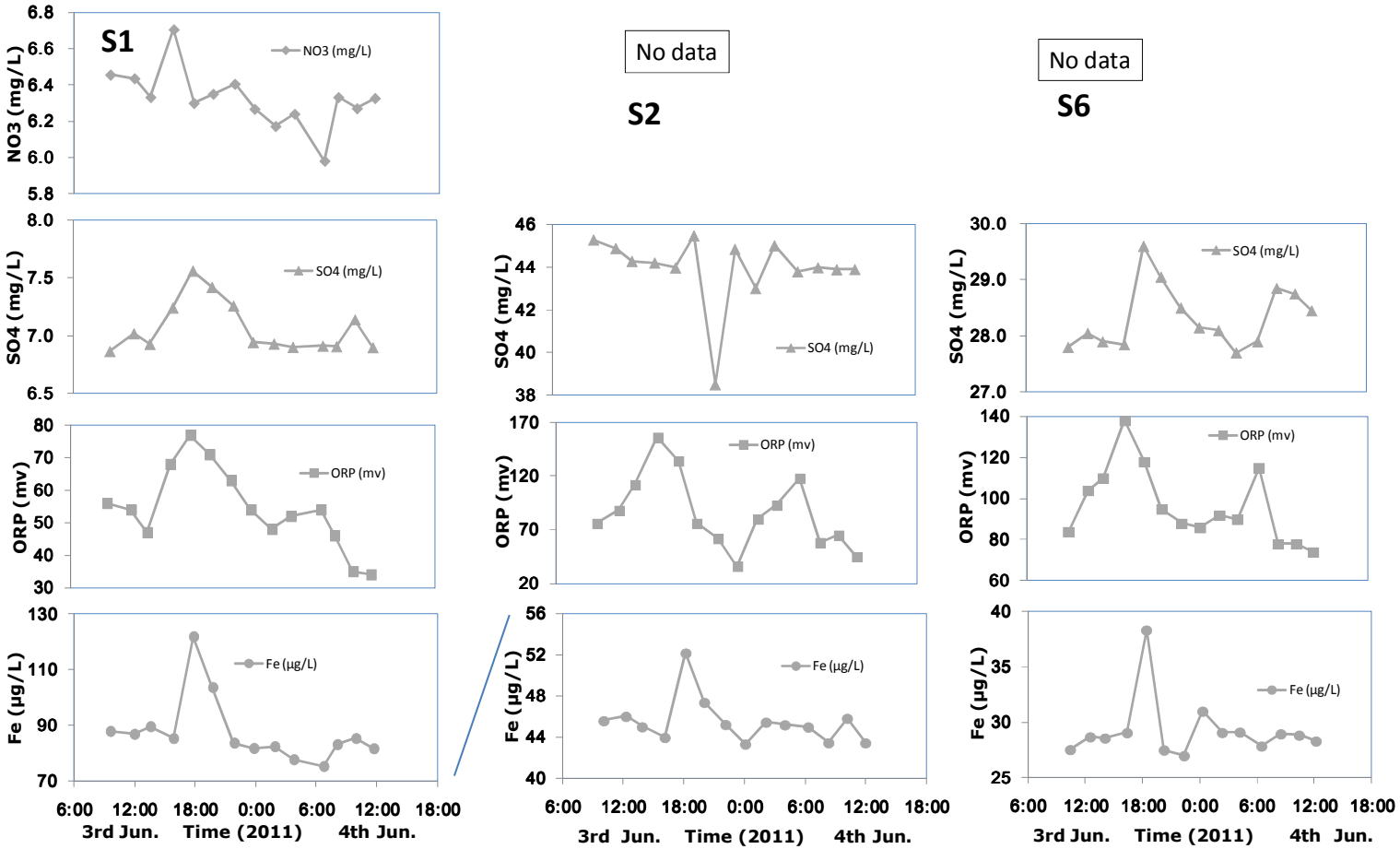

Fig. 4.25 Time series plot to show relationship between trace metal and different ions for all three samples S1, S2 and S6 during June, 2011 to depict the reaction mechanism responsible for its mobilization

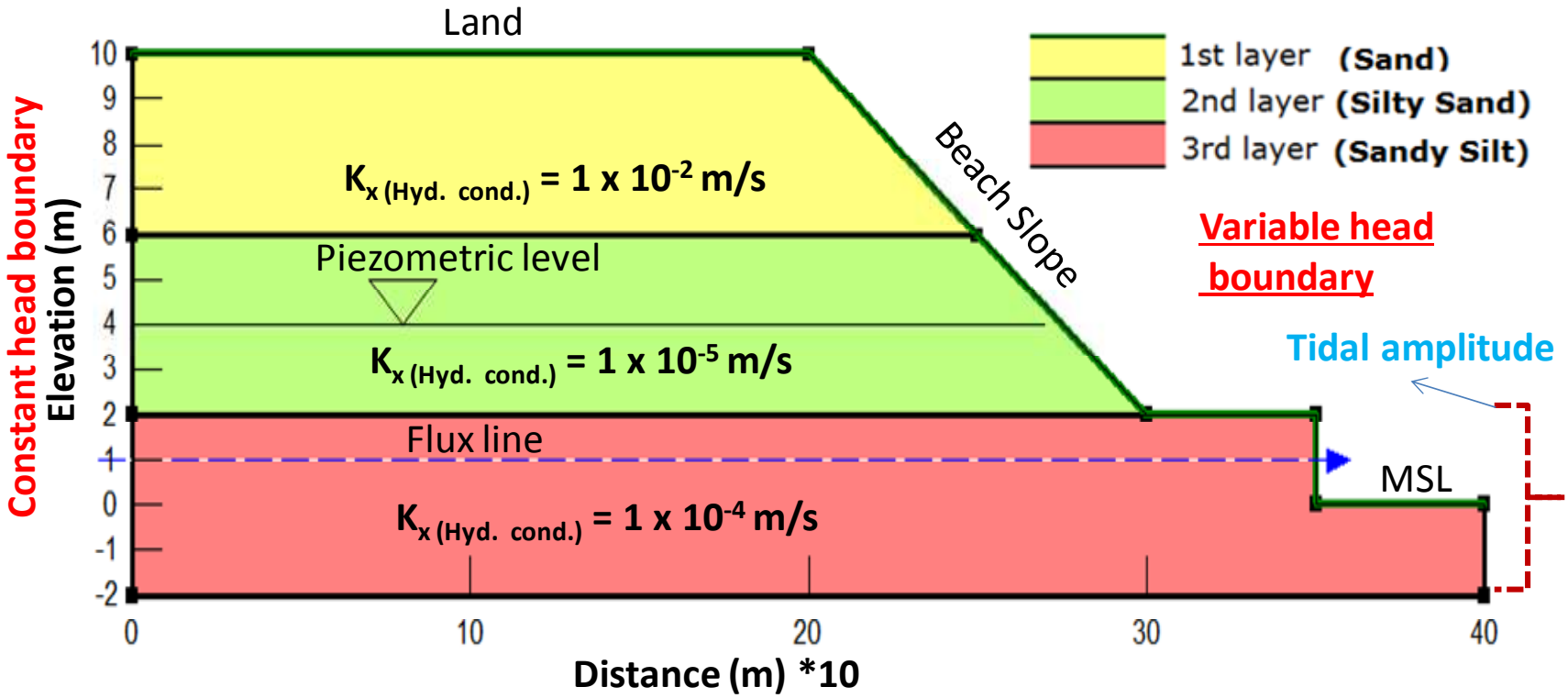

Fig. 4.26 Problem domain consisting of unconfined aquifer for numerical simulation

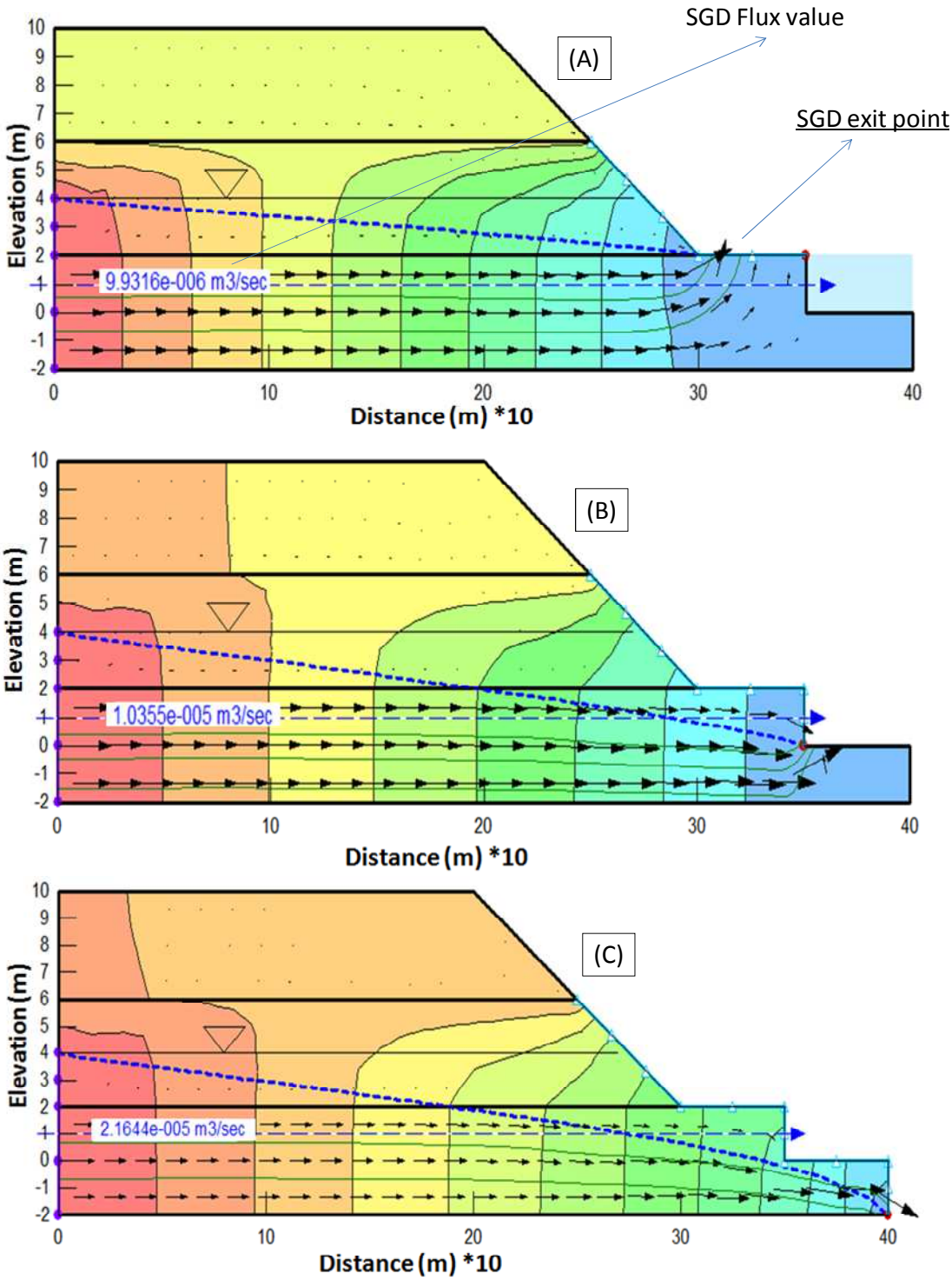

Fig. 4.27 Simulation output for submarine groundwater discharge for the domain with lower boundary at two meter deeper than mean sea level. Here (A), (B), and (C) are denoting results for high tide, zero tide and low tide situation respectively

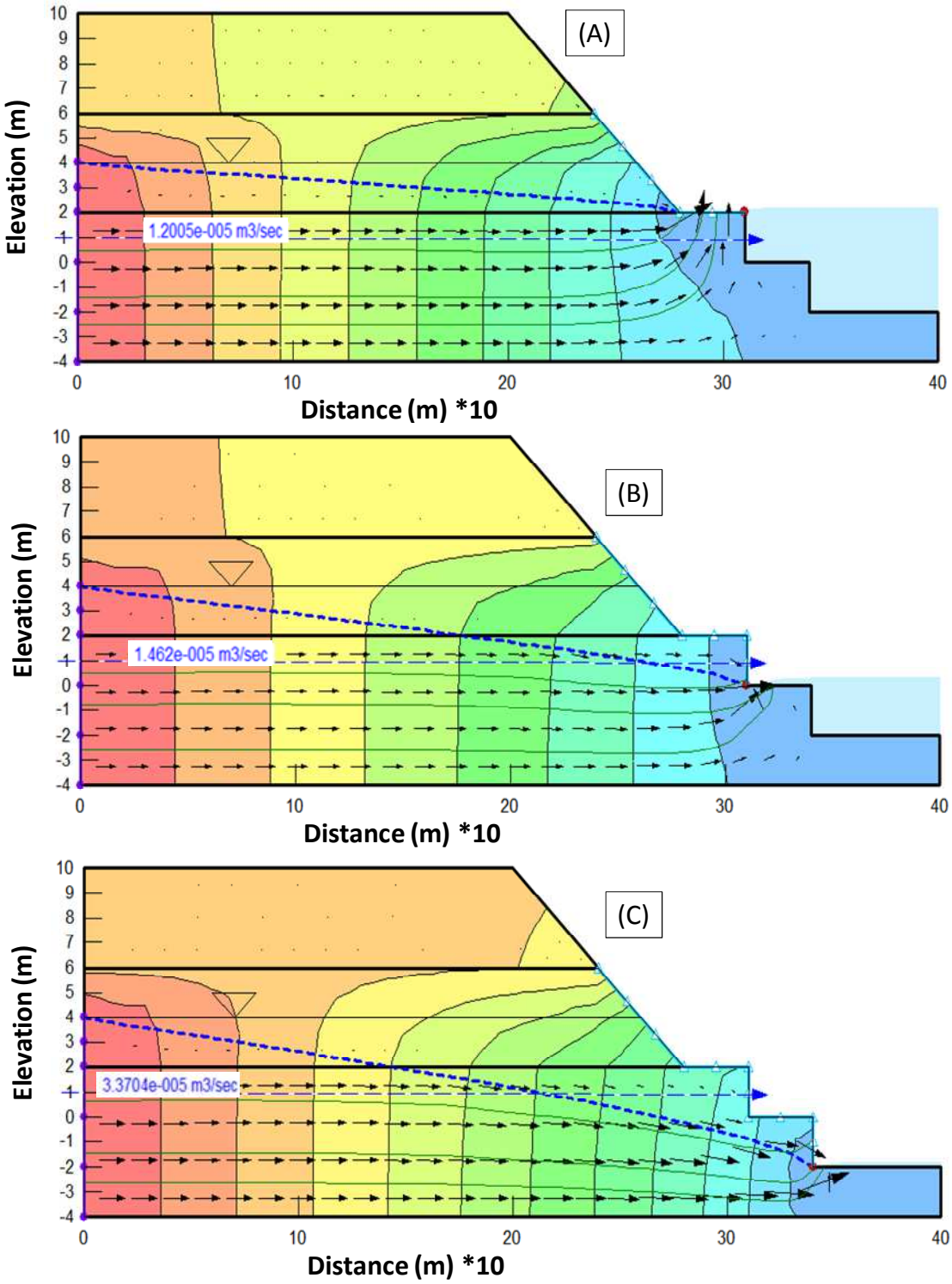

Fig. 4.28 Simulation output for submarine groundwater discharge for the domain with lower boundary at four meter deeper than mean sea level. Here (A), (B), and (C) are denoting results for high tide, zero tide and low tide situation respectively

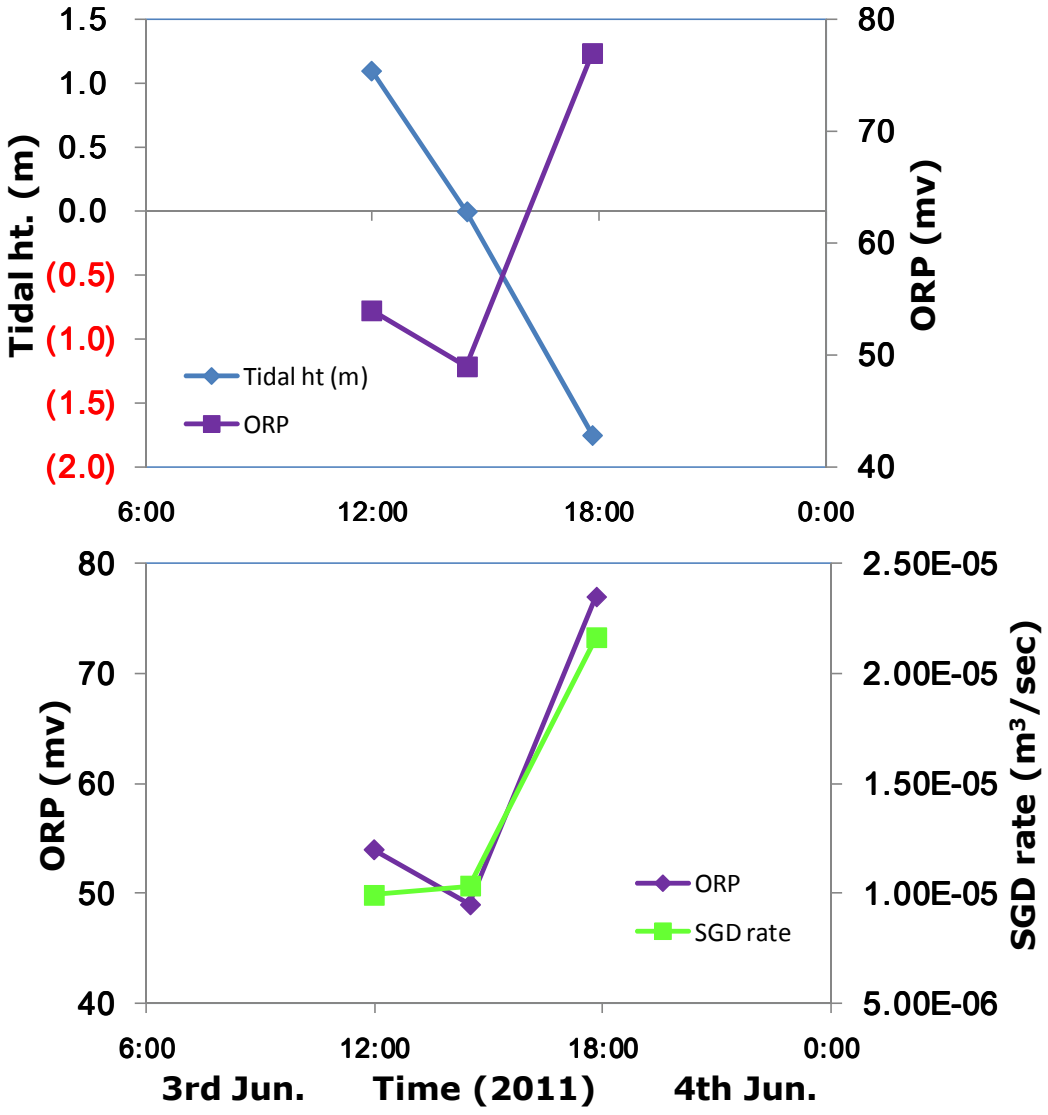

Fig. 4.29 Comparative presentation of time series fluctuation of SGD (obtained from simulation) and ORP (obtained from field observation) with different tidal phase

Table 4.2 Summary for aquifer properties, tidal efficiency and time lag for both the monitoring sites

Site	Distance from coast (D) (in meter)	Storage coefficient (S)	Aquifer thickness (b) (in feet)	Tidal efficiency	Average time lag (hours)
S1	200	0.17	20.0	0.516	2.90
S2	200	0.0001	65.6	0.522	4.65

Table 4.3 Saturation indices for the selected five iron minerals for all three water samples during different sampling campaign. (Shaded portion indicating values at lower low tide situation and low tide situation respectively

		S1 (Jul., 2010)						S2 (Jul., 2010)				
S. No.	Pyrite	FeS	Geothite	Siderite	Scorodite		S. No.	Pyrite	FeS	Geothite	Siderite	Scorodite
1	−0.15	−2.28	−10.95	−12.15	−8.59		1	−0.85	−5.03	−6.70	−8.79	−8.65
2	−0.15	−2.27	−10.89	−12.08	−8.60		2	−0.85	−5.33	−6.62	−8.72	−8.84
3	−0.15	−2.27	−10.86	−12.02	−8.59		3	−0.85	−5.53	−6.57	−8.66	−8.97
4	−0.16	−2.45	−10.94	−12.14	−8.58		4	−0.86	−5.01	−6.69	−8.78	−8.62
5	**−0.37**	**−2.66**	**−10.86**	**−11.98**	**−8.26**		5	**−1.07**	**−5.29**	**−6.52**	**−8.62**	**−8.81**
6	**−0.33**	**−2.68**	**−10.84**	**−11.62**	**−8.45**		6	**−1.07**	**−5.31**	**−6.15**	**−8.26**	**−8.83**
7	−0.18	−2.54	−10.90	−11.36	−8.51		7	−0.95	−5.69	−5.90	−8.00	−9.09
8	−0.16	−2.35	−10.96	−11.56	−8.54		8	−0.84	−5.74	−6.10	−8.20	−9.15
9	−0.16	−2.32	−10.98	−11.72	−8.58		9	−0.85	−5.79	−6.26	−8.36	−9.15
10	−0.15	−2.48	−10.90	−11.04	−8.57		10	−0.85	−5.61	−5.59	−7.68	−9.03
11	**−0.35**	**−2.48**	**−10.97**	**−11.00**	**−8.59**		11	**−0.93**	**−4.85**	**−5.54**	**−7.64**	**−8.53**
12	**−0.28**	**−2.57**	**−10.91**	**−12.11**	**−8.58**		12	**−0.96**	**−5.44**	**−6.65**	**−8.75**	**−8.92**
13	−0.16	−2.33	−10.88	−12.07	−8.57		13	−0.84	−5.42	−6.61	−8.71	−8.90
							14	−0.84	−5.28	−6.66	−8.76	−8.83
		S1 (Oct., 2010)						S2 (Oct., 2010)				
S. No.	Pyrite	FeS	Geothite	Siderite	Scorodite		S. No.	Pyrite	FeS	Geothite	Siderite	Scorodite
1	−0.35	−3.43	−11.41	−11.16	−7.97		1	−1.13	−4.65	−8.48	−10.06	−6.85
2	−0.33	−3.47	−11.48	−11.34	−7.96		2	−1.12	−5.42	−8.61	−10.24	−7.38
3	−0.34	−3.40	−10.54	−9.89	−7.97		3	−1.12	−4.95	−7.2	−8.79	−7.04
4	−0.32	−3.41	−11.19	−10.91	−7.96		4	−1.12	−5.35	−8.18	−9.81	−7.3
5	**−0.50**	**−3.40**	**−10.95**	**−10.55**	**−7.96**		5	**−1.16**	**−5.41**	**−7.82**	**−9.45**	**−6.64**
6	**−0.32**	**−3.40**	**−11.30**	**−11.07**	**−7.94**		6	**−1.21**	**−5.2**	**−8.34**	**−9.97**	**−7.05**
7	−0.32	−3.51	−11.05	−10.72	−7.94		7	−1.14	−5.06	−7.97	−9.62	−7.09
8	−0.31	−3.41	−11.39	−11.24	−7.89		8	−1.13	−5.35	−8.48	−10.14	−7.3
9	−0.30	−3.45	−11.28	−11.10	−7.90		9	−1.13	−6.07	−8.32	−10.00	−7.76
10	−0.31	−3.38	−10.46	−9.85	−7.91		10	−1.15	−6.15	−7.99	−8.75	−7.86
11	−0.31	−3.41	−10.20	−9.46	−7.93		11	−1.13	−5.94	−8.7	−8.36	−7.69
12	−0.31	−3.49	−11.43	−11.30	−7.95		12	−1.14	−5.79	−8.54	−10.20	−7.58
13	−0.30	−3.43	−11.27	−11.08	−7.94		13	−1.13	−4.74	−8.31	−9.98	−6.89
14	**−0.41**	**−3.47**	**−11.17**	**−10.93**	**−7.92**		14	**−1.12**	**−5.43**	**−8.16**	**−9.83**	**−7.34**
15	**−0.43**	**−3.46**	**−11.72**	**−11.77**	**−7.89**		15	**−1.18**	**−4.52**	**−8.99**	**−10.67**	**−6.73**
16	−0.30	−3.49	−11.18	−10.95	−7.89		16	−1.19	−5.34	−8.17	−9.85	−7.27
17	−0.30	−3.43	−10.69	−10.21	−7.91		17	−1.13	−7.95	−7.44	−9.11	−8.99
18	−0.28	−3.44	−11.85	−12.00	−7.89		18	−1.11	−6.29	−9.19	−10.90	−7.9
19	−0.30	−3.35	−12.00	−12.18	−7.89		19	−1.12	−6.45	−9.41	−11.08	−7.99
		S1 (Jun., 2011)						S2 (Jun., 2011)				
S. No.	Pyrite	FeS	Geothite	Siderite	Scorodite		S. No.	Pyrite	FeS	Geothite	Siderite	Scorodite
1	−0.23	−3.58	−12.30	−12.60	−9.04		1	−0.63	−6.13	−9.84	−11.66	−7.84
2	−0.23	−3.57	−12.24	−12.53	−9.05		2	−0.63	−6.43	−9.76	−11.59	−8.03
3	−0.23	−3.57	−12.21	−12.47	−9.04		3	−0.63	−6.63	−9.71	−11.53	−8.16
4	−0.23	−3.55	−12.29	−12.59	−9.03		4	−0.64	−6.11	−9.83	−11.65	−7.81
5	**−0.42**	**−3.55**	**−12.21**	**−12.43**	**−8.71**		5	**−0.85**	**−6.39**	**−9.66**	**−11.49**	**−8**
6	**−0.42**	**−3.63**	**−12.19**	**−12.07**	**−8.90**		6	**−0.85**	**−6.41**	**−9.29**	**−11.13**	**−8.02**
7	−0.21	−3.54	−12.25	−11.81	−8.96		7	−0.73	−6.79	−9.04	−10.87	−8.28
8	−0.23	−3.57	−12.31	−12.01	−8.99		8	−0.62	−6.84	−9.24	−11.07	−8.34
9	−0.22	−3.58	−12.33	−12.17	−9.03		9	−0.63	−6.89	−9.4	−11.23	−8.34
10	−0.23	−3.57	−12.25	−11.49	−9.02		10	−0.63	−6.71	−8.73	−10.55	−8.22
11	**−0.37**	**−3.57**	**−12.32**	**−11.45**	**−9.04**		11	**−0.71**	**−5.95**	**−8.68**	**−10.51**	**−7.72**
12	**−0.23**	**−3.57**	**−12.26**	**−12.56**	**−9.03**		12	**−0.74**	**−6.54**	**−9.79**	**−11.62**	**−8.11**
13	−0.22	−3.56	−12.23	−12.52	−9.02		13	−0.62	−6.52	−9.75	−11.58	−8.09
14	−0.20	−3.58	−12.26	−12.57	−9.02		14	−0.62	−6.38	−9.8	−11.63	−8.02

Table 4.4 Summary for the processes responsible for the water quality change with tidal fluctuation

Survey	S1(Fresh water)	S2 (Salinized water)	S3 (Salinized water)
1st Survey	Cation exchange > Sea water mixing	Sea water freshening + Cation echange	Data not available
2nd Survey	Sea water mixing > Cation exchange	Sea water mixing > Cation exchange	Data not available
3rd Survey	Cation exchange > Sea water mixing	Cation exchange > Sea water mixing	Cation exchange > Sea water mixing

Part - III

4.3 Conceptual model for the tidal implication on coastal ground water quality

From above results, possible mechanisms for the tidal implication in case of the different aquifers were shown by simple conceptual sketching (Fig. 4.30). Here it is clear that during low tide situation, position of brackish water- fresh water interface front also changes which results into solute exchange between different water (selective movement) without replacing the water as a whole for unconfined aquifer. On the other hand for the confined aquifer, presence of confining layer doesn't allow direct movement of tidal wave, however little change at ionic level might took place because of dilution through nearby pounded water.

To make this idea more clear, schematic diagram considering the screen depth of monitoring well from unconfined region i.e. "S1" (assuming very less or no tidal effect for confined aquifer) for both high tide and low tide situation were plotted in Fig. 4.31 & 4.32. As it was observed from the land use – land cover map (Fig. 2.4), that coastal area (around the "S1" and "S2") is mainly occupied by industrial set up. Among this setup, dominant types are water consuming industries e.g. mineral processing, textile, and beverage industry (Saijo City report, 2008). Because of this high pumping rate, saline plume is induced more towards the inland and there is flow of brackish water from sea towards the land. At high tide situation, Piezometric level is relatively lower than that of sea level, however high enough to cover the screen depth of the monitoring well which means ground water in the monitoring well is under reducing

condition and trace metals concentration is low. Also at the lower depth of inland aquifer matrix, sea water is in transitional equilibrium with ground water.

During low tide situation, lowering of Piezometric level is less than that of sea level which causes creation of hydraulic gradient towards the coast. This leads to increase in submarine groundwater discharge (SGD) rate (shown by black arrow in Fig. 4.32) and thus aquifer matrix near capillary fringe gets oxidized very quickly ultimately results in trace metal mobilization. Following this phenomenon, because the creation of unsaturated zone in fresh water aquifer; tidal wave energy pushes the brackish font more toward inland with high magnitude. As a result of the above process, brackish water touches the monitoring well screen as recharging source for short term and mass flux between these two different density water bodies causes a short term change in water quality through solute exchange between different water types via soil matrix.

Calculation of distance inland at which Piezometric fluctuation reduce to 1% that at shore

After getting a fair amount of idea about the tidal effect on water quality it is also necessary to understand about the extent and limit of this effect in order to implement better ground water management plan at coastal aquifers around the world.

Considering vertical land-ocean interface with no seepage face and with only one tide, Li et al. (1999) stated that distance at which the magnitude of water table fluctuations is reduced to 1% of that at the shore was calculated by the equations (4.11) and (4.12):

$$\kappa = \sqrt{\frac{\omega n_e}{2DK}} \qquad \text{…….(4.11)}$$

κ = wave number, ω = tidal frequency, D= mean aquifer thickness, K = hydraulic conductivity, n_e = effective porosity

$$L = 4.6/\kappa \qquad \ldots\ldots(4.12)$$

For sample "S1"

Geological signature of aquifer – Sand and Silt type

T = 14/21 day, D = 65.6 feet, n_e = 20 %, K = 0.01 m/sec

Putting all these values in above equations (4.11) and (4.12), we get

κ = 0.00669 m^{-1} and L = 687.6 meter

For sample "S2"

Geological signature of aquifer – Sand and Silt type

T = 14/21 day, D = 65.6 feet, n_e = 1 %, K = 2.8 x 10^{-5} m/sec

Putting all these values in above equations (4.11) and (4.12), we get

κ = 0.04935 m^{-1} and L = 93.2 meter

Using respective aquifer properties, calculated landward distance for both "S1" and "S2" were 687.6 and 93.2 meters respectively. This means that at Saijo plain, beyond this distance there should not be any tidal effect on water characteristics for respective aquifer types. However, field condition is more complex than our consideration, so there might be chances for some discrepancies.

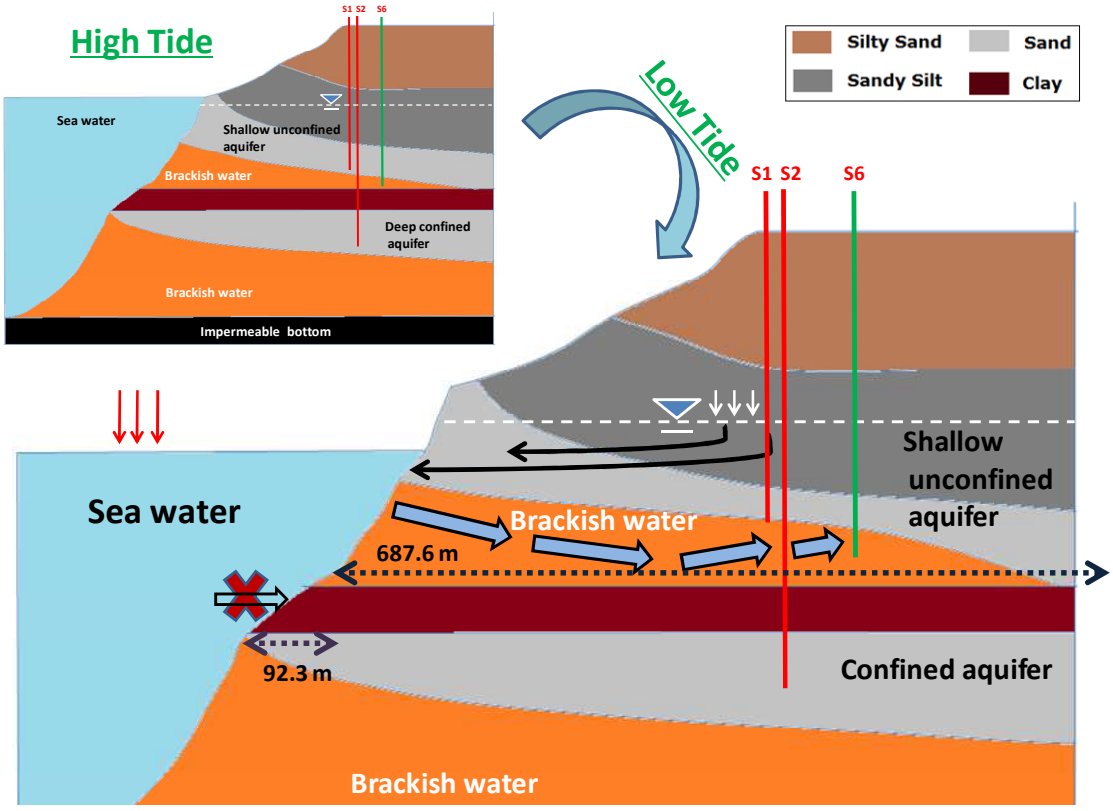

Fig. 4.30 Conceptual sketching showing the mechanism responsible for tidal effect on water characteristics in case of different aquifers. Lower part of the figure represents low tide situation where dotted line shows brackish water – fresh water interface temporarily shifted towards land

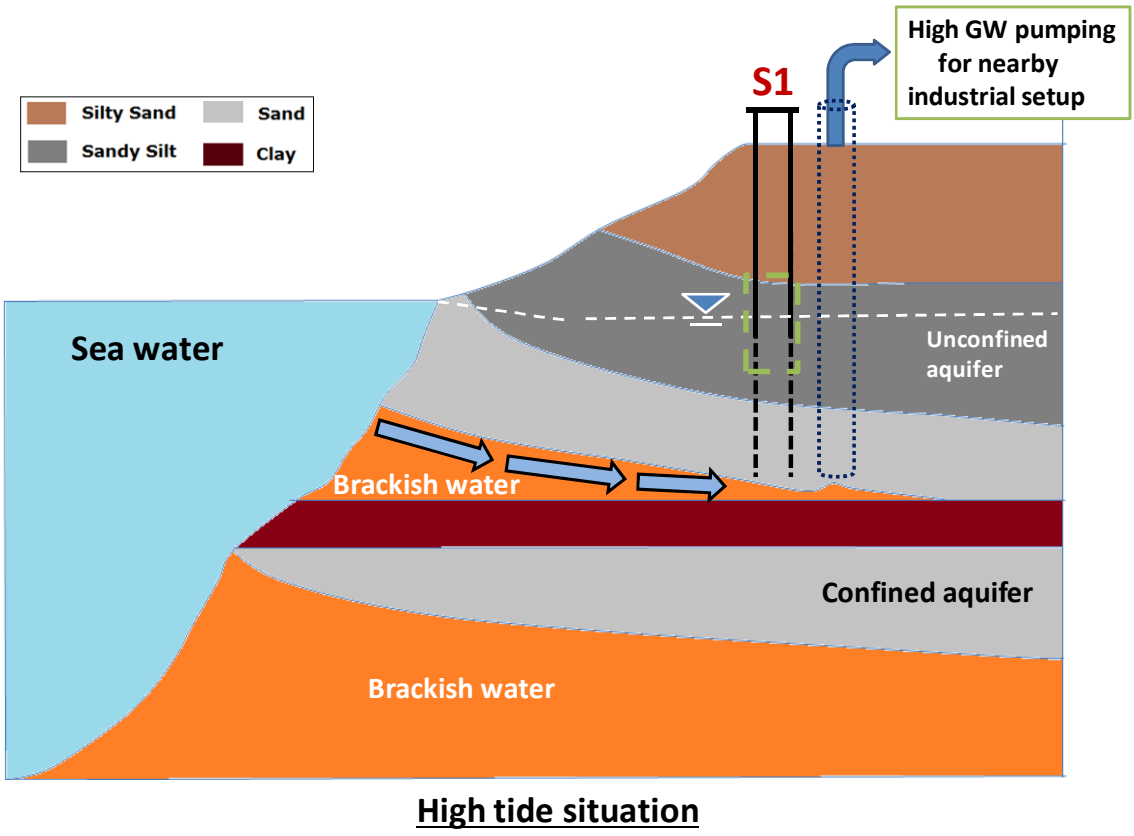

Fig. 4.31 Conceptual sketching showing the recharging condition in case of unconfined aquifers (monitoring well with screen depth) at high tide situation

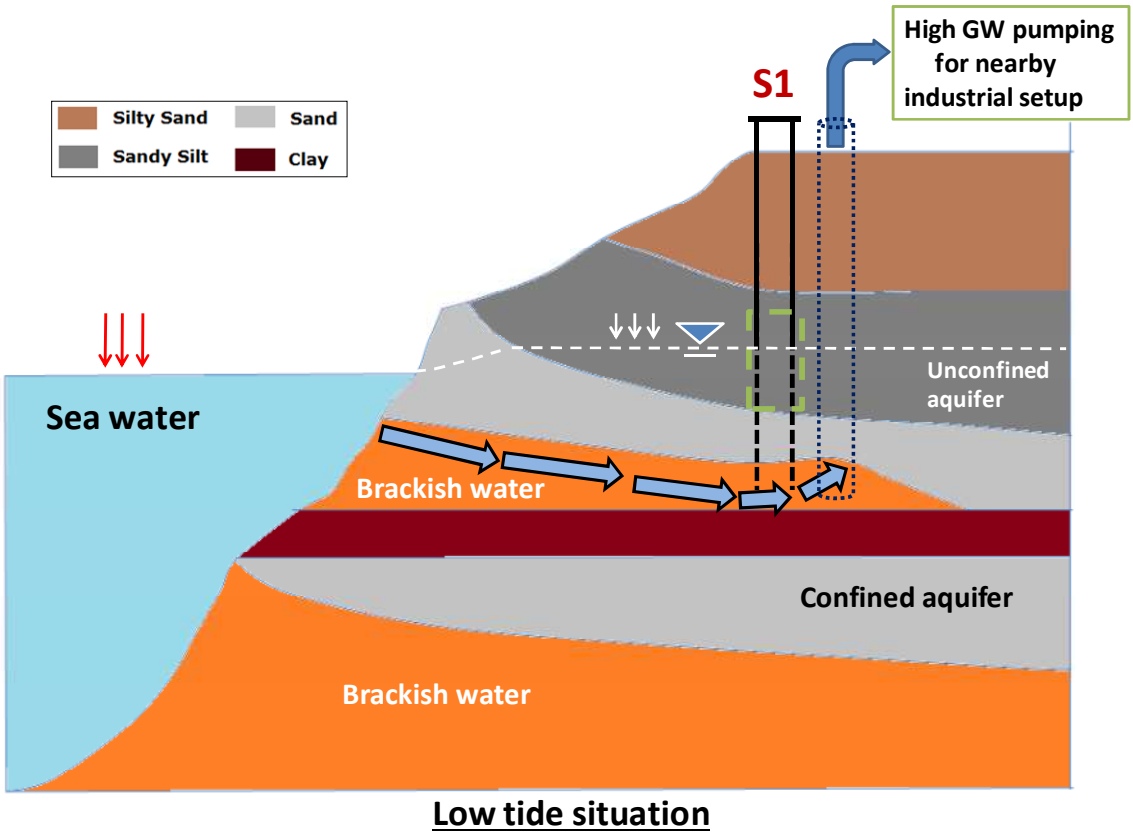

Fig. 4.32 Conceptual sketching showing the change in recharging condition in case of unconfined aquifers (monitoring well with screen depth) at low tide situation. Also because of high SGD rate the aquifer get quickly oxidized and facilitates trace metal mobilization. Here two headed arrow shows the inland distance at which tidal effect reduces to 1% that at shore for different aquifers

Chapter 5

Conclusions

From hydro-geochemical study at spatio-temporal scale in Saijo plain, water type found very heterogeneous in nature even in small area which is an elemental signature of complex geology and patchy distribution of aquifer system. Major ion analysis suggests that most of the water samples were showing good quality i.e. all the physico-chemical parameters were less than the highest desirable or maximum permissible limit set by WHO, while two samples show higher chloride concentration i.e. nascent state of salinization which needs immediate attention. Temporal variation of water quality is mainly controlled by cation exchange process due to rock water interaction or simple mixing with aquifers of different ionic strength. Isotopic ($\delta^{18}O$, δD and $^{87}Sr/^{86}Sr$) study revealed that most of the water samples are meteoric in origin and some of the samples have a primary problem of salinization caused mainly through simple local SW-FW mixing.

Findings for the study of tidal effects on water quality for different aquifers at Saijo plain can be concluded in following points: First, tidal fluctuation at diurnal scale, significantly affects ionic signature of groundwater along with Piezometric level for unconfined aquifer whereas the effect is less prominent with confined aquifer. The mechanism responsible here (i.e. for the change in ionic characteristics) is horizontal mass movement i.e. mass flux generated due to change in boundary condition towards sea. In other words, during the low tide situation, brackish water plume gets further pushed towards inland and acts as a recharging source for the ground water (very short

time phenomenon) results in to change in the water type. Cation exchange and local mixing of brackish water – fresh water is suggested to be main physiochemical processes operating during this time interval. However, mobilization for heavy metal in groundwater samples from both aquifers occurs mainly because of second process i.e. local mass movement across Piezometric level. Oxidation-reduction in the capillary zone of the aquifer matrix is suggested to be the main physiochemical process responsible here. Results from numerical simulation also depicts that tidal height affects the amount and position of submarine groundwater discharge (SGD) and thus value for oxidation reduction potential (ORP) for groundwater fluctuates which ultimately play a positive role for trace metal mobilization. Though changes/fluctuations in magnitude of many chemical parameters caused by these processes are not very high but the phenomenon is significantly necessary to be pointed out.

Second, seasonal change of rainfall amount is also one of the important factors affecting the intensity of tidal effect on water quality.

Third, presence of aquitard /aquiclude (e.g. Clay) hinder partially or completely the propagation of tidal wave to affect water quality parameters in coastal aquifers. In other words, position/location of screen depth for the borehole is an important factor controlling the characteristics of tidal effect on the ground water type at point scale.

Fourth, distance for which tidal effect will diminish for unconfined and confined aquifers are 687.6 and 93.2 meters respectively in Saijo plain. At last the general framework mentioning the trend of tidal effect on ground water characteristics with respect to the different aquifer properties is shown in Figure 5.1.

From above work it was found that for samples taken from bore well with deeper screen depth (about 25 meter) has a problem of salinization so it will be

recommended to have an alternate tube/bore well with shallow screen depth (about 15 meter) in order to prevent the encounter of SW–FW interface as a short term solution. However, for long term solution, it is better to study ground water budget in order to calculate safe extraction yield per capita for sustainable growth. On the other hand, from the geological point of view, since there are many faults which occur in older rock of hard nature and affecting the overlying sediment in this plain, so it is very hard to think about the building barrier to prevent sea water encroachment.

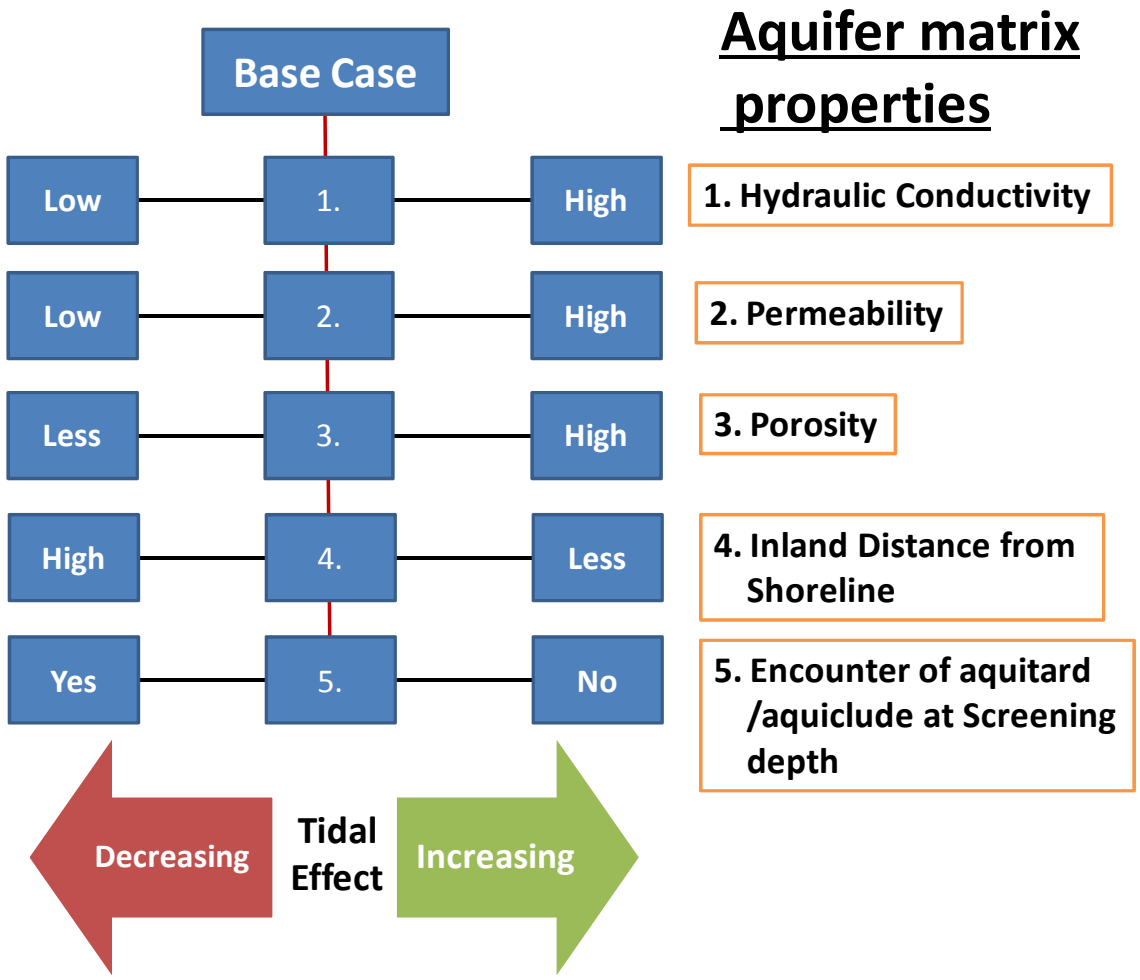

Fig. 5.1 General framework showing the trend of tidal effect on ground water characteristics with respect to the different aquifer properties

ACKNOWLEDGEMENTS

Author would like to express gratitude to his mentor, Prof. MAKI TSUJIMURA for his expert guidance, patient hearing, constant encouragement, enthusiasm and sense of understanding towards author which makes him able to work according to his style of working. Words cannot convey author`s respect and thankfulness for him. Author can never forget his co-operation and contribution to this dissertation through out of his life. He has not only helped at each and every stage of this investigation but also enabled author with the many abilities like thinking scientifically, critically, rationally and big, which will continue to guide author in future.

Author expresses his sincere gratitude to Dr. Takanori Nakano, his co-adviser for allowing him to discuss anything, anytime. He was always there whenever author was in need of him. Author has never seen such a loyal and down to earth person, till date. He is having such a magical understanding of the need of a student that one needs not to open their mouth for anything they require. He was very easily approachable in spite of his busy schedule.

Author should not forget to convey his heartiest thanks to Prof. Norio Tase for his keen guidance coupled with practical approach, critical comments and ability of finding author`s minute mistakes, which has been proven immensely fruitful to make author`s understanding precise. Author would like to offer his sincere gratitude to Prof. Michiaki Sugita, Prof. Jun Asanuma and Dr. Tsutomu Yamanaka who have provided him help and support throughout this work and many a times, sweet & sour discussion. Despite of their busy schedule, they all were always beside him, whenever author needed them.

Author is also very much thankful to Tokumasu San for giving a tirelessly help during his sampling in Saijo City along with his kind help for giving author and his colleagues a tour to glimpse to natural beauty of Saijo Plain. Author would also like to sincerely thank to all members of life and environment section, Municipal office of Saijo city for their valuable help to our field work. Author would like to give sincere

thank to Dr. Yu Saitoh and Dr. Ki-Cheol Shin for providing the necessary logistic support to conduct experiments at RIHN, Kyoto, Japan.

Author would like to give his heartiest thanks to Sho Iwagami for being his tutor cum first friend in Japan and for giving such a fantastic company not only in daily life but in academics as well. Author takes this opportunity to express his sincere thanks to his lab mates Abe-San, Anis-San, Kumasaka-San, Zang-San, Matsumoto-San, Ikeda San, Takahashi-san, Yamada-Kun, Kawaguchi Kun, Sakakibara Kun, Wakabayashi-Kun and Yoshizawa san who have provided him help and support throughout his stay in Japan. Author's work association with desk mates like Matsuno-San, Wei-San made his much tedious work easy by providing cheerful environment. Heartily thanks to his friends Ram Avtar and Amit Mishra who have kept him smiling through their sincere support, help and also for providing him the support for lending an ear to whatever author said. Author has no hesitation to say that contribution of all and each of these persons are immense.

Author is grateful to the Government of Japan for supporting his study and stay in Japan through Monbu-kagakusho scholarship.

At the end no words can explain the gratitude for the unexpressed immense patience and encouragement given to him by his family who have sustained his energy levels throughout the work and inspired him to put his best efforts in everything author did. Author is feeling lucky for having such a lovely family and this dissertation may not be a reality today without their support. Finally author would like to thank almighty god for giving him cheerful life and good health to finish this work with great enthusiasm.

Bibliography

Abdullah, M.H., Mokhtar, M.B., Tahir, S.H.J., Awaluddin, A. B.T. (1997). Do tides affect water quality in the upper phreatic zone of a small oceanic island, Sipadan Island, Malaysia? Environmental Geology, 29, 1/2, 112-117.

Adams, S., Titus, R., Pietersen, K., Tredoux, G. (2001). Hydrochemical characteristics of aquifers near Sutherland in the Western Karoo, South Africa. Journal of Hydrology, 241, 91-93.

Appelo, C.A.J., Postma, D. (2005). Geochemistry, Groundwater and Pollution. Second edn, Balkema, pp. 649.

Aryafar, A., Ardejani, F.D. (2009). Anisotropy and bedding effects on the hydro geological regime in a confined aquifer to design an appropriate dewatering system. International Journal of Environmental Science and Technology, 6, 4, 563-570.

Banno, S., Sakai, C. (1989). Geology and metamorphic evolution of the Sanbagawa metamorphic belt, Japan. Evolution of Metamorphic Belts, Geological Society Special Publication, 43, 519–32.

Bullen, T.D., Kendall, C. (1998). Tracing of Weathering Reactions and Water Flowpaths: A Multi-isotope Approach. In: C. Kendall and J.J. McDonnell (Eds.), Isotope Tracers in Catchment Hydrology. Elsevier, Amsterdam, 611-646.

Carr, P.A., Kamp, G.S.V.D. (1969). Determining aquifer characteristics by the tidal method. Water Resources Research, 5, 5, 1023-1031.

Chan, S.Y., Mohson, M.F.N. (1992). Simulation of tidal effects on contaminant transport in porous media. Ground Water, 30, 1, 78-86.

Chen, K.P., Jiao, J.J. (2007). Seawater intrusion and aquifer freshening near reclaimed

coastal area of Shenzhen. Water Science and Technology, 7, 137-145.

Cheng, J.M., Chen, C.X. (2001). Three Dimensional modeling of density-dependent salt water intrusion in multilayered coastal aquifers in Jahe River Basin, Shandong Province, China. Ground Water, 39, 1, 137-143.

Church, T.M. (1996). A groundwater route for the water cycle. Nature, 380, 18, 579-580.

Coetsiers, M., Walraevens, K. (2006). Chemical characterization of the Neogene Aquifer, Belgium. Hydrogeology Journal, 14, 1556–1568.

Datta, B., Vennalakanti, H., Dhar, A. (2009). Modeling and control of saltwater intrusion in a coastal aquifer of Andhra Pradesh, India. Journal of Hydro-environment Research, 3, 148-159.

Drever, J.I. (1997). The geochemistry of natural waters: surface and groundwater environment, Third edition. Prentice-Hall, pp. 436.

Erskine, A.D. (1992). The effect of tidal fluctuation on a coastal aquifer in the UK. Groundwater, 29, 4, 556-562.

Fakir, Y., Razack, M. (2003). Hydrodynamic characterization of a Sahelian coastal aquifer using the ocean tide effect (Dridrate Aquifer, Morocco). Journal of Hydrological Sciences, 48, 3, 441-454.

Farrell, E.R. (1994). Analysis of groundwater flow through leaky marine retaining structures. Geotechnique, 44, 2, 255-263.

Faure, G., Mensing, T.M. (2005). Isotopes: Priciples and applications. Third edition, John Wiley and Sons, New York, pp.897.

Fisher, C.W. (1986). Tidal circulation in Chesapeake Bay. PhD Thesis of Old Dominion University, pp.255.

Forcada, E.G. (2010). Dynamics of Sea water interface using hydrochemical facies evolution diagram. Ground Water, 48, 2, 212-216.

Forcada, E.G., Bencini, A., Pranzini, G. (2010). Hydrochemical consideration about the origin of groundwater salinization in some coastal plains of Elba Island (Tuscany, Italy). Environmental Geochemistry and Health, 32, 243-257.

Freeze, R. A., Cherry, J. A. (1979). Groundwater, Prentice-Hall. Inc., Englewood. Cliffs, New Jersey, pp. 604.

Frost, G.D., Toner, R.N. (2004). Strontium isotopic identification of water-rock interaction and groundwater mixing. Ground Water, 42, 3, 418-432.

Garrels, R.M., Christ, C.L. (1965). Solutions, minerals and equilibria. New York: Harper & Row, pp.450.

Gibbes, B., Robinson, C., Li, L., Lockington, D. (2007). Measurement of hydrodynamics and pore water chemistry in intertidal groundwater systems. Journal of Coastal Research SI, 50, 884 – 894.

Grant, U.S. (1948). Influence of the water table on beach aggradation and degradation. Journal of Marine Research, 7, 655-660.

Gregg, D.O. (1966). An analysis of groundwater fluctuation caused by the ocean tides in Glynn country, Georgia. Ground Water, 29, 3, 24-32.

Hachani, F. (2011). Application of Self-potential Measurements to Investigate Groundwater Flow in the Saijo Plain, Ehime prefecture, Western Japan. Unpublished Doctoral thesis. University of Tsukuba, Japan.

Harbison, P. (1986). Diurnal variation in the chemical environment of a shallow tidal inlet, Gulf St Vincent, South Australia: Implication for water quality and trace metal migration. Marine Environment Research, 20, 161-195.

Hughes, C.E., Binning, P., Willgoose, G.R. (1998). Characterisation of the hydrology of an estuarine wetland. Journal of Hydrology, 211, 34-49.

Jacob, C.E. (1950). Flow of groundwater, in Engineering Hydraulics, edited by H. Rouse, John Wiley, New York, 321-386.

Jeng, D.S., Li, L., Barry, D.A. (2002). Analytical solution for tidal propagation in a coupled semi-confined/phreatic coastal aquifer. Advances in Water Resources, 25, 5, 577-584.

Jha, M.K., Namgial, D., Kamii, Y., Peiffer, S. (2008). Hydraulic Parameters of Coastal Aquifer Systems by Direct Methods and an Extended Tide–Aquifer Interaction Technique. Water Resource Management, 22, 1899–1923.

Jiao, J. J., Tang, Z. (1999). An analytical solution of groundwater response to tidal fluctuation in a leaky confined aquifer. Water Resources Research, 35, 3, 747-751.

Jiao, J. J., Tang, Z. (2001). Reply to comment by R. E. Volker and Q. Zhang on “An analytical solution of groundwater response to tidal fluctuation in a leaky confined aquifer” by J. J. Jiao and Z. Tang. Water Resources Research, 37, 1, 187-188.

Jorgensen, N.O., Andersen, M.S., Engesgaard, P. (2008). Investigation of a dynamic seawater intrusion event using strontium isotopes ($^{87}Sr/^{86}Sr$). Journal of Hydrology, 348, 257– 269.

Kim, J., Lee, J., Cheong, T., Kim, R., Koh, D., Ryu, J., Chang, H. (2005). Use of time series analysis for the identification of tidal effect on groundwater in the coastal area of Kimje, Korea. Journal of Hydrology, 300, 188–198.

Kim, K.Y., Seong, H., Kim, T., Park, K., Woo, N., Park, Y., Koh, G., Park, W. (2006). Tidal effects on variations of fresh–saltwater interface and groundwater flow in a multilayered coastal aquifer on a volcanic island (Jeju Island, Korea). Journal of Hydrology, 330, 525– 542.

Kim,Y., Lee, K.S., Koh, D.C., Lee, D.H., Lee, S.G., Park, W.B., Koh, G.W., Woo, N.C. (2003). Hydrogeochemical and isotopic evidence of groundwater salinization in a coastal aquifer: a case study in Jeju volcanic island, Korea. Journal of Hydrology, 270, 282-294.

Knight, J.H. (1981). Steady period flow through a rectangular dam. Water Resources Research, 17, 4, 1222-1224.

Kopsiaftis, G., Mantoglou, A., Giannoulopoulos, P. (2009). Variable density coastal aquifer models with application to an aquifer on Thira Island. Desalination, 237, 65–80.

Kubota, Y., Takeshita, T. (2008). Paleocene large_scale normal faulting along the Median Tectonic Line, western Shikoku, Japan. Island Arc, 17, 129-151.

Kumar, P., Kumar, M., Ramanathan, A.L., Tsujimura, M. (2010). Tracing the factors responsible for arsenic enrichment in groundwater of the middle Gangetic Plain,

India: a source identification perspective. Environmental Geochemistry and Health, 32,129–146.

Kumasaka, H. (2010). Estimation of Groundwater Residence Time Using CFCs as Tracer in Saijo and Shuso plain. Unpublished Master thesis. University of Tsukuba, Japan, pp. 83.

Kurihara, G. (1972). Geology of the alluvial plains of the southern coastal area of Setouchi. Tohoku Univ. Inst. Geol. Pal. Center, **7**3, 31-65 (in Japanese with English abstract).

Langman, J.B., Ellis, A.S. (2010). A multi-isotope (δD, δ18O, $^{87}Sr/^{86}Sr$, and $\delta^{11}B$) approach for identifying saltwater intrusion and resolving groundwater evolution along the Western Caprock Escarpment of the Southern High Plains, New Mexico. Applied Geochemistry. 25, 159–174.

Langmuir, C.H., Vocke, R.D., Hanson, G.N., Hart, S.R. (1978). General Mixing Equation with Applications to Icelandic Basalts. Earth and Planetary Science Letters, 37, 380-392.

Langmuir, D. (1997). Aqueous environmental geochemistry. Prentice Hall, Engelwood Cliffs, New Jersey, pp.600.

Lanyon, J.A., Eliot, I.G., Clarke, D.J. (1982). Groundwater–level variation during semidiurnal spring tidal cycles on a sandy beach. Australian Journal of Marine and Freshwater Research, 33, 377-400.

Li, G., Chen, C. (1991). Determining the length of confined aquifer roof extending under the sea by the tidal method. Journal of Hydrology, 123, 97-104.

Li, L., Barry, D.A., Parlange, J.Y., Pattiaratch, C.B. (1997). Beach water table fluctuations due to wave run-up: Capillarity effects. Water resources research, 33, 5, 935-945.

Li, L., Barry, D.A., Stagnitti, F., Parlange, J.Y. (1999). Tidal along-shore groundwater flow in a coastal aquifer. Environmental Modeling and Assessment, 4, 179-188.

Li, H., Jiao, J.J. (2001a). Tide-induced groundwater fluctuation in a coastal leaky confined aquifer system extending under the sea. Water Resources Research, 37, 5, 1165-1171.

Li, H., Jiao, J.J. (2001b). Analytical studies of groundwater-head fluctuation in a coastal confined aquifer overlain by a leaky layer with storage. Advances in Water Resources, 24, 5, 565-573.

Li, H., Jiao, J.J., Luk, M., Cheung, K. (2002). Tide-induced groundwater level fluctuation in coastal aquifers bounded by L-shaped coastlines. Water Resources Research, 38, 3, 61- 68.

Li, H., Jiao, J.J. (2002b). Tidal groundwater level fluctuations in L-shaped leaky coastal aquifer system. Journal of Hydrology, 268, 1-4, 234-243.

Li, H., Jiao, J.J. (2003a). Influence of the tide on the mean watertable in an unconfined, anisotropic, inhomogeneous coastal aquifer. Advances in Water Resources, 26, 1, 9-16

Liu, K. (1996). Tide-induced ground-water flow in deep confined aquifer. Journal of Hydraulic Engineering, 122, 2, 104-110.

Lu, J.C.S, Chen, K.Y. (1977). Migration of trace metals in interfaces of seawater and polluted surficial sediments. Environmental Science and Technology, 11, 174-82.

Maas, C., Lange, W.J.D. (1987). On the negative phase shift of groundwater tides near shallow tidal rivers-The Gouderak anomaly. Journal of Hydrology, 92, 333-349.

Mao, X., Enot, p., Barry, D.A., Li, L., Binley, A., Jeng, D.S. (2006). Tidal influence on behavior of a coastal aquifer adjacent to a low- relief estuary. Journal of Hydrology, 327, 110-127.

Marquis, S.A. Jr., Smith, E.A. (1994). Assessment of ground-water flow and chemical transport in a tidally influenced aquifer using geostatistical filtering and hydrocarbon fingerprinting. Ground Water, 32, 2, 190-199.

Mizuno, K., Okada, A., Sangawa, A., Shimizu, F. (1993). Strip map of the median tectomedian tectonic line active fault system in Shikoku. Geological Survey of Japan.

Moore, W.S. (1996). Large groundwater inputs to coastal waters revealed by ^{226}Ra enrichment, Nature, 380, 18, 612-614.

Nakamura, Y., Hosokawa, T., Jinno, K., Iwamitu, K. (2005). Estimation of Residence Time of Fresh Water and Salt Water in Coastal Aquifers and Their Characteristics. Journal of Hydraulic Engineering, 49, 103-108. (in Japanese with English abstract).

Nakano, T., Saitoh, Y., Tokumasu, M. (2008). Geological and human impacts on the aquifer system of the Saijo basin, western Japan. Proceedings of 36th IAH Congress.

Nielsen, P. (1990). Tidal dynamics of the water table in beaches. Water Resources Research, 26, 2127-2134.

Oude Essink, G.H.P. (2001). Improving Fresh Groundwater Supply - Problems and Solutions. Ocean and Coastal Management, 44, 5, 429-449.

Parkhurst, D.L., Appelo, C.A.J. (1999). User's Guide to PHREEQC: a Computer Program for Speciation, Reaction-path, 1-D Transport, and Inverse Geochemical Calculations, U.S. Geological Survey Water-Resources Investigations Report, 99–4259.

Ray, R.K., Mukherjee, R. (2008). Reproducing the Piper Trilinear diagram in Rectangular Coordinates. Ground Water, 46, 6, 893-896.

Petalas, C., Pisinaras, V., Gemitzi, A., Tsihrintzis, V.A., Ouzounis, K. (2009). Current conditions of saltwater intrusion in the coastal Rhodope aquifer system, northeastern Greece, Desalination, 237, 22-41.

Philip, J.R. (1973). Periodic nonlinear diffusion: An integral relation and its physical consequences. Australian Journal of Physics, 26, 513-519.

Robinson, M.A., Gallagher, D.L., Reay, W.G. (1998). Field observations of tidal and seasonal variations in ground water discharge to estuarine surface waters. Ground Water Monitoring and Remediation, 18, 1, 83-92.

Robinson, M.A., Gallagher, D.L. (1999). A model of ground water discharge from an unconfined coastal aquifer. Ground Water, 37, 1, 80-87.

Robinson, C., Li, L., Barry, D.A. (2007). Effect of tidal forcing on a subterranean estuary. Advances in Water Resources, 30, 851–865.

Saijo city. (2008). Survey of groundwater resources in Dozen plain, Nippon Koei Co., Ltd., p. 94 (in Japanese).

Schiavo, M.A., Hauser, S., Povinec, P.P. (2009). Stable isotopes of water as a tool to study groundwater-seawater interactions in coastal south-eastern Sicily. Journal of Hydrology, 364, 40-49.

Shalev, E., Lazar, A., Wollman, S., Kington, S., Yechieli, Y., Gvirtzman, H. (2009). Biased monitoring of Fresh Water-Salt Water Mixing Zone in Coastal Aquifers. Ground Water, 47, 1, 49–56.

Shiklomanov, I.A. (1993). World fresh water resources. Chapter 2 in part I, In the book entitled Water in crisis: A guide to the World's fresh Water Resources, edited by Peter H. Gleick, Oxford University Press, 473, 13-23.

Sophocleous, M. (2002). Interactions between groundwater and surface water: the state of the science. Hydrogeology Journal, 10, 52–67.

Spiteri, C., Slomp, C.P., Tuncay, K., Meile, C. (2008). Modeling biogeochemical processes in subterranean estuaries: Effect of flow dynamics and redox conditions on submarine groundwater discharge of nutrients, Water Resources Research, 44, W02430, doi: 10.1029/2007WR006071.

Steyl, G., Dennis, I. (2010). Review of coastal-area aquifers in Africa. Hydrogeology Journal, 18, 217–225.

Stuyfzand, P.J. (2008). Base Exchange Indices as Indicators of Salinization or Freshening of (Coastal) Aquifers. 20th salt water Intrusion Meeting, Naples, Florida, USA.

Sun, H. (1997). A two-dimensional analytical solution of groundwater response to tidal loading in an estuary. Water Resources Research, 33, 6, 1429-1435.

Tanikawa, S. (1998). Comparative study of the salinization affect to groundwater quality - Case study in Saijo Plain, Ehime Pref. Proceedings of the General Meeting of the Association of Japanese Geographers, 54, 76-77.

Turner, I. (1993). The total water content of sandy beaches. Journal of coastal research, 15, 11-26.

USGS. (2011). United State Geological Survey for the estimation of water distribution over the planet earth, http://ga.water.usgs.gov/edu/earthwherewater.html.

Urish, D.W., McKenna, T.E. (2004). Tidal effects on ground water discharge through a sandy marine beach. Ground water (Oceans Issue), 42, 7, 971–982.

Van der Kamp, G. (1972). Tidal fluctuations in a confined aquifer extending under the sea. 24th International Geological Congress, Section 11, 101-106.

Van der Kamp, G. (1973). Periodic flowof groundwater. Ph.D. dissertation, Free University of Amsterdam. The Netherlands.

Vengosh, A., Kloppmann, W., Marei, A., Livshitz, Y., Gutierrez, A., Banna, M., Guerrot, C., Pankratov, I., Raanan, H. (2005). Sources of salinity and boron in the Gaza strip: natural contaminant flow in the southern Mediterranean coastal aquifer. Water Resource Research, 41, W01013, doi: 10.1029/2004WR003344.

Volker R.E., Zhang, Q. (2001). Comments on “An analytical solution of groundwater response to tidal fluctuation in a leaky confined aquifer” by Jiu Jimmy Jiao and Zhonghua Tang. Water Resources Research, 37, 1, 185-186.

Voudouris, K.S. (2006). Groundwater Balance and Safe Yield of the coastal aquifer system in NEastern Korinthia, Greece. Applied Geography, 26, 291–311.

WHO (2004). Guidelines for drinking water quality-II pp 333. Geneva, Environmental Health Criteria, 5.

Weisman, R.N., Seidel, G.S., Ogden, M.R. (1995). Effect of watertable manipulation on beach profiles. Journal of Waterway, Port, Coastal and Ocean Engineering, 121, 2, 134– 142.

Woods, T.L., Fullagar, P.D., Spruill, R.K., Sutton, L.C. (2000). Strontium isotopes and major elements as tracers of ground water evolution: Example from Upper Castle Hayne aquifer of North Carolina. Ground water, 38, 5, 762-771.

Xia, Y., Li, H., Boufadel, M.C., Guo, Q. (2007). Tidal wave propagation in a coastal aquifer: Effects of leakages through its submarine outlet-capping and offshore roof. Journal of Hydrology, 337, 249-257.

Yim, C.S., Mohsen, M.F.N. (1992). Simulation of tidal effect on contaminant transport in porous media. Ground water, 30, 1, 78-86.

Younger, P. L. (1996). Submarine groundwater discharge. Nature, 382, 121-122.